INFORMATION TO USERS

This reproduction was made from a copy of a manuscript sent to us for publication and microfilming. While the most advanced technology has been used to photograph and reproduce this manuscript, the quality of the reproduction is heavily dependent upon the quality of the material submitted. Pages in any manuscript may have indistinct print. In all cases the best available copy has been filmed.

The following explanation of techniques is provided to help clarify notations which may appear on this reproduction.

1. Manuscripts may not always be complete. When it is not possible to obtain missing pages, a note appears to indicate this.

2. When copyrighted materials are removed from the manuscript, a note appears to indicate this.

3. Oversize materials (maps, drawings, and charts) are photographed by sectioning the original, beginning at the upper left hand corner and continuing from left to right in equal sections with small overlaps. Each oversize page is also filmed as one exposure and is available, for an additional charge, as a standard 35mm slide or in black and white paper format.*

4. Most photographs reproduce acceptably on positive microfilm or microfiche but lack clarity on xerographic copies made from the microfilm. For an additional charge, all photographs are available in black and white standard 35mm slide format.*

***For more information about black and white slides or enlarged paper reproductions, please contact the Dissertations Customer Services Department.**

UMI Dissertation Information Service

University Microfilms International
A Bell & Howell Information Company
300 N. Zeeb Road, Ann Arbor, Michigan 48106

Synovec, Robert Eugene

INSTRUMENTAL AND COMPUTATIONAL TECHNIQUES FOR OBTAINING ANALYTICAL DATA IN HIGH PERFORMANCE LIQUID CHROMATOGRAPHY

Iowa State University PH.D. 1986

Instrumental and computational techniques for obtaining analytical data in high performance liquid chromatography

by

Robert Eugene Synovec

A Dissertation Submitted to the
Graduate Faculty in Partial Fulfillment of the
Requirements for the Degree of
DOCTOR OF PHILOSOPHY

Department: Chemistry
Major: Analytical Chemistry

Approved:

Signature was redacted for privacy.

In Charge of Major Work

Signature was redacted for privacy.

For the Major Department

Signature was redacted for privacy.

For the Graduate College

Iowa State University
Ames, Iowa
1986

TABLE OF CONTENTS

CHAPTER 1.

INTRODUCTION TO LIQUID CHROMATOGRAPHY DETECTION

Current Status and Future Trends

Liquid chromatography (LC) detectors and their development are unavoidably guided by the specific requirements of the chromatographic system in which the detector will be applied (1, 2). The goal in an analysis is to provide useful qualitative and quantitative information about a sample or set of samples in order to answer some pertinent chemical question. In a chromatographic analysis, this goal translates into a process in which the column produces a separation due to differing molecular properties of sample components, in time, with subsequent detection of the sample components by a suitable detector. Both the chromatographic separation process and the detection process provide qualitative information about the sample components. That is, the information may be inferred from the retention times of eluting peaks, or provided by the use of a suitable detector. Chemical identification of eluting species is often the goal of studying this qualitative information. Concurrent with providing qualitative information, a LC detector will provide a signal that is a function of sample component concentration. This will provide the means to quantitate the amount of the various components present in a sample. While not always possible, it is useful to choose a detector that yields qualitative information that is

orthogonal to the information inferred in the separation process. This helps to optimize the information content in a chromatogram. Quantitative and qualitative information that can be obtained with a given detector is dependent upon the detector specificity and detectability. Specificity implies what species will be detected, often in the presence of co-eluting species that are not "specified" by the LC detector (3). Detectability implies the minimum amount or concentration of a species that can be detected with a minimum of statistical certainty (4). In the context of LC detector development, the peak broadening introduced in the detector must be kept to a minimum, while maintaining the detectability quality.

Developments for LC detectors have been, and will continue to be, in designing detectors that provide new or improved information. Detectors that provide new chemical information are slow to develop, but the consequences of such work can often be rewarding. The recent analytical interest in microbore (ca 1 mm i.d. columns), packed capillary (ca 250 μm i.d. columns), and open tubular (ca 10 μm i.d. columns) LC column technology has given the field of detector development further purpose in providing compatible detectors. Thus, the improvements in detectors have been in an effort to maintain detectability in absolute terms and improve mass detectability, while not sacrificing peak band broadening during detection. This may be accomplished, in concert, with providing new information. The challenges are both conceptual and technical, in nature, and often quite formidable.

A justification for scaling down LC detectors is dependent upon the justification for investigating the use of smaller-scale LC columns (5). These columns have already been listed. One advantage for their use is reduced solvent consumption. This translates into reduced cost for applications involving conventional solvents, and the possibility of using more exotic solvents that would have been cost prohibitive at conventional LC flow rates. Improved mass detectability is another advantage, allowing the injection, separation, and detection of extremely small quantities of samples, that may not have been as easily analyzed with conventional systems. Finally, smaller-scale LC has made it possible to interface, more compatibly, the LC system with certain detection principles, such as electrochemical and mass spectrometric detectors.

It is anticipated that the trend of reducing chromatographic column size will continue to some extent. As some of the state-of-the-art detectors designed for microbore, capillary, and open tubular (OT) LC become commercially available, it is quite reasonable to expect chromatographic separations, themselves, to become better understood. From this, investigations with more exotic solvent systems and novel detection concepts, based upon fundamental principles, will produce new directions and solutions to a variety of important analytical problems (6, 7).

Concurrent with this trend, is the necessity to optimize the use of the gathered chromatographic data. This involves the optimization of the chromatographic data collection process, and subsequent

utilization of algorithms that derive useful information from the data (8, 9). These tasks are interdependent with understanding statistical and computational relationships that govern the credibility of the quantitative results provided by an analysis (4, 10). Many novel computational procedures are dependent upon chromatographic detectors providing signals that are related, in an absolute way, to a fundamental physical chemistry relationship (6, 11, 12, 13, 14). While signal linearity and predictability is an important property for LC detectors, it is also important that there exist a relationship between different eluent systems for a given LC detection system. This provides the means for absolute quantitation procedures, such as with refractive index detection (15). A direct result of this study was the development of an on-line procedure for the LC analysis of motor oils (16) and crude oils (17, 18) without collecting and individually analyzing fractions. Both quantitative and qualitative information were simultaneously determined in the procedure.

As other technical fields provide improvements in fabricated materials and electronic devices, it is anticipated that state-of-the-art LC detectors will be developed and improved by taking advantage of these insights. This is the case for the recent development of state-of-the-art optical activity detectors for both transmission detected circular dichroism (19) and fluorescence detected circular dichroism (20) in LC.

LC is a single step in the process of answering a meaningful question about a chemical problem. An LC detector merely samples a

chemical system, providing information. So, in considering LC detection, one is considering the broader task of collecting appropriate data, processing the data, and interpreting the data. In each phase of this task, optimization is the key. Novel developments, within the context of this broader focus, were accomplished, and will be the subject of this manuscript. But first, it is of interest to discuss LC detectors in more detail. Both commercially available (conventional) and state-of-the-art LC detectors will be reviewed. This will provide a basis for discussion. LC columns and separations are not reviewed, since LC, itself, is used in demonstration, for the most part, in each of the projects.

Conventional and State-of-the-art Liquid Chromatography Detectors

There are a few LC detectors that because of commercial availability at low cost, ease of applicability, and trustworthiness of operation, can be considered as favorites for routine use. The list includes absorbance, fluorescence, electrochemical, conductivity and refractive index detectors. Table 1 contains some pertinent data for a discussion of LC detectors.

UV-Visible absorbance detection

UV-Visible absorbance detection is by far the most popular routinely used detector. Detectors are available with anywhere from single-wavelength to simultaneous multi-wavelength detection capabilities. Wavelength selectivity and often excellent analyte

sensitivity in the absorption process are two key advantages for this mode of detection. For conventional conditions, typical detectability with commercial absorbance detectors is 1 ng of injected analyte, at an injected concentration of 5×10^{-7} M. These values are improved by a factor of 10 with commercially available cells adapted for microbore LC. Pathlength and injection volume offset each other in comparing conventional and microbore LC, while the difference in detectability is due to superior separation efficiency with microbore LC. Apart from being quite sensitive, selectivity in absorbance detection is quite useful. Unresolved peaks in a chromatographic analysis can be diagnosed using simultaneous multi-wavelength detection (21, 22). For instance, the presence of unresolved peaks can be diagnosed from the shifting of retention times as a function of detection wavelength. Analyte identification and purity determination within the chromatographic separation are often quite easily performed with multi-wavelength absorbance techniques (23). In the other extreme, absorbance detection at a single wavelength in the range of 185- to 210 nm can provide sensitive, and almost universal detection of analytes, with proper choice of eluent (24). Another feature of absorbance detection, which is also true of this universal detection scheme, is the compatibility of detection with the use of gradient elution.

State-of-the-art absorbance detection is involved with microbore LC. The pathlength dependence of absorption has limited the development for capillary and OT LC. In an effort to maintain as long

Table 1. Detection capabilities of liquid chromatography detectors

Liquid Chromatography Detector	Commercially Available	Mass LOD[a] (commercial detectors)	Mass LOD[b] (state-of-the-art detectors)
Absorbance	Yes[c]	100pg - 1ng	1 pg
Fluorescence	Yes[c]	1 - 10pg	10 fg
Electrochemical	Yes[c]	10pg - 1ng	100 fg
Refractive Index	Yes	100ng - 1µg	
Conductivity	Yes	500pg - 1ng	500 pg
Mass Spectrometry	Yes[d]	100pg - 1ng	1 - 10pg
FT-IR	Yes[d]	1 µg	100 ng
Optical Activity	No	-	1 ng
Element Selective	No	-	10 - 100 ng
Photoionization	No	-	1pg - 1ng

[a]Mass limit of detection (LOD) is calculated for injected mass that yields a peak height equal to 5 times the standard deviation of the baseline noise, using a molecular weight of 200 g/mole, and either 10 µL injected volume for conventional or 1 µL injected volume for microbore LC.

[b]Same definition as in a, above, but the injected volume is generally smaller.

[c]Commercially available for microbore LC, also.

[d]Commercially available, yet somewhat cost prohibitive.

a pathlength as possible, without sacrificing chromatographic resolution in detection, lasers have been readily applied in recent absorbance detector development. Both spatial and polarization properties have been utilized to develop microbore LC absorbance detectors capable of detecting low pg amounts of injected analytes. These novel approaches include thermal lense (25, 26, 27), photothermal (28, 29), and indirect (7) absorbance detection. The absorbance limit-of-detection (LOD) is about 3×10^{-6} AU cm^{-1} in each case, for typical eluent systems.

Fluorescence detection

Fluorescence detection is more selective than absorbance detection, since all species that absorb light do not necessarily fluoresce. Detection of fluorescence can be made more selective by adjusting both the excitation and emission wavelengths. Since the fluorescence emission is often well removed to longer wavelengths, from the excitation wavelength, the fluorescence measurement is not as affected by the background detected signal. This is in contrast to transmission mode absorbance measurements. Subsequently, fluorescence detection is capable of better detectability than common transmission mode absorbance detection. Commercially available fluorescence detectors for conventional LC and microbore LC produce mass detectabilities of 10 pg and 1 pg, respectively, for a typical fluorescing analyte. This is about 100 times better than that provided by commercial absorbance detectors. Also, fluorescence spectra can be measured on-line with some commercial detectors. If an

analyte does not fluoresce originally, various derivatization procedures, both on-line and in sample preparation, have been devised to take advantage of the excellent detectabilities provided by fluorescence detection in LC.

Both microbore and capillary LC have benefitted by the development of laser-based fluorescence detectors. The ability to put a large amount of light, via a laser, into a very small volume has produced excellent state-of-the-art fluorescence detectabilities (30). Proper design considerations has allowed detection cells to be less than 100 nL for use with capillary LC (31). The reward is LOD values for 10 to 20 femtograms (fg) of an injected, fluorescing test analyte. Fluorescence spectra can be obtained in such small detection volumes, providing a powerful qualitative tool for analyte identification for extremely small injected quantities (32).

Electrochemical detection

Electrochemical (EC) detectors offer selectivity capabilities analogous to absorbance and fluorescence detection. Sensitive detection is for species exhibiting a reversible electron transfer for a particular functional group. Thus, EC detection is particularly useful for the analysis of aromatic amines and phenols. Detectabilities for conventional LC are quite favorable for these type of species, ranging from about 10 pg to 1 ng injected material for the LOD.

Because EC detection is a surface phenomena and not a solution phenomena, in contrast to many other detectors, it is uniquely well-

suited to be scaled down for capillary and OT LC. State-of-the-art EC detection volumes have been reported in the sub-nL range (33). LOD of phenols is on the order of 100 fg for OT-LC. Rapid-scanning and dual-electrode techniques have provided a means to further enhance the selectivity already implicit in EC-LC detection (34, 35).

Conductivity and refractive index detection

Although quite different in many ways conductivity and refractive index (RI) detectors are similar in one important respect. Conductivity detection is the method of choice for simple, universal detection of ionic species, while RI detection is quite popular as a universal detector of neutral species. Only conventional LC detectors are commercially available for both. Detectability for the conductivity detector is about 500 pg to 1 ng for a system with temperature control for anion chromatography with or without suppression (36). The LOD is about 10 times worse if temperature effects are neglected. For RI detection, a typical eluent-analyte combination can produce detectabilities from 100 ng to about a 1 ug of injected material. Again, the use of lasers has allowed for the development of small volume RI detectors for microbore detection (37, 38). Detectabilities on the order of 10 to 50 ng have been reported. Light scattering detection is often used in conjunction with size-exclusion chromatography and, for example, polymer analysis. This detector is also laser-based (39, 40).

Mass spectrometry, Fourier transform infrared spectroscopy and related detectors

Though both are commercially available, they are somewhat cost prohibitive to be considered bench-top instruments. This should not detract from the realization that both mass spectrometry (MS) and Fourier transform infrared (FTIR) detection are excellent tools for analyte identification in chemical analysis. Both provide molecular structure information that can be invaluable in answering many analytical questions. A possible limitation is that neither adequately provides optical activity information. Detectabilities for state-of-the-art LC-MS systems are on the order of 1 to 10 pg for OT LC with direct-liquid-injection (DLI) (41). However, FTIR detection has been developed only to the point of being interfaced with microbore LC, with an LOD of about 100 ng injected material (42, 43).

Much of the original work in combining MS with conventional and microbore LC has dealt with removing the eluent without losing or distorting the eluting analyte peak shape. Various LC-MS interfaces have been developed such as the moving-belt interface (44), and the thermospray interface (45). The advent of capillary and OT LC columns has allowed for DLI to be more readily developed. Essentially, the flux of material due to the eluent flow for these chromatographic systems is found to be small enough to allow for DLI. As an advantage, LC-MS in such systems is quite favorable for thermally labile species that could not survive a gas chromatograph-MS analysis, but can be analyzed by LC-MS procedures (46). If total ion current is

measured, LC-MS offers universal detection at sub-ng levels (46). Real-time mass spectra of eluting species can be provided to show the ability of LC-MS in providing information for definitive molecule identification. Nuclear magnetic resonance (NMR) has also been coupled to LC (47), while the success in terms of detectability is rather poor. Yet, LC-NMR is an area of some interest with many future possibilities (48, 49). Many detection concepts have been proposed for element specific detection (ESD). These include flame photometric detection (FPD) (50) and thermionic detection (51). Thermionic and FPD provide detectabilities on the order of 10 to 100 ng injected analyte with ESD. Techniques such as photoionization detection (PID), with (52) or without (53) EC detection, offers functional group selectivity with LOD values ranging from 1 pg to 1 ng.

Optical activity detection

Optical activity detection (OAD) is an area of recent interest. While many of the detectors previously described provide information that infers molecular identity with a separation, the optical activity (OA) of sample constituent is not provided. The OA is best determined without derivatization due to racemization problems. Thus, the development of a suitable OAD for conventional and microbore LC is of interest in order to solve a variety of analytical problems. An OAD-LC system, based upon polarimetry and suitable for microbore LC, has been reported (6). It provided low ng detectabilities in a 1 μL detection cell. OAD is extremely useful for the analysis of biologically important materials, where the OAD is of prime concern

(54, 55). Sample preparation is often at a minimum, since OAD provides ample selectivity and resistance to matrix effects.

OAD based upon circular dichroism (CD) offers another level of selectivity, beyond that of OAD based upon polarimetry. CD requires a sample to be both optically active and to absorb at the laser wavelength utilized. Detectabilities for microbore LC with CD detection (8) are comparable to those obtained with polarimetry (6).

CHAPTER 2.

QUANTITATIVE ANALYSIS WITHOUT ANALYTE IDENTIFICATION USING REFRACTIVE INDEX DETECTION

Introduction

Chemical analysis deals with the solution to scientific questions through the identification and the quantitative determination of the composition of matter. It is generally accepted that the former precedes the latter. That is, one must identify or specify the species of interest before one can determine its concentration. This is because all analytical methods are based on some particular physical and/or chemical property of the species. The experimental observable must be calibrated against this particular property so that a concentration can be deduced. Analytical working curves thus serve to provide the needed calibration, but they can only be constructed if the identify of the species is not in doubt. There are certain situations where it is desirable to know the concentrations of the components before any attempts at identification. One example is the assay of supposedly pure material. There, one tries to determine the type and the amount of each impurity present, the latter being of primary concern. Since quantitative methods are generally species specific, it is difficult to be sure that all possible impurities have been searched for. If however one can first ascertain the amount of all impurities present, the scope of the problems becomes much more tractable. Another example is the control of pollution emission and

waste discharge. Knowing the concentrations of any foreign matter released without first requiring speciation is advantageous. A third example is forensic chemistry, where finding out whether any contamination exists at all is an important first step. A fourth example is in organic synthesis, where it may be desirable to know the yields of the various reaction products on the microscale, even when these products cannot be identified. And, when the products are identified, it may not be possible to isolate sufficient quantities of each to use traditional analytical calibration curves. It is therefore appropriate to pose the question whether qualitative analysis is a prerequisite for quantitative analysis.

By quantitative analysis one means the determination of concentrations in terms of volume fraction, weight fraction, or mole fraction of a species, and not secondary properties like oxygen uptake or total carbon. Naturally, the first two can always be determined in conjunction with some separation procedure, as long as the quantities are large enough for direct measurements, for example in prep scale LC. This discussion is restricted to trace analysis and microanalysis. There are a few known analytical methods that come close to providing quantitative information for an unidentified analyte. Coulometry relates electrochemical equivalents to an observable, the current, that can be independently calibrated. To obtain the concentration, however, one needs to know the change in the number of electrons in the reaction, as well as the current efficiency of the system. Mass spectrometry can in principle determine the

number and the molecular weight of a species simultaneously, but the choice of conditions affects the ionization efficiency and the extent of fragmentation, and thus the quantitation. Furthermore, the same number of ions of different types need not produce the same ion count in the detector. The electron capture detector for gas chromatography (GC) has been suggested as an absolute gas-phase coulometer (56, 57), but positive ions, dissociation, and instrumental effects create problems. Besides, only compounds with very high capture cross-sections are suitable for applying this scheme.

The scheme proposed here can be explained qualitatively using the following example. Suppose a refractive index (RI) detector is used to monitor the elution of an analyte in a flowing system. Suppose that no signal (from baseline) is observed even at the highest sensitivity setting of the detector. On changing to a different eluent, however, a detector response is obtained from the same injected amount. The lack of response in the first experiment is in fact an important piece of information, that is, the RI of the analyte is essentially the same as that of the first eluent. If the RI of both eluents are known from independent measurements, this then allows one to calculate the concentration of the analyte. In general, it is fortuitous if in fact no response is obtained from a particular eluent. But, as long as the two eluents have different RIs, it can be seen that the two experiments provide two equations with two unknowns, the RI and the concentration of the analyte, and the latter can be uniquely determined.

Theory

It is necessary to start from first principles to see how RI depends on the components in a mixture. From the basic relations among the electric field, the electric displacement vector, and the polarization, one obtains the Clausius-Mosotti relation (58):

$$\chi_i = \frac{3}{4\pi} \frac{M}{N_0 \rho} \left(\frac{\varepsilon'-1}{\varepsilon'+2}\right) \tag{1}$$

where χ_i is the susceptibility per molecule, M is the molecular weight, N_0 is Avogadro's number, ρ is the density of the material, and ε' is the dielectric constant. It can be shown that, except at high densities or high field intensities, neither of which is true in LC, the susceptibility of a mixture is additive (58)

$$\chi = \sum_i x_i \chi_i \tag{2}$$

where x_i is the mole fraction of component i with susceptibility of χ_i. It may be noted that for sufficiently low field strengths or high temperatures

$$\chi_i = \alpha_i + \frac{D_i^2}{3kT} \tag{3}$$

where α_i and D_i are the polarizability and the permanent dipole moment of the species i, k is the Boltzmann constant, and T is the absolute temperature. Now, the volume fraction of the component i, C_i, is given by

$$C_i = \frac{x_i(M_i/\rho_i)}{\sum_j x_j(M_j/\rho_j)} \tag{4}$$

The refractive index of component i, n_i, is given by

$$n_i = \sqrt{\mu_i' \varepsilon'_i} \tag{5}$$

where μ_i' is the permeability of the medium. But since μ' is very nearly unity (typical deviating by less than 10^{-3}), one can replace ε'_i with n_i^2 in Equation 1. Grouping Equations 1, 2, 4, and 5, one has

$$\frac{n^2 - 1}{n^2 + 2} = \sum_i C_i\left(\frac{n_i^2 - 1}{n_i^2 + 2}\right) \tag{6}$$

with n being the RI of the mixture.

Now consider the case of a binary mixture, which is composed of an analyte species and an eluent. At any particular instant, the measured RI response is determined by the volume fraction of the analyte of RI n_x in the flow cell, C_x, and the volume fraction of the eluent in the flow cell, $(1-C_x)$. Using Equation 6 and the subscript 1 for the eluent, one obtains

$$\frac{n^2-1}{n^2+2} - \frac{n_1^2-1}{n_1^2+2} = C_x\left[\frac{n_x^2-1}{n_x^2+2} - \frac{n_1^2-1}{n_1^2+2}\right] \tag{7}$$

Combining the two terms on the left of Equation 7, one gets $3(n^2 - n_1^2)/[(n^2 + 2)(n_1^2 + 2)]$, which in turn equals $3\Delta n_1(n+n_1)/[(n^2+2)(n_1^2+2)]$. Δn_1 is in fact the experimental

observable from any of the differential RI detectors. Note that for low concentrations, errors much less than 0.1% are expected if all n's are now replaced by n_1's. Rearranging and redefining terms:

$$\Delta n_1 K_1' = C_x(F_x - F_1) \tag{8}$$

where $F_i \equiv (n_i^2-1)/n_i^2+2)$, and $K_i' \equiv 6n_i/(n_i^2+2)^2$. So, Equation 8 shows that by using two eluents 1 and 2 for the same injected quantity of the analyte,

$$C_x = \frac{\Delta n_1 K_1' - \Delta n_2 K_2'}{F_2 - F_1} \tag{9}$$

and the concentration is thus determined. To relate these to the volume fraction of the analyte at injection, one must integrate these C_x values over the entire detector response curve, which is shaped like a peak, and then multiply by the ratio of the total peak volume to the injection volume. It is therefore much more convenient to think in terms of peak areas, in units of RI•volume. This can be derived from the RI versus time detector response curve that is normally obtained by measuring the eluent flow rate. After this, one can insert Equation 9 into Equation 8 and determine the value n_x. It is important to note that the denominator in Equation 9 is the order of (n_2-n_1), and that the K' values are the order of unity. So, no loss in sensitivity or in significance is expected in applying this scheme. In fact, the choice of two eluents of substantially different RIs guarantees that a signal will be obtained in at least one of the

eluents for any analyte. Also, it is important to use the correct signs for Δn_i throughout, otherwise an analyte with n_x intermediate between n_1 and n_2 will incorrectly show a cancellation in the numerator of Equation 9.

One can expand further on this concept. It is known that RI depends on the temperature, the pressure and the wavelength of light used. It is also known that commercial detectors for RI show a response that is dependent upon the RI of the eluent (59), unlike RI detectors based on interferometry (37, 60). It may also be necessary to use different eluent flow rates for the two experiments. It is therefore desirable to rewrite Equation 8 in terms of the observed signal, S, which is an area in arbitrary units

$$S_1K_1 = V_x(F_x - F_1) \qquad (10)$$

where K is a new constant grouping together the old K', the particular flow rate for this eluent, the injection volume, the conversion factor from Δn_1 to the units of the signal (such as a voltage, or a number in the computer), and V_x is the volume fraction of the analyte at injection. As long as the same light source, the same temperature, and the same pressure are used throughout, F_x and F_1 are true constants. For the same injection using a second eluent,

$$S_2K_2 = V_x(F_x - F_2) \qquad (11)$$

K_2 is a different constant because it includes the RI of the second eluent, a different conversion factor for response, and the flow rate of the second eluent. From Equations 10 and 11,

$$V_x = \frac{S_1K_1 - S_2K_2}{F_2 - F_1} \tag{12}$$

One can now obtain two other detector response curves, injecting equal amounts (for example, equal volumes with equal volume fractions) V of each eluent into the other under the same conditions. So,

$$S_3K_1 = V(F_2 - F_1) \tag{13}$$

and

$$S_4K_2 = V(F_1 - F_2) \tag{14}$$

From these, one can see that

$$K_1/K_2 = - S_4/S_3 \tag{15}$$

Combining Equations 12, 13, and 15, the result is

$$V_x = V(\frac{S_1}{S_3} + \frac{S_2}{S_4}) \tag{16}$$

In other words, the volume fraction of the analyte injected is determined without any knowledge of the instrumental response factor, or the identities of the two eluents and the analyte! The only requirement is that the same conditions are used throughout for these measurements. Again, no loss of sensitivity or significance is

expected. To then solve for F_x and thus n_x, it is necessary to know the two values n_1 and n_2. From Equations 10 and 11, one has

$$\frac{S_1K_1}{S_2K_2} = \frac{F_x - F_1}{F_2 - F_2} \tag{17}$$

So, making use of Equation 15, one can solve for F_x.

Experimental

All reagents and eluents used were reagent grade materials without further purification. A conventional chromatographic system was used, although not necessarily for the demonstration of the concept. It consisted of a reciprocating pump (Milton Roy, Riviera Beach, FL, Model 196-0066), a 25 cm x 4.6 mm, 10-μ C_{18} column (Alltech, Deerfield, IL), a 5-μL sample loop at a conventional injection valve (Rheodyne, Berkeley, CA, Model 7010), and a commercial RI detector (Waters Associates, Milford, MA, Model R401) with the reference cell used in the static mode filled with the eluent being used. A flow rate of 0.60 mL/min was used throughout. Solutions with specified volume fractions were made by pipetting a well defined volume of the minor component into a volumetric flask, and then filling to mark with the major component.

The output of the RI detector (10 mV full scale) was connected to a digital voltmeter (Keithley, Cleveland, OH, Model 160B), the analog output of which was in turn connected to a computer (Digital Equipment, Maynard, MA, Model PDP 11/10 with LPS-11 laboratory

interface). The computer took readings every 0.05 s, and averaged each set of 10 before storing the information. Typically about 100 of these averaged data points define an analyte peak. The area was determined by locating and determining the peak maximum, and then summing all points that were more than 1.0% of this peak value above the baseline. The numerical values of these areas were then used directly as S_i defined earlier. All areas were determined using multiple injections (three or more) and were found to be reproducible to ±2.5% (relative standard deviation). The linearity of the attenuation settings on the RI detector was determined by injections of successively diluted samples, and was found to be ±2.5% from 32X to 2X, which covers all of the scales used in this work.

Measurements of RI for various mixtures were performed with a standard Abbe refractometer (Spencer Optical, Buffalo, NY) after calibration with pure solvents.

Results and Discussion

To appreciate the implications of Equations 7 and 8, the actual dependence of RI of a mixture of heptane and benzene as a function of the volume fraction of benzene is plotted in Figure 1. The ordinates are shifted on the left compared to the right to facilitate visualization. The solid horizontal line is a linear interpolation of the RIs for the two pure solvents, and is commonly assumed in elementary discussions of applications of refractometry (61). The curved line is the actual dependence from Equation 7. It can be seen

Figure 1. RI dependence on volume fraction for benzene in heptane Solid horizontal line - linear interpolation; solid curve - true dependence; dashed lines - limiting slopes.

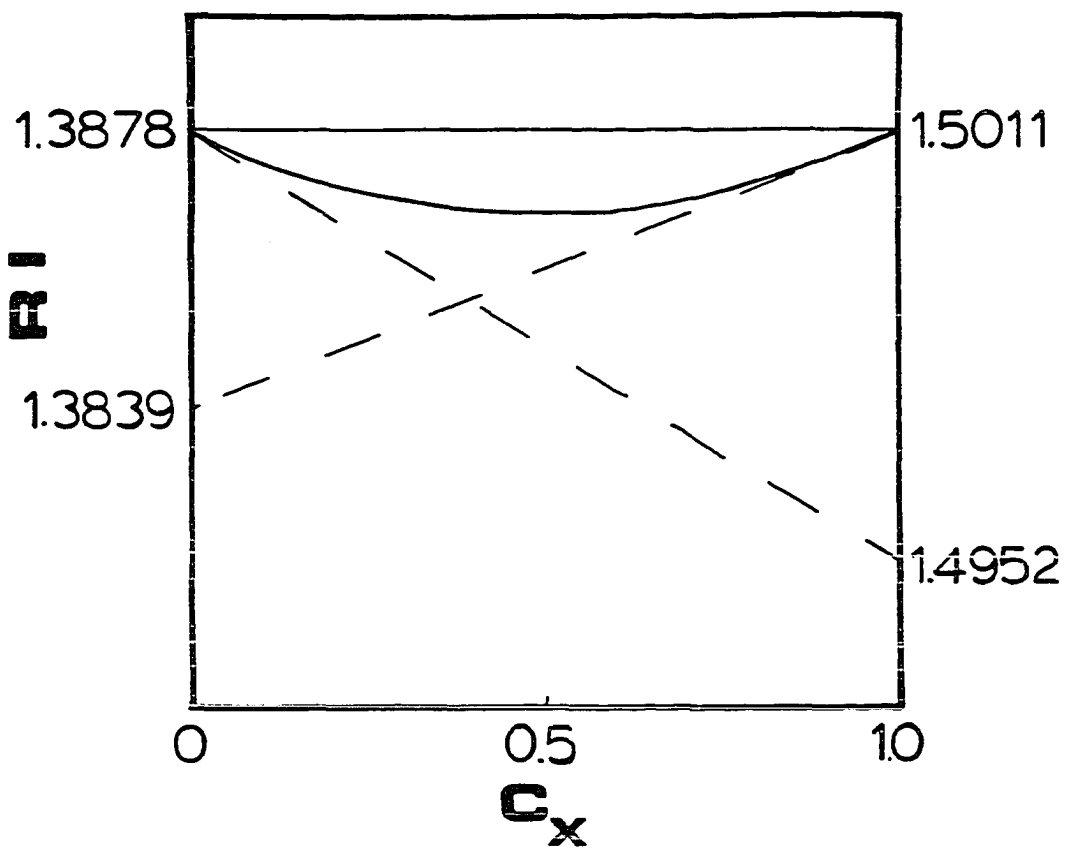
1.3878
1.5011
n
1.3839
1.4952
0
0.5
1.0
C_x

that the linear interpolation does extremely poorly throughout. Note that the correct curvature shown is not due to a nonideal solution. A nonideal solution simply changes the implication of the volume fraction C_x and in a sense makes the horizontal scale nonlinear. The deviation from an ideal solution will introduce a corresponding amount of error in a determination. Unless either the analyte or eluent is extremely polar, one can safely assume that an ideal solution is formed. In LC, for instance, this assumption is made implicitly in all measurements. Otherwise, the concentration at the detector cannot be related to the concentration of the injected sample in a linear fashion. The dashed lines in Figure 1 are the tangents to the curve for small concentrations of each of the components. From Equation 8, the two slopes are given by $(F_x - F_1)/K_1'$ and $(F_1 - F_x)/K_x'$, respectively. The fact that these slopes are different for each of the two solvents used allows us to determine the value C_x independent of the particular value of F_x. Using a standard refractometer, linearity and the limiting slope were independently confirmed, as specified by Equation 8 for cases with the minor component present below 4% by volume for a number of binary mixtures involving combinations of hexane, benzene, $CHCl_3$, CCl_4, and CS_2.

The raw data, averaged for each set of multiple injections onto the LC system, are shown in Table 2. Full scale corresponds to 10 mV from the detector module, amplified to 1.0 V by the digital voltmeter, and converted to a numerical value of 2048 by the A/D converter in the laboratory interface. The 10 measurements in Table 2 involving

Table 2. Areas of eluted peaks

Eluent	Analyte	Injected Volume Fraction	Attenuation	Area ($\times 10^4$)
Heptane	Benzene	0.02	32	3.86
Heptane	Benzene	0.01	16	3.92
Heptane	Benzene	0.005	8	3.88
Heptane	Benzene	0.00167	4	2.65
Heptane	Benzene	0.00167	2	5.25
Heptane	CCl_4	0.03	32	4.12
Heptane	CCl_4	0.003	4	3.13
Heptane	$CHCl_3$	0.03	16	5.54
Heptane	$CHCl_3$	0.003	2	4.59
Benzene	Heptane	0.02	32	-4.75
Benzene	Heptane	0.01	16	-4.76
Benzene	Heptane	0.005	8	-4.70
Benzene	Heptane	0.00167	4	-3.08
Benzene	Heptane	0.00167	2	-6.14
Benzene	CCl_4	0.03	32	-2.02
Benzene	CCl_4	0.003	4	-1.66
Benzene	$CHCl_3$	0.03	32	-3.39
Benzene	$CHCl_3$	0.003	4	-2.76

heptane and benzene only can be used to calibrate the attenuation settings of the refractometer and to determine the goodness of Equation 8. In order, the five values involving benzene injected into heptane give calibrations for full scale at each attenuation of 11.5, 5.66, 2.86, 1.40, and 0.71, in 10^{-5} RI units. The five values involving heptane injected into benzene give calibrations for full scale at the corresponding attenuation of 10.2, 5.08, 2.57, 1.31, and 0.66, in 10^{-5} RI units. Linearity of the scales and of Equation 8 is thus confirmed to ±2.5%. The ratios of the two sets of RI scales are consistent with a slight nonlinearity in the particular instrument design.

With these calibrated scales for RI, one can now relate the areas for CCl_4 and for $CHCl_3$ to RI•volume units. Since the injected volume is 0.005 mL and the flow rate used provides also 0.005 mL per integration interval, the areas in Table 2 are simply multiplied by the full scale equivalent RI and then divided by the range of the A/D converter, 2048. From published work (62), it was found that $n_{heptane}$ = 1.3878, and $n_{benzene}$ = 1.5011. This gives F_1 = 0.2359, F_2 = 0.2947, K_1' = 0.5402 and K_2' = 0.4979. So, the concentration of the "unknowns" can be found using Equation 9, and are tabulated in Table 3. Compared to the "true" volume fractions, the agreement is good, with an average relative error of 3%, which is consistent with the standard deviations of the individual area measurements in each set of multiple injections. Also tabulated in Table 3 are the predicted values of the RI of the unknowns using Equation 8 and the RI of

Table 3. Predictions for simulated mixtures

Sample	True C_x	True RI	Eq. (9), (8)		Eq. (16), (17), (15)	
			C_x	RI	C_x	RI
CCl_4	0.030	1.4601	0.0298	1.460	0.0299	1.4679
	0.0030	1.4601	0.00286	1.4661	0.00287	1.4647
$CHCl_3$	0.030	1.4459	0.0284	1.4461	0.0286	1.4435
	0.0030	1.4459	0.00296	1.4436	0.00295	1.4425

benzene. The agreement with known values is again good, especially since the wavelengths used in the RI detector are not the sodium D lines, and the temperature of the eluent is not controlled to be at 20°C. On careful inspection it was noted that the sample of $CHCl_3$ contained an unknown impurity. This impurity was not resolved chromatographically by the system used. This is probably a preservative for the reagent. So, even though the volume fraction is correctly predicted, a slight systematic error in the RI calculated is expected. Using Equation 8 and the RI of n-heptane, similar values are obtained for the unknown RIs. However, it is known that the eluent used actually contained about 2% of impurities, so that any comparison is inappropriate.

The problems with the above procedure are now obvious. It is necessary to calibrate the instrument in actual RI units (which typically changes from one eluent to the next), and to maintain conditions so that the temperature, pressure, and wavelength all correspond to the chosen values for n_1 and n_2. If this quantitation concept is applied to LC, this concern becomes even more serious if a mixed solvent provides the best chromatographic condition (63), and an accurate value for n is not available. All these problems can be avoided if instead Equation 16 is used. Concentrations for the "unknowns" have been calculated in this manner. These are shown in Table 3. The agreement with the true values are again within the relative standard deviations of each set of area measurements. In fact, the average relative error of 2.7% is slightly better than that

using the previous procedure, as expected. The calculated values for the n's for the unknowns are found using Equations 15 and 17, and are listed in Table 3. Again, the comparison with the true values is good in view of the discussions in the preceding paragraph.

The application of this quantitation concept for LC should be considered. For instance, extend this concept to the case of a mixture of analytes x and y, in which the analytes are not chromatographically resolved. One can obtain the analogue to Equation 8,

$$\Delta n_1 K_1' = C_x F_x + C_y F_y - (C_x + C_y) F_1 \qquad (18)$$

It can be seen that by following the procedure described above, one can uniquely determine the total concentration, $C_x + C_y$, contributing to the particular chromatographic peak, regardless of the individual refractive indices. In this case, the calculated refractive index will be intermediate between those of components x and y, and will have a volume fraction weighted dependence. Note that if one uses 4 eluents (different n_i) to elute this sample, there will then be available 4 equations of the form in Equation 18. However, these equations are not independent and can be reduced to only 2 independent equations. So, the 4 unknowns, C_x, C_y, F_x, and F_y cannot be solved for uniquely.

The calculations above require that the chromatographic peaks must be correlated between the chromatograms obtained with the two eluents, i.e., the order of elution must be known. In gel permeation

chromatography using selected pairs of solvents, this is not a major problem. In other cases, one can obtain a third chromatogram with an eluent with a RI different from the other two. There are a total of N! possible different elution orders for a sample with N components in the first two chromatograms. If one now uses the above procedure to determine V_x and n_x based on the first pair of chromatograms, one can predict the response, S, in the the third chromatogram for every one of the N peaks. If the elution order changed in any of the three eluents, consistency will not be achieved. It is possible for the computer to go through all N! combinations until consistency is obtained in the predictions. This way, the elution order for each of the N peaks in each of the three eluents can be uniquely determined. It is easy to see that the only time this consistency test fails is if both the concentration and the RI for two or more of the components are identical. In this unlikely case, one does not worry about the individual concentrations anyway. Applications of this kind of consistency test include the optimization of chromatographic conditions in LC, when 3 chromatograms rather than 3(N-1) chromatograms are needed to check the elution order.

An intriguing question is whether there are other similar methods in chemical analysis that can be adapted to this scheme. An inspection of the basic operations show that the experimental observable must be related (linearly, if possible) simultaneously to some property of the analyte and the environment (the eluent). It must be possible to change the environment while keeping the

concentration of the analyte and the property of the analyte the same. For this reason, some chromatographic method that allows a change of eluent is the simplest solution. Following the procedure here, the peak area is meaningful regardless of the change in actual separation conditions (different k's or different number of theoretical plates), as long as one can correlate the peaks in each chromatogram. The detector must be a true differential detector, so that the contributions of the pure environment can be used as the baseline. Otherwise, one will end up subtracting two large numbers to detect the small change in the experimental observable, losing sensitivity and significance at the same time.

The other common differential detector in LC is the absorption detector. It satisfies all of the conditions outlined above. To be adapted to this scheme, one must use at least two eluents with different molar absorptivities at the wavelength of interest (11, 12). A difficulty is that when the highly absorbing eluent is used, so little light reaches the sensor of the detector that the normal electronics will not function as well. Then, it can be seen that mole fraction (rather than volume fraction) becomes the appropriate unit for concentration. Technical problems not withstanding, the micropolarimeter for LC (64) can be used in conjunction with optically active eluents and a nonchiral analogue (6). The differential measurement is essentially accomplished by setting the appropriate mechanical null for the analyzer. Applying the scheme with micropolarimetry detection is particularly useful, since both

chromatograms used in the calculations are entirely correlated with respect to elution properties for an achiral stationary phase.

It is particularly interesting to apply this scheme to gel permeation chromatography, where almost all eluents produce the same chromatogram. The molecular size information in the chromatogram can be used in conjunction with the volume fraction determined here to give a count of the molecules. This concept should work even for poorly resolved chromatograms (fairly continuous distribution of molecular sizes), by using Equation 16 for each well-defined "slice" of the chromatogram. In the characterization of polymers or of fossil fuels, this is valuable new information. All these can be performed using analytical scale LC, with instrumentation that is available in most analytical laboratories.

The concepts of predicting the elution order for a series of unknown peaks in three chromatograms (10) will be discussed next. This will be followed by the application of this absolute quantitation scheme in the development of procedures for the analysis of motor oils (16) and crude oils (17).

Conclusion

A concept has been presented in a mathematical form based upon known principles of refractive index detection in LC. The concept has been developed into a method that allows quantitation of eluting species in LC without prior identification. Possible applications of this method were discussed.

CHAPTER 3.

CORRELATION OF ELUTION ORDERS IN DIFFERENT LIQUID CHROMATOGRAPHIC SYSTEMS WITHOUT ANALYTE IDENTIFICATION

Introduction

The use of high performance liquid chromatography for the analysis of complicated mixtures of organic substances is a common occurrence. In some cases the analyst has previously identified the analyte or analytes of interest before doing any chromatography. Usually this is not the case. It is more likely that an analyst is faced with the task of providing qualitative and quantitative information on a sample with little or no initial information. The problem of providing the information of interest and optimizing the chromatographic separation for routine analyses can become a time consuming and expensive task. When analyte identification has not preceded the chromatography, the implementation of methods such as standard additions or construction of a calibration curve are obviously impossible. In principle, the response of many LC detectors can provide quantitative information simultaneous with the identification. In practice, mass spectrometry (65, 66), infrared spectrometry (67, 68) or nuclear magnetic resonance applied to detection in LC can only provide semi-quantitative information, because analyte identification using any of these techniques alone is still not completely unambiguous.

In the last chapter it was shown that both qualitative and quantitative information about a sample can be obtained from the chromatograms produced by two eluents with different refractive indices (RI) using RI detection. No prior identification of any solutes was necessary. If, however, an analyte mixture produces more than one peak in a chromatogram, it is necessary to know which peaks correlate with the peaks in the other chromatogram. The RI detector gives a response that depends on the RI of the eluent, so the peak areas alone cannot be used directly to determine elution orders. This is unlike the case of an absorption detector, where peak areas for the individual analytes are expected to remain constant for most non-absorbing eluents. To obtain quantitative information, one must either be able to preserve the elution order for the individual analytes when changing eluents, or be able to separately correlate the elution orders in the two eluents. The former approach works in certain cases, such as in gel-permeation chromatograph (16) and in ion chromatography (11, 12). The latter is the subject of this investigation.

It is well known that predictions about elution orders from the same column for an arbitrary set of analytes in different eluents are difficult, except for the cases mentioned above. If different columns are used, the situation is even more serious. This is especially true if the first chromatographic system performs a normal phase separation and the second chromatographic system provides a reversed phase separation. In the process of optimizing the chromatographic

conditions for an unknown sample, the analyst is thus faced with the difficult task of following the retention behaviors of each of the unidentified components using different columns and different eluents. This then is another reason for developing some scheme to correlate the observed elution orders from different chromatographic systems without analyte identification.

Theory

The correlation scheme for determining the elution orders for a sample consisting of N analytes in two different eluents (regardless of the columns used) is based on obtaining the chromatogram of the same sample in a third eluent (regardless of the column used). To use the RI detector, this third eluent should have an RI different from those of the first two eluents. It is assumed that the N chromatographic peaks obtained in each of the three eluents are resolved well enough to obtain areas for each peak, by deconvolution if necessary. If the peaks are poorly resolved in either one of the first two eluents, the particular eluent-column combination will not be useful for studying that sample anyway. If the peaks are poorly resolved in this third eluent, one can find a different eluent-column combination that gives better separation. It has been shown (15, 16) that if the correct elution orders are known, then any two of these chromatograms will provide enough information to predict the peak areas in the third, or any other, chromatogram. This is because the two chromatograms can be used to calculate, without analyte

identification, the concentration and the RI of each component in the sample. This information can then be used to predict the response of each of the components in an arbitrary third eluent. So, the unknown elution order in the third eluent can be determined simply by matching up the peak areas found experimentally and the predicted peak areas. However, if the elution orders are not known in either of the first two eluents, there can then be a total of N! possible combinations of predictions from the first two chromatograms. The idea then is to find the one combination out of the N! combinations that best predicts the third chromatogram with respect to the individual peak areas, with the help of some least-squares criterion. Thus, one relies on achieving consistency in the quantitative information among the assigned elution orders in the three chromatograms to arrive at the best choice, without requiring analyte identification. Note that peak areas are used rather than peak heights because they reflect the total amount of each component injected, independent of differences in the retention times, the efficiencies of the columns, and the flow rates used for the three separations.

It was shown in the previous chapter that to obtain quantitative information, one does not even need to independently determine the RIs of the eluents or the actual response factor of the detector, if two "calibrating" substances A and B of known amounts V (volume fraction) can be eluted from the chromatographic system under the same conditions that produced the three chromatograms. The response S_1^A in arbitrary area units, of substance A in eluent 1 is given by

$$S_1^A K_1 = V\ (F_A - F_1) \tag{19}$$

where K_1 is a constant that contains the RI and the flow rate of eluent 1 and the conversion factor relating S to the real RI units, and $F_i \equiv (n_i^2-1)/(n_i^2+2)$ is a function of the RI of the material i. By successively obtaining the responses of the two calibrating substances in the three eluents, one has six expressions of the form in Equation 19. One can show that

$$\frac{K_2}{K_1} = \frac{S_1^A - S_1^B}{S_2^A - S_2^B} \tag{20}$$

and

$$\frac{K_2}{K_3} = \frac{S_3^A - S_3^B}{S_2^A - S_2^B} \tag{21}$$

Note that this "calibration" need only be performed once for a given eluent at a given operating condition. Now, for any one of the analytes in the sample, its concentration, V_x (volume fraction), can be calculated from its peak areas in any pair of chromatograms, so

$$V_x = V\left[\frac{S_1^x - S_2^x\ (K_2/K_1)}{S_1^A - S_2^A\ (K_2/K_1)}\right] \tag{22}$$

or

$$V_x = V\left[\frac{S_3^x - S_2^x\ (K_2/K_3)}{S_3^B - S_2^B\ (K_2/K_3)}\right] \tag{23}$$

Combing Equations 22 and 23, one can then predict the peak area observed for this analyte in the third eluent, $S_3^{x'}$, from its peak areas in the other two eluents, S_1^x and S_2^x. The result is

$$S_3^{x'} = (aS_1^x + bS_2^x)/c \tag{24}$$

where $a = S_2^A S_3^B - S_2^B S_3^A$

$b = S_1^B S_3^A - S_1^A S_3^B$

and $c = S_2^A S_1^B - S_1^A S_2^B$

For the N peaks in each of the first two eluents, there is then a total of N^2 possible predicted areas according to Equation 24, arranged in N! distinct combinations. These predictions are obtained without analyte identification, and without knowing any physical property of the analytes, the eluents, and the calibrating substances. Now, each of these N! combinations can be tested against the experimentally observed third chromatogram, with areas S_3^x for each of the peaks, by a least-squares criterion. Since the choice is ordinal, each peak should contribute equally to the decision making regardless of its magnitude. It is thus appropriate to weigh the squares of the residuals, $[S^{x'} - S^x]^2$, by the estimated variances for the predicted area, $\sigma^2_{Sx'}$, and for the experimental area, σ^2_{Sx}, before applying the least-squares criterion (69). These estimated variances

can be obtained if multiple chromatograms are available for each eluent so that each S value has associated with it an experimentally determined variance. The variance for the predicted area can be calculated from the individual variances of each of the terms in Equation 24 by considering the statistical propagation of errors (70), and is given in Appendix 1. The result is that, for each of the N! combinations, one can calculate a relative standard deviation for the fit, given by

$$\sigma_{INST} = \frac{1}{(\Sigma|S^X|)} \sqrt{\frac{\Sigma \frac{1}{\sigma^2_{S^{X'}} + \sigma^2_{S^X}} (S^{X'} - S^X)^2}{(N-2)\ \Sigma \frac{1}{\sigma^2_{S^{X'}} + \sigma^2_{S^X}}}} \qquad (25)$$

where the sums are over all peaks in the chromatogram. The number of degrees of freedom is (N-2) because both $S^{X'}$ and S^X are estimates of the "true" values in the chromatogram. The subscript INST denotes this method of weighting, commonly called instrumental weighting. When experimental variances are not available, for example, when only one trial is used, one can use statistical weighting (69), that is, the weights are the reciprocals of the squares of the individual areas. The implication is that the standard deviation of a given peak is proportional to its magnitude. Thus,

$$\sigma_{STAT} = \frac{1}{(\Sigma|S^X|)} \sqrt{\frac{\Sigma \left(\frac{2}{|S^{X'}|+|S^X|}\right)^2 (S^{X'} - S^X)^2}{(N-2)\Sigma \left(\frac{2}{|S^{X'}|+|S^X|}\right)^2}} \qquad (26)$$

The least-squares criterion simply requires that the sum of squares of the residuals, appropriately weighted, be minimized. In other words, the relative standard deviation calculated either from Equation 25 or 26 should be minimized. This then produces a unique choice among the N! combinations of elution orders as the one that is the most consistent for all three chromatograms. This set of elution orders can then be taken as the "correct" set for describing the N analytes in the three chromatographic systems. Once the correct elution order is found, quantitation of each component following Equation 22 or 23 is straightforward. One can also proceed to calculate the refractive index of each of the N components, as given by Equation 17 in Chapter 2, since

$$F_x = \left[F_2 \left(\frac{S_1^x K_1}{S_2^x K_2} \right) - F_1 \right] \Bigg/ \left[\left(\frac{S_1^x K_1}{S_2^x K_2} \right) - 1 \right] \qquad (27)$$

Naturally, one needs to associate some level of confidence with the chosen elution order as derived from minimizing either Equation 25 or 26. That is, how good is the choice with the minimum σ compared to that with the next smallest σ? One can think of σ as simply a quantity derived from the set of all experimental measurements, namely, the 3N peak areas. It is thus possible to use standard techniques for propagation of errors to determine the variations in σ as a function of uncertainties in the individual area measurements. To a first approximation, one can consider the weighting factors in

either Equation 25 or 26 to be constants. This greatly simplifies the calculations, so that one obtains an estimate of the uncertainty in the σ values as derived in Appendix 1, with

$$\sigma(\sigma) = \left[\left(\frac{2}{N-2}\right) \frac{\Sigma w^2(\sigma_S^2 x' + \sigma_S^2 x)\ (S^{x'} - S^x)^2}{(\Sigma w^2\ (S^{x'} - S^x)^2)(\Sigma w^2)\ (\Sigma|S^x|)^2}\right]^{1/2} \tag{28}$$

The weighting factors, w, are $1/(\sigma_S^2 x' + \sigma_S^2 x)$ for $\sigma(\sigma_{INST})$ and $4/(|S^{x'}|+|S^x|)^2$ for $\sigma(\sigma_{STAT})$ respectively. Assuming normal Gaussian distribution of errors, this means that since each experimental area has a 68% chance for being within the range of $S^x \pm \sigma_S x$ in any particular trial, the value of σ in either Equation 25 or 26 also has a 68% chance for being within the range of $\sigma \pm \sigma(\sigma)$. If the best choice and the second-best choice, according to the summed least squares of the residuals, are separated by an amount equal to $\sigma(\sigma)$, there is better than a 76% chance that this particular ranking of the σ's will be preserved in future experiments. The probability can be calculated explicitly following the procedure given in Appendix 1. The chosen elution order has associated with it a 76% or better confidence level. Similarly, if the two best choices have σ's separated by $2\sigma(\sigma)$, one can show that the confidence level of the choice is better than 92%.

Finally, there are two additional checks for the chosen elution order, although neither can be used independently to provide a clear choice among the N! possible elution orders. First, the total area

calculated from Equation 24 for all peaks in the third chromatogram should equal the total experimental area so that the entire area is accounted for. One can define

$$r = \frac{\Sigma|S^{x'}|}{\Sigma|S^{x}|} \tag{29}$$

Ideally, r should equal unity. Second, one can calculate the analogue of a correlation coefficient (70) as the ratio of the experimental deviations from the best-fit to the combined variances of the predicted areas and the experimental areas. So,

$$R = \sqrt{\frac{\Sigma(\sigma^2_{Sx'} + \sigma^2_{Xx})}{\sigma^2_{NW}}} \tag{30}$$

where σ^2_{NW} is the unweighted sum of the squares of the residuals, given by

$$\sigma_{NW} = \sqrt{\frac{\Sigma(S^{x'} - S^{x})^2}{N-2}} \tag{31}$$

Equation 20 tells whether the lack of fit is fully explained by the uncertainties in the predicted and the experimental areas. If R is larger than unity, the fit is better than the experimental uncertainties. If R is smaller than unity, the fit is worse than is expected from the experimental uncertainties. These two additional checks can be used to decide whether there exists some unusual

problems with the chromatograms, such as some components not eluting off the column or that one has N peaks for a sample with more than N components, some of which are not resolved.

Experimental

All reagents and eluents used were reagent grade with no further purification. Three chromatographic systems were employed. A high pressure pump (ISCO, Lincoln, NE, Model 314), a 1-μL sample loop at a conventional injection valve (Rheodyne, Berkeley, CA, Model 7410), and a commercial RI detector (Waters Associates, Milford, MA, Model R401) with the reference cell used in the static mode filled with the eluent being used, were used in all three chromatographic systems. The differences are in the columns and eluent composition. The first system used a 25 cm x 4.6 mm, 5 μm, silica column (Anspec, Warrensville, IL) and an eluent composed of 99.8% toluene and 0.2% methanol by volume. The second system used the same column as the first system while the eluent was composed of 99.8% n-butylchloride and 0.2% methanol by volume. The third system used a 25 cm x 4.6 mm, 10 μm, C_{18} column (Anspec, Warrensville, IL) and an eluent composed of 60% distilled and deionized H_2O and 40% CH_3CN by volume.

RI values for the eluents are as follows: n(toluene/methanol) = 1.4936, n(n-butylchloride/methanol) = 1.4009, and n(60% H_2O/40% CH_3CN) = 1.3443. These RI values were calculated by considering literature n_D^{20} values and the theory in Chapter 2. The first system operated at an eluent flow rate of 1.00 mL/min. The second system had a flow rate

of 0.67 mL/min., and the third system was operated at 1.09 mL/min. Mixtures, for the analysis, with specified volume fractions were made by pipetting volumes of each component.

The output of the RI detector (10 mV full scale) was connected to a digital voltmeter (Keithley, Cleveland, OH, Model 160B), the analog output of which was in turn connected to a computer (Digital Equipment, Maynard, MA, Model PDP 11/10 with a LPS-11 laboratory interface). The computer took readings every 0.05 s, and averaged each set of 10 before storing the information. The peaks in each chromatogram were, then, baseline adjusted via software before integration to produce peak areas or integrated response values. All areas were determined using multiple injections (three or more). Linearity of the detector had been previously confirmed over the attenuation settings used in this study (32X to 2X). The computer was used in all calculations pertaining to the correlation scheme used. Basically no time delay was observed for the calculations necessary to do the correlation with N=4 peaks in three chromatograms, although the computer time should increase at roughly an N! rate.

Results and Discussion

To test this correlation procedure, the three eluent-column combinations were chosen to provide a range of RIs and different separation mechanisms. The former is necessary to retain significance in the subtractions in Equations 22 and 23. The latter results in at least some scrambling of the elution orders to simulate real

situations. The first step is to use calibrating substances A and B to standardize the three chromatographic systems. The chemicals p-anisaldehyde (n_D^{20} = 1.5730) and ethylacetate (n_D^{20} = 1.3724) were chosen because of their very different RI values, again to assure significance in the calculations. The observed areas are tabulated in Table 4. The σ_S values are determined from the individual set of repeated injections (≥ 3).

Two mixtures of four components each are used to test the correlation scheme. The four components chosen are chloroform (n_D^{20} = 1.4458), benzaldehyde (n_D^{20} = 1.5463), 3-pentanone (n_D^{20} = 1.3924), and tetrahydrofuran (n_D^{20} = 1.4050). These provide a large variation of RIs, as well as a small difference in RI for two of the components. An equal-volume mixture, I, allows an evaluation of the case in which two components have similar RIs and are at similar concentrations. Another mixture, II, consists of the same components at different concentrations, chosen so that the peak areas in one of the eluents are quite close to one another. These four components are well separated in each of the three chromatographic systems. To show the separation in the three chromatographic systems, chromatograms for mixture II were reconstructed from the experimental retention times and experimental peak-widths, and plotted on the same scale expansion (8X). These are shown in Figure 2. As indicated, chromatogram 3 has peak areas that are quite similar for all four components. Also, the area of the fourth peak in chromatogram 2 was

Table 4. Experimental results for the calibrating substances

Sample[a]	$S(x10^3)$[b]	$\sigma_S(x10^3)$[b]
S_1^A	230.0	1.9
S_1^B	-474.0	9.8
S_2^A	773.0	4.9
S_2^B	-199.0	1.4
S_3^A	610.0	4.1
S_3^B	103.0	0.7

[a]A, anisaldehyde; B, ethylacetate; 1, toluene; 2, n-butylchloride; 3, 60:40 H_2O:CH_3CN. 1.0 µL injected in each case.

[b]Integration interval - 0.5s; full scale on 8x attenuation = 2048 units.

Figure 2. Reconstructed chromatograms showing the separation of the four components in mixture II in the three eluents 1, toluene; 2, n-butylchloride; 3, 60:40 H_2O:CH_3CN.

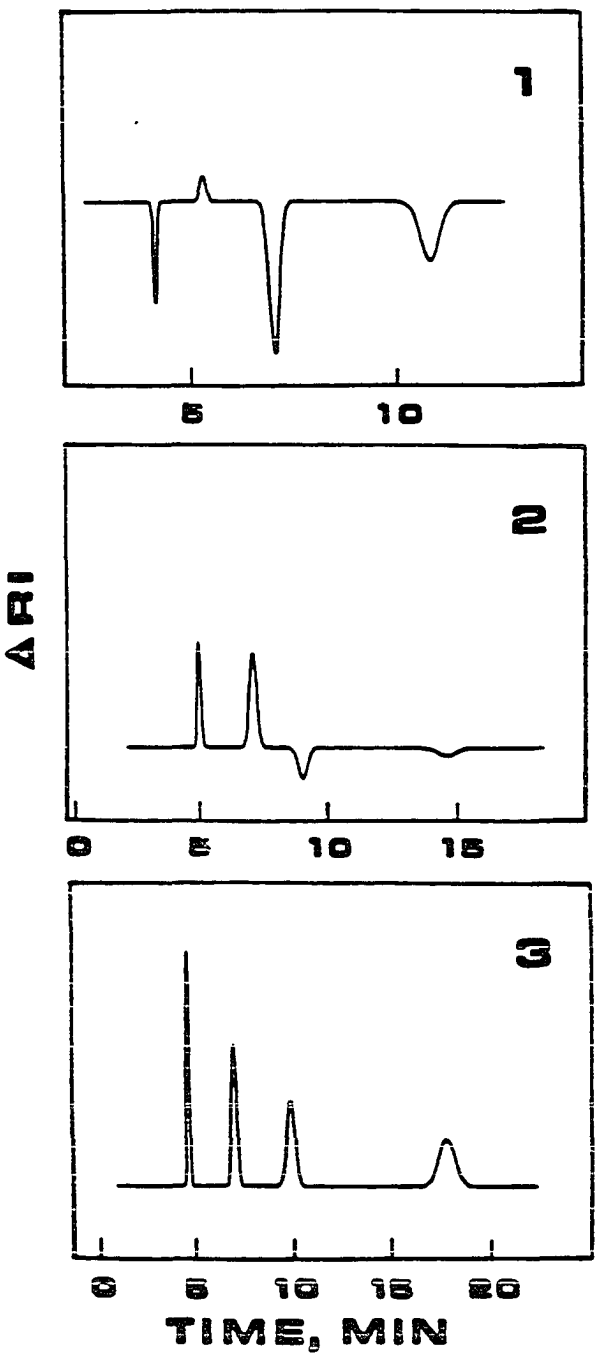
1
5
10
2
ΔRI
0
5
10
15
3
0
5
10
15
20
TIME, MIN

actually measured with reasonable precision because a different scale expansion was used during data acquisition. The experimentally determined areas for each peak in the three eluents are listed in Table 5 for mixture I and in Table 6 for mixture II, together with the corresponding standard deviations for the multiple trials. These data are listed with the particular analyte because the true elution orders have been determined by independent experiments. Naturally, the areas are simply indexed 1 through 4 in their order of elution in that particular chromatographic system when they are used in the correlation calculations.

With these results one can proceed to use Equation 24 to form the N^2 possible area predictions arranged in N! different elution orders. For each of these possible elution orders, one can calculate the relative standard deviation of the fit with either instrumental weighting, Equation 25, or with statistical weighting, Equation 26, and even the corresponding uncertainties in these relative standard deviations, Equation 28. The two additional parameters r and R from Equations 29 and 30 can also be calculated. These are tabulated in Table 7 for mixture I and in Table 8 for mixture II. Since any two of the three chromatograms for each mixture can be used to predict the areas in the third chromatogram, results are included for the three possible choices for the first two eluents. Only the three best fits in each case, as dictated by σ_{INST} and by σ_{STAT}, of the N! combinations are tabulated.

Table 5. Experimental results for mixture I

Eluent[a]	Analyte[b]	$S(x10^3)^c$	$\sigma_s(x10^3)^c$
1	1	-42.7	0.64
1	2	39.1	0.94
1	3	-91.7	1.16
1	4	-78.5	4.2
2	1	52.4	0.73
2	2	164.8	1.43
2	3	-18.8	0.73
2	4	-10.2	1.16
3	1	68.6	1.00
3	2	134.1	0.50
3	3	37.9	0.25
3	4	41.2	0.63

[a]1, toluene and silica column; 2, n-butylchloride and silica column; 3, 60:40 H_2O:CH_3CN and C_{18} column.

[b]1, chloroform; 2, benzaldehyde; 3, 3-pentanone; 4, tetrahydrofuran. 0.25 μL of each injected.

[c]Integration interval - 0.5 s; full scale on 8x attenuation = 2048 units.

Table 6. Experimental results for mixture II

Eluent[a]	Analyte[b]	$S(x10^3)^c$	$\sigma_s(x10^3)^c$
1	1	-34.6	0.43
1	2	14.8	1.14
1	3	-153.6	3.26
1	4	-93.2	8.4
2	1	42.5	0.84
2	2	66.5	0.44
2	3	-30.1	1.21
2	4	-11.9	0.90
3	1	55.3	0.23
3	2	52.9	0.57
3	3	62.4	1.32
3	4	49.5	0.74

[a]1, toluene and silica column; 2, n-butylchloride and silica column; 3, 60:40 H_2O:CH_3CN and C_{18} column.

[b]1, 0.20 µL of chloroform; 2, 0.10 µL benzaldehyde; 3, 0.40 µL of 3-pentanone; 4, 0.30 µL of tetrahydrofuran.

[c]Integration interval - 0.5 s; full scale on 8x attenuation = 2048 units.

Table 7. Results of least-squares fit for mixture I

Eluents[a]	Rank of fit	σ_{INST}[b]	$\sigma(\sigma_{INST})$[c]	σ_{STAT}[d]	$\sigma(\sigma_{STAT})$[c]	R[e]	r[f]
X	1	1.43	0.35	0.91	0.31	0.64	1.04
X	2	1.80	0.37	1.76	0.59	0.47	1.04
X	3	4.23	0.33	3.68[g]	0.35[g]	0.17	1.04
Y	1	1.70	0.41	0.68	0.77	0.64	0.95
Y	2	1.74	0.41	0.71	0.60	0.63	0.95
Y	3	4.94	0.39	1.76[g]	0.31[g]	0.17	0.85
Z	1	2.64	0.60	2.98	0.69	0.63	0.96
Z	2	2.71	0.62	2.98	0.69	0.63	0.96
Z	3	13.4	0.55	12.8	0.53	0.15	1.08

[a]The eluents are respectively 1 -toluene, 2 - n-butylchloride, and 3 - 60:40 H_2O:CH_3CN. X - areas in 1 and 2 used to predict area in 3; Y - areas in 1 and 3 used to predict area in 2; and Z - areas in 2 and 3 used to predict area in 1.

[b]Equation 25.

[c]Equation 28.

[d]Equation 26.

[e]Equation 30.

[f]Equation 29.

[g]A different combination compared to σ_{INST} was chosen.

Table 8. Results of least-squares fit for mixture II

Eluents[a]	Rank of fit	σ_{INST}[b]	$\sigma(\sigma_{INST})$[c]	σ_{STAT}[d]	$\sigma(\sigma_{STAT})$[c]	R[e]	r[f]
X	1	1.82	0.37	1.52	0.58	0.96	1.06
X	2	2.65	0.37	4.91[g]	0.48[g]	0.31	1.06
X	3	6.16	0.46	5.20[g]	1.44[g]	0.29	1.06
Y	1	1.83	0.58	1.62[g]	2.33[g]	0.66	1.07
Y	2	1.97	0.62	1.82[g]	2.07[g]	0.77	1.04
Y	3	2.28	0.58	1.91[g]	2.07[g]	0.51	1.07
Z	1	1.53	0.46	0.57	0.23	0.65	0.93
Z	2	1.60	0.49	0.75[g]	0.25[g]	0.76	0.96
Z	3	1.91	0.46	1.06[g]	0.49[g]	0.51	0.93

[a]The eluents are respectively 1 -toluene, 2 - n-butylchloride, and 3 - 60:40 H_2O:CH_3CN. X - areas in 1 and 2 used to predict area in 3; Y - areas in 1 and 3 used to predict area in 2; and Z - areas in 2 and 3 used to predict area in 1.

[b]Equation 25.

[c]Equation 28.

[d]Equation 26.

[e]Equation 30.

[f]Equation 29.

[g]A different combination compared to σ_{INST} was chosen.

Since there is only one correct set of elution orders, it should not matter in principle which two of the three chromatograms are used to predict the third. This is evident in Table 7, where the choice giving the smallest σ_{INST} for each eluent combination refers to the identical set of elution orders is always chosen. These are also the true elution orders. One has to be more careful, however, in making such interpretations. For example, the tabulated $\sigma(\sigma)$ values imply that both σ_{INST} and σ_{STAT} for the 4th vs. 5th entry, and for the 7th vs. 8th entry, are really not significantly different. For eluent combinations (Y) and (Z), one therefore has insufficient grounds to decide whether the lowest σ or the second lowest σ should be chosen to represent the best set of elution orders. It is therefore fortuitous that the correct elution orders were also predicted by eluent combinations (Y) and (Z). A clearer choice results from eluent combination (X), where one finds that the 1st and 2nd entries are separated by about one $\sigma(\sigma)$ for σ_{INST} and even better for σ_{STAT}. One can pick the elution order corresponding to the lowest σ_{INST} with 76% confidence, as discussed above. In examining the third lowest σ for each eluent combination, one finds that the values are all separated from the second lowest σ by several $\sigma(\sigma)$'s. One can then reject the third and higher choices in each case as being correct with at least 99.9% confidence. As expected, the top two choices in each eluent combination correspond to interchanging the assigned elution order for components 3 and 4, which have nearly identical RIs and identical

concentrations. Note that for the 6th entry, the two σ's did not produce the same ranking. In general, if experimental σ_S values are available, one should rely on σ_{INST}. σ_{INST} is used only if single chromatograms are obtained, or if there is a reason to believe the uncertainties are proportional to the magnitudes of S. The bottom line is that one should use only the first entry in Table 7, based on σ_{INST} and $\sigma(\sigma_{INST})$, for a correlation of the elution orders at a 76% confidence level.

Table 8 provides a much more difficult case for testing the correlation scheme, because of the proximity of the areas in one chromatogram. For eluent combination (X), the two smallest σ_{INST} are separated by about two times $\sigma(\sigma)$. One can thus choose this particular elution order with 92% confidence. If one examines the other two eluent combinations, it is not even possible to distinguish among the top three choices in each case based on the $\sigma(\sigma)$ values. In fact, many other choices (not tabulated) beyond the the first three are also less than one $\sigma(\sigma)$ away from the minimum value. Therefore, the only valid prediction is offered by the eluent combination (X), which also corresponds to the correct elution order as determined independently. All of the tabulated choices in Table 8 for eluent combinations (Y) and (Z) were incorrect elution orders. The point of interest is that the overall smallest σ is not necessarily the one corresponding to the best choice. One must be able to establish a

confidence level for the choice, which may mean trying each combination of the two "predicting" eluents until a reasonable confidence level is achieved in one of them.

A qualitative explanation can be given as to why in this particular sample the eluent combination of (X) used for prediction seems to outperform the others in the correlation scheme. An examination of the raw data shows that the data obtained in eluent 3 for either mixture are overall more precise than those in the other eluents. In calculating the residuals in Equation 25 or 26 it is better to have a precise, and thus presumably more accurate, value for one of the terms, namely S_X, rather than to have the precision (and accuracy) of this data set diluted when it is incorporated into the $S^{X'}$ term.

The value of R in Equation 30 is not a true correlation coefficient, but does give an indication of the "accountability" of the errors. The value is always positive, and can be larger than unity. Tables 7 and 8 show that R alone cannot be used to determine the elution order. However, the better fits all show a reasonable value for R of the order of unity. The value of r in Equation 29 accounts for all the areas observed in the third chromatogram. Tables 7 and 8 show that for the best fits, the areas are properly accounted for, and that one did not "lose" area by having some material not eluting in the third chromatographic system, and did not "gain" area by eluting some extra components off the column.

After the elution orders are determined, the concentration of each component can be calculated from Equation 22, and its RI can be calculated from Equation 27. These are tabulated in Table 9. The "true" volumes are also listed there and the literature RI values were given earlier in this section. One should note that the RIs here are measured at a wavelength of 520 nm because of the particular instrument. The comparison with literature values is only appropriate if one assumes that the RIs of the analytes and of the eluents can linearly extrapolated from their Na-D line values. The tetrahydrofuran volumes are somewhat low, and may be related to non-ideal solutions, as evidenced by heat produced when the mixtures are prepared. Good agreement is indicated therefore in all cases.

This procedure was repeated for a third mixture consisting of benzaldehyde, methylacetate, methylethylketone, and cyclohexanone in the same three chromatographic systems. In normal-phase LC, this was the elution order. In reversed-phase LC, benzaldehyde became the last component to elute while the others maintained their order of elution. This correlation scheme works even in this case with some scrambling of the peaks. The other findings are about the same as in mixtures I and II. There, the precision of the three chromatograms were about the same, and the level of confidence in the least-squares choice of elution orders turns out to be about the same regardless of which eluent pair is used for the predictions.

Table 9. Correlation results and calculated parameters

Analyte	Predicted elution order[a]			Calculated Volume (μL)	True Volume (μL)	Calculated[b] RI
	Eluent 1	Eluent 2	Eluent 3			
Mixture I						
Chloroform	1	1	4	0.25	0.25	1.4437
Benzaldehyde	2	2	3	0.24	0.25	1.5412
3-pentanone	3	3	2	0.24	0.25	1.3854
Tetrahydrofuran	4	4	1	0.22	0.25	1.3916
Mixture II						
Chloroform	1	1	4	0.20	0.20	1.4438
Benzaldehyde	2	2	3	0.10	0.10	1.5367
3-pentanone	3	3	2	0.40	0.40	1.3861
Tetrahydrofuran	4	4	1	0.26	0.30	1.3918

[a]These are also the correct elution orders.

[b]Assuming $n_1 = 1.4936$ and $n_2 = 1.4009$.

It is useful to discuss the limitations of this correlation procedure. First, if the values of the peak areas in each chromatographic system are separated by more than the individual precisions, σ_S, and if precision i implies accuracy, one can expect to arrive at a reliable correlation at a high confidence level. The more different the peak areas are from each other, the higher is the confidence level of the correlation. Note that similar areas will be produced by substances with both similar concentrations and similar RIs, such as the last two entries in Table 5. However, similar areas can also be produced by fortuitous combinations of substances with different concentrations and different RIs, such as the last four entries in Table 6. To obtain the initial correlation in three eluents, their RIs must be quite different to allow Equation 24 to become significant. Once the initial correlation is obtained, however, any two of these chromatograms can be used to predict the areas, and thus correlate the elution order, in an arbitrary fourth eluent, regardless of its RI. This is because one no longer needs to go through N! combinations. The problem reduces to one for the direct application of Equation 24. To obtain the best quantitative information after the elution orders are determined, one needs only two of the chromatograms. The best choice will be either the pair that is most different in RI (for the best detection limit) or the pair that has the most precisely determined peak areas (for the best precision) while providing a moderate RI difference. When some of the peaks in the chromatograms can be correlated independently, such as

with previously identified analytes, one can eliminate these (mathematically) before using the correlation scheme. This reduces the number N that must be correlated without identification. This is in fact closer to a "real" situation. For the difficult unknown cases, for example, the 4th versus 5th entries in Table 7, one has actually limited the choices to 2!. A more sensitive test for consistency then results, particularly if the experiments can be repeated to produce more precise results for these two analytes in the three eluents.

Conclusion

In summary, a completely objective scheme for correlating elution orders in arbitrary eluents without analyte identification was developed. This should aid in the development of the optimum chromatographic conditions for separating the components in an unknown sample. It also extends the usefulness of the quantitation scheme outlined in Chapter 2 to allow for changes in elution orders in different chromatographic systems.

CHAPTER 4.

QUANTITATIVE GEL-PERMEATION CHROMATOGRAPHY WITHOUT STANDARDS

Introduction

In gel-permeation chromatography (GPC), very often one is dealing with samples that have a distribution of components of varying sizes. This is particularly true in applications to characterize fossil fuels (71) and polymers (72). It is unlikely that complete separation of the components in these samples can be achieved in LC. Still, it is meaningful to obtain a quantitative distribution curve for these samples, for the purpose of characterization. The difficulty is that since the nature of the components is generally not known, concentration standards are not available to calibrate the response of the detectors. One can, therefore, only obtain chromatograms that show an arbitrary response. The only alternative currently practiced involves the use of prep-scale columns and the collection of fractions afterwards (73). By evaporating off the eluent, one can in principle obtain the volume or the weight of sample collected in each fraction. Not only is the procedure tedious and time-consuming, but the results obtained can also be easily influenced by the volatility and the chemical stability of the collected materials. It is thus desirable to develop a procedure to obtain the same information using analytical or micro scale LC.

Theory

It was demonstrated in Chapter 2 that quantitative analysis is possible without analyte identification using HPLC and the refractive index (RI) detector when well-resolved peaks can be obtained for the chromatograms. This concept can be extended to the case of unresolved chromatograms. Very briefly, the procedure is based on the relationship between the RI observed for a mixture (the eluent and the solutes), n, and the individual RIs, n_i

$$\frac{n^2 - 1}{n^2 + 2} = \sum_i V_i \left(\frac{n_1^2 - 1}{n^2 + 2} \right) \tag{32}$$

where V_i is the corresponding volume fraction of each component at the detector. For a well-resolved chromatographic peak (single solute), one can see that the concentrations are, respectively, V_x and $(1-V_x)$ for the solute and the eluent, while the RIs are, respectively, n_x and n_1. Equation 32 then reduces to

$$F_n - F_{n_1} = V_x(F_{n_x} - F_{n_1}) \tag{33}$$

where F is a defined function such that $F_{n_i} \equiv (n_1^2 - 1)/(n_i^2 + 2)$. For all practical levels of concentration in LC, the left hand side in Equation 33 can be simplified for the case of a differential refractometer to give

$$S_1K_1 = V_x(F_{n_x} - F_{n_1}) \tag{34}$$

where S_1 is the integrated response (peak area) for the analyte in eluent 1 and K_1 is a constant for the conditions used with eluent 1, including the eluent flow rate, the integrating interval, the scale expansion used at the detector, and the RI of the eluent. If the same sample is then eluted with a different eluent, that is, one having a different RI of n_2, V_x and F_{n_x} remain constant while a different peak area is obtained, such that

$$S_2K_2 = V_x(F_{n_x} - F_{n_2}) \tag{35}$$

where 2 indicates parameters relevant to eluent 2. Equations 34 and 35 together allow unique values of V_x and F_{n_x} to be obtained. The concentration of the analyte is thus determined without analyte identification.

It was shown in Chapter 2 that it is not necessary to know even n_1 or n_2 if only V_x is to be determined. This is done by obtaining the chromatographic peak areas when known concentrations of each eluent are used alternately as samples in the other eluent. This eliminates contributions due to uncertainties in the experimental parameters, as long as those remain fixed throughout. In GPC, however, the eluents are usually of low molecular sizes and may not conveniently elute as samples in each other. In such cases, one can use two additional compounds, with RIs n_3 and n_4, to obtain two more sets of areas in the same two eluents. So,

$$S_3K_1 = V_3(F_{n_3} - F_{n_1}) \tag{36}$$

$$S_4K_2 = V_3(F_{n_3} - F_{n_2}) \tag{37}$$

$$S_5K_1 = V_4(F_{n_4} - F_{n_1}) \tag{38}$$

$$S_6K_2 = V_4(F_{n_4} - F_{n_2}) \tag{39}$$

It is more convenient, but not necessary, to use the same concentration V for these two compounds, so that $V = V_3 = V_4$. Doing this Equations 36 through 39 give

$$\frac{K_2}{K_1} = \frac{S_3 - S_5}{S_4 - S_6} \tag{40}$$

Now, Equations 36 and 37 give

$$\frac{F_{n_2} - F_{n_1}}{K_1} = \frac{S_3 - (K_2/K_1)S_4}{V} \tag{41}$$

And, Equations 34 and 35 give

$$\frac{F_{n_2} - F_{n_1}}{K_1} = \frac{S_1 - (K_2/K_1)S_2}{V_x} \tag{42}$$

Combining Equations 40 through 42, the final result is

$$V_x = V \left[\frac{S_1 - S_2 \left(\frac{S_3 - S_5}{S_4 - S_6}\right)}{S_3 - S_4 \left(\frac{S_3 - S_5}{S_4 - S_6}\right)} \right] \tag{43}$$

Equation 43 implies that quantitative determination is possible without knowing any of the properties of the eluents, the analyte, or the two "calibrating" compounds. The only requirements are that the two RIs n_3 and n_4 are quite different, so that $(S_3 - S_5)$ and $(S_4 - S_6)$ can both be determined with good precision, and that the two RIs n_1 and n_2 are quite different (but not necessarily different from n_3 or n_4), so that the subtractions in the numerator and in the denominator of Equation 43 can retain significance. Note that S_3 and S_6 need only be determined once for a given set of eluents 1 and 2.

If now one can independently obtain the values n_1 and n_2, the RI of the analyte, n_x, can be determined. This is because Equations 34, 35 and 40 give

$$\frac{F_{n_x} - F_{n_1}}{F_{n_x} - F_{n_2}} = \frac{S_1 K_1}{S_2 K_2} = \frac{S_1}{S_2}\left(\frac{S_4 - S_6}{S_3 - S_5}\right) \tag{44}$$

The function F_{n_x} can then be solved for in terms of the peak areas and the functions F_{n_1} and F_{n_2}.

When several components, x, y, z, etc., coelute at a given point in the chromatogram, one notes that V_x, V_y, V_z, etc., represent their individual concentrations, and $(1 - V_x - V_y - V_z - \ldots)$ represents the concentration of the eluent. Using the same procedure above, one obtains an expression identical to Equation 43 except that the left hand side is replaced by $(V_x + V_y + V_z + \ldots)$. The total concentration is then determined for that point in the chromatogram.

Equation 44 can still be used, but the calculated refractive index becomes the concentration-weighted RI of all components at that point.

The above procedure requires that the chromatograms in the two different eluents be correlated, so that the correct set of peak areas is used for the calculations. The problem is simplified in GPC, where separation depends on the sizes of the analyte molecules and is relatively independent of the eluent used. Even though the chromatograms are not necessarily totally resolved, the elution order is retained. One can then correlate each slice of the two chromatograms and apply Equations 43 and 44. In what follows, a study of the distribution of components in motor oils using GPC and this scheme is presented.

Experimental

All reagents and eluents used were reagent grade materials without further purification. The chromatographic system used was conventional, and consisted of a metering pump (Micrometrics, Norcros, GA, Model 750), a 30 cm x 4.6 mm, 100 Å, 5-μ PL gel permeation column (Anspec, Warrensville, IL), a 1-μL sample loop at a conventional injection valve (Rheodyne, Berkeley, CA, Model 7410), and a commercial RI detector (Waters Associates, Milford, MA, Model R401) with the reference cell used in the static mode filled with the eluent being used. A flow rate of 0.67 mL/min was used throughout. Solutions with

specified volume fractions were made by pipetting well-defined volumes of the minor component into a volumetric flask, and then filling to mark with the major component.

The output of the RI detector (10 mV full scale) was connected to a digital voltmeter (Keithley, Cleveland, OH, Model 160B), the analog output of which was in turn connected to a computer (Digital Equipment, Maynard, MA, Model PDP 11/10 with LPS-11 laboratory interface). The computer took readings every 0.05 s, and averaged each set of 10 before storing the information. These numbers then represented the areas (S values) for each 0.5 s of elution time. All areas were determined using multiple injections (three or more) and were found to be reproducible to ±2.5% (relative standard deviation). Linearity of the detector was independently confirmed by the analysis of a series of samples at successive dilutions.

Results and Discussion

It is important to first establish the optimum experimental conditions. The two eluents should be chosen to have significantly different RIs but similar chromatographic properties. A consideration of the solubility parameters, δ, for the eluents recommended by the manufacturer of the column shows that tetrahydrofuran (THF) and benzene are good candidates. The nature of the neutral polystyrene/divinylbenzene particles in the PL-gel columns provides a minimum of adsorptive and other interactions in addition to the desired molecular-size selectivity. The similarity in δ for benzene

and THF further guarantees closely matching interactions, if any. To test this, a mixture of phthalate esters (Supelco, Bellefonte, PA, Kit 606-N) was used to establish retention volumes, V_R, in each eluent. The molecular weights and the densities of these esters (74) allows one to derive the molar volumes, V_M, for each of them. The results are

$$\text{Benzene:} \quad \log V_M = -0.0894\ V_R + 4.352 \tag{45}$$

$$\text{THF:} \quad \log V_M = -0.1044\ V_R + 4.582 \tag{46}$$

Despite the careful choice of conditions, the retention volumes are not reproduced exactly on changing eluents. The discrepancy can be attributed to slight differences in the degree of swelling of the resins in the two eluents, modifying the effective pore sizes, and probably not the presence of other mechanisms of retention. This is further verified by the close agreement between observed and predicted retention volumes for heptane, bromoethane, and carbon tetrachloride, using Equations 45 and 46. It is expected that for nonpolar substances that form ideal solutions with each of the eluents, the retention volumes will be predicted with reasonable accuracy. Equations 45 and 46 allows one to correlate particular portions of the two chromatograms and allow application of Equations 43 and 44. This could be checked with the procedure described in Chapter 3.

In Figure 3 are shown the RI chromatograms obtained for a sample of synthetic motor oil (AMSOIL, Superior, WI, synthetic 10W-40) in THF

Figure 3. Refractive index gel permeation chromatograms of a synthetic motor oil in (A) THF and (B) benzene as eluents

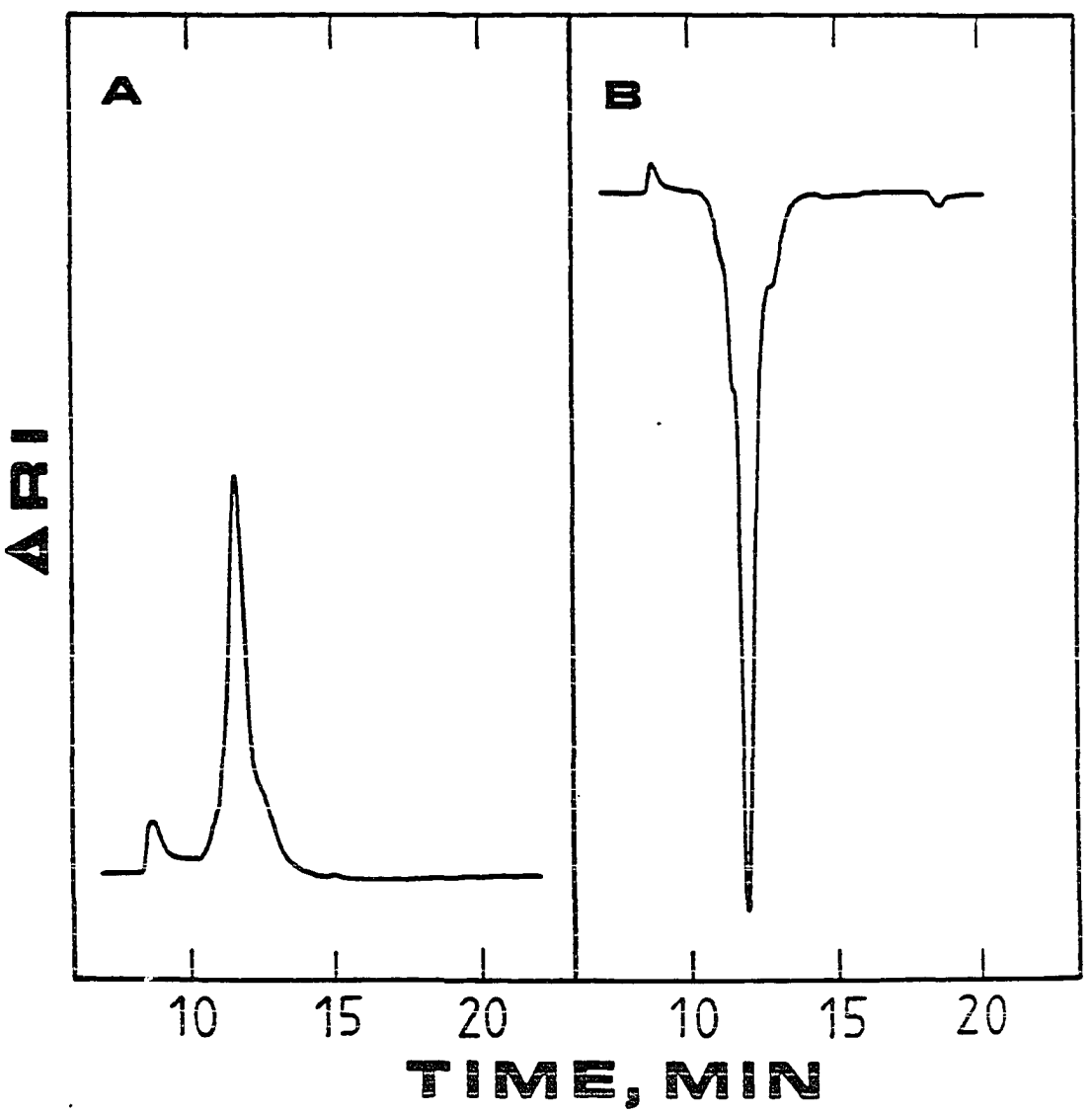
A
B
ΔRI
10
15
20
10
15
20
TIME, MIN

(A) and in benzene (B). The chromatograms show two major features, at 8.7 min and 11.6 min for THF, and at 8.7 min and 11.9 min for benzene. Trials with other natural motor oils (e.g., PENNZOIL, Oil City, PA, multi-vis 10W-40) give similarly reproducible retention times in the two eluents for the major features. This confirms the feasibility of obtaining correlated chromatograms in two different eluents for these samples. It is interesting to note that the main features in most of these chromatograms appear around 10 min., or a retention volume of 6.7 mL. This is the retention volume at which Equations 45 and 46 give the same V_M. In other words, molecules eluted in this region are expected to show the least variations in retention volumes in the two eluents. Little error is introduced if one assumes that a given component of the sample has identical elution volumes in each of the two eluents.

To provide the values S_3 through S_6, samples of known concentrations V_3 and V_4 of heptane and α-chloronaphthalene, respectively, were used. These were chosen based on the large difference in RI for the two compounds. Using Equation 40 it was found that the experimental conditions correspond to a value of K_2/K_1 = 1.044. As a check, Equation 43 was used for samples of known concentrations of CCl_4, (bis(2-ethylhexyl)-phthalate, butylbenzylphthalate, and dimethylphthalate, and an average accuracy of 3.7% was obtained, which can be attributed to uncertainties in the area measurements.

The chromatograms in Figure 3 are then divided into 0.5 s intervals. The areas for each interval are successively used as S_1 and S_2 in Equation 43 to determine the concentrations eluted at each interval. The results are presented in Figure 4. The ordinate then corresponds to the volume-fraction concentration eluted every 0.5 s, or every 5.6 μL of eluent. The integration interval was chosen to produce a smooth and continuous display, and not based on the available efficiency of the column. Note that the peak consists of a distribution of components rather than a single component, as judged from the total elution time involved. The total integrated area in Figure 4 is in good agreement with the 1 μL injection volume. Similar results are obtained with other motor oils, as seen in Figure 5. Apparently the synthetic motor oil has a sharper distribution of components compared to the natural motor oil, which is a reasonable result. The utility of this quantitative scheme is now obvious. Figure 3(A) or 3(B) alone does not provide a correct picture of the distribution of the components, since the RIs of the components are not known. Figure 4, however, gives the correct amount of materials eluted at any time regardless of the RI of the components, and should be identical to results obtained by the tedious method of collecting fractions.

Using values for $n_{THF} = 1.4050$ and $n_{benzene} = 1.5011$, Equation 44 can be used to predict the RIs of the components as they elute off the column. The results are shown in Figure 6. Equation 44 naturally becomes meaningless when little or no material is being eluted, i.e.,

Figure 4. Concentration of components as the volume fraction eluted in a 0.5 s interval (5.6 μL) for a synthetic motor oil

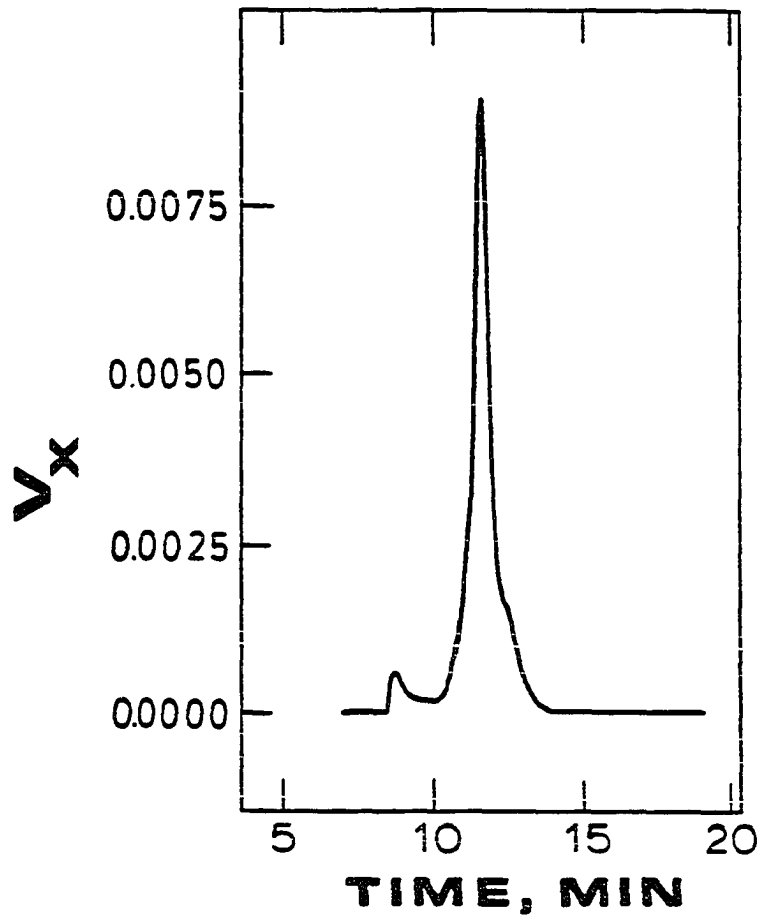
0.0075
0.0050
0.0025
0.0000
V_x
5
10
15
20
TIME, MIN

Figure 5. Concentration of components as the volume fraction eluted in a 0.5 s interval (5.6 μL) for a natural motor oil

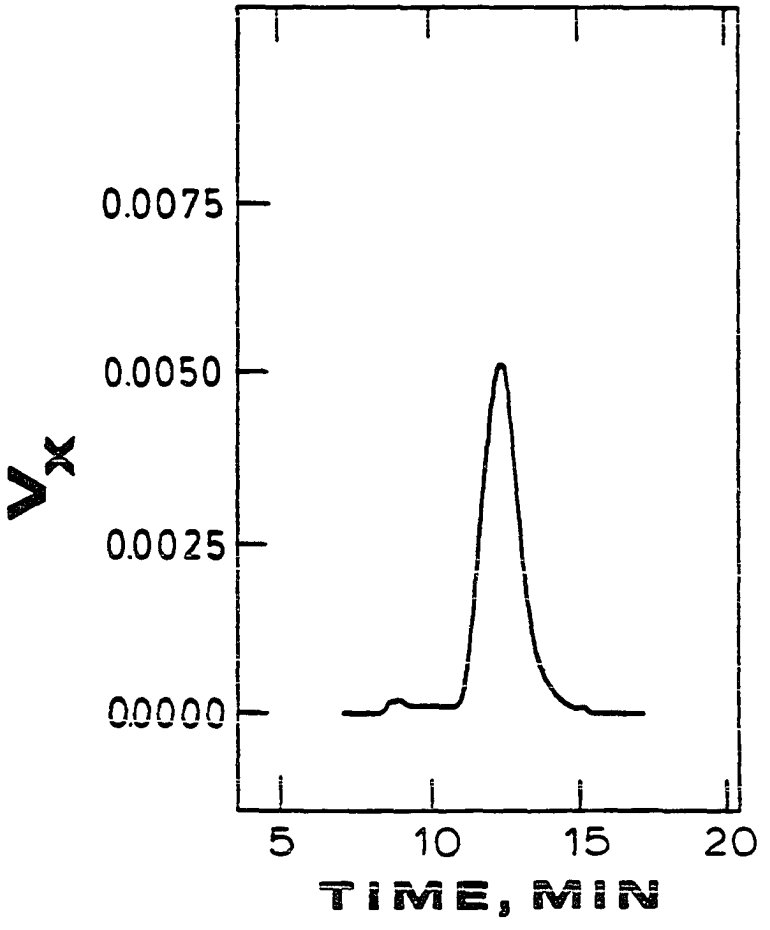
0.0075
0.0050
0.0025
0.0000
V_x
5
10
15
20
TIME, MIN

Figure 6. Refractive indices of the components as they elute from the column for a synthetic motor oil

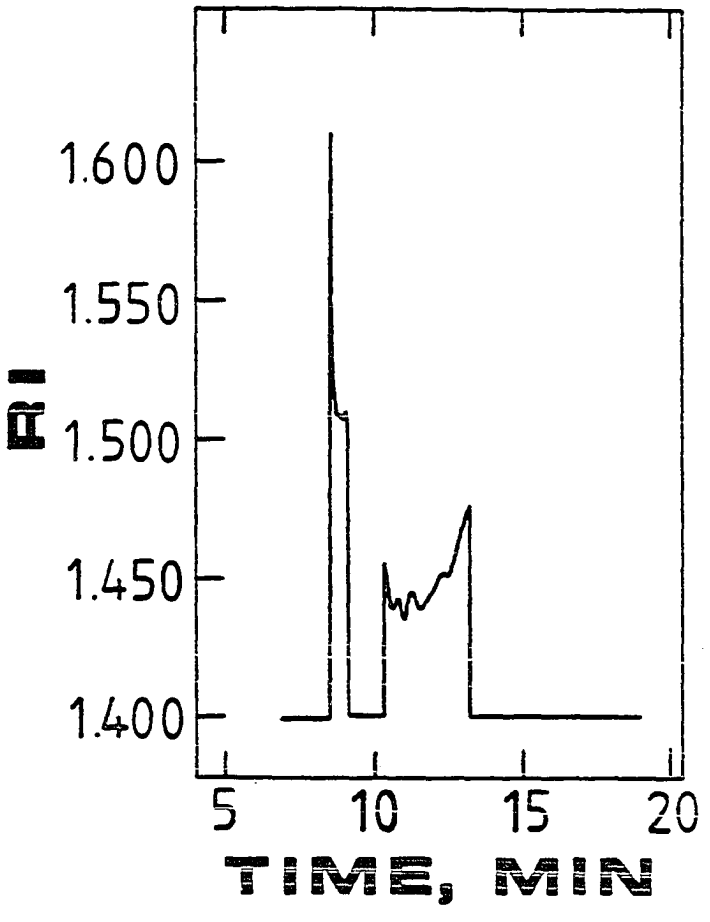
1.600
1.550
1.500
1.450
1.400
RI
5
10
15
20
TIME, MIN

when S_1 and S_2 approach the baseline noise level. The "baseline" was arbitrarily set at 1.400 whenever the fraction eluted fell below 3% of the peak volume fraction in Figure 4. Figure 6 provides interesting insight into the nature of the components in the sample even though it represents only the concentration-weighted RIs, and shows information usually not available using other methods. The structure between 10 and 12 minutes is real considering the typical efficiencies of this type of column. As expected, the RI distributions obtained are quite different between natural and synthetic motor oils.

Finally, it should be emphasized that correlated chromatograms in different eluents may not be available for the sample of interest. A very tedious consistency test must then be applied as described in Chapter 3. For example, similar studies have been performed using various solvent-refined coals (75). There, the presence of polar compounds and possible hydrogen bonding with THF contribute to uncertainties in the correlation. It may be possible, however, to first obtain, say, the nonpolar aliphatic fraction of these solvent-refined coals before applying this scheme.

Conclusion

In summary, a method has been devised for obtaining quantitative information in GPC that does not require identification of the analytes. The procedure is not only more efficient and more convenient, but the results are also more reliable and more illuminating.

CHAPTER 5.

QUANTITATION OF COMPONENTS IN CRUDE OILS USING LIQUID CHROMATOGRAPHY WITHOUT IDENTIFICATION

Introduction

Quantitative and qualitative characterization of fossil fuels and their commercial by-products is a common analytical consideration. Various combinations of chromatographic separation and detection systems have been successfully demonstrated. Coal extracts have been analyzed by Fourier transform infrared (FTIR) spectrometry using either size-exclusion chromatography (71, 76) or normal-phase chromatography (77, 78). Characterization of coal extracts can also involve a series of separation and detection methods such as extraction, prep-scale LC, and analysis of LC fractions by gas chromatography to form a detailed picture of the sample (79). Often, mass spectrometry via a GC interface, NMR, and UV absorption are used to provide structural information about the solutes (80). Also, optical activity (OA) detection has been recently used with reverse-phase chromatography for studying coal extracts (81).

Generally, the complicated nature of a fossil fuel sample requires separation and detection methods selective towards a narrow range of organic functionalities in the sample (82). Utilizing both highly selective separation techniques and highly selective detectors is necessary when identification of only a few species in a petroleum sample is desired (83, 84). A more complete picture about a sample

may require application of a relatively universal detector, such as the refractive index (RI) detector (85). More importantly, quantitation must be accomplished without analyte identification, since the latter is often impractical. Such an application was discussed for the analysis of motor oils by size-exclusion chromatograph (SEC) with RI detection in Chapter 4. It was shown that concentration and absolute RI chromatograms can be generated if the sample is eluted consecutively in two eluents with different RIs in an otherwise identical chromatographic system. This type of information about the samples gave a much more complete characterization than would be available with more selective analytical methods.

One of the major considerations in applying this absolute quantitation method is definitive solute correlation between the two chromatograms required for quantitation. In certain types of LC this is not a problem because an essentially identical chromatographic separation can be produced by proper choice of eluting solvents. That is, if the retention order of solutes stays the same (same eluent selectivity) and the retention time stays the same (same eluent strength), the solute correlation in the two chromatograms is straightforward. For well-resolved solutes, ion chromatography (11, 12) provides straightforward correlation between chromatograms, and has been successfully utilized with this quantitation method. For nonpolar materials in SEC, good correlation can be expected. Using optical activity (OA) detection (6) the correlation is also very easy because the eluents are chromatographically identical with respect to

the column separating mechanisms. In other forms of LC/detector combinations, such as reverse-phase (RP) or normal-phase (NP) with RI detection, one must choose two eluents with different RI values to optimize the sensitivity of the quantitation scheme as discussed in Chapter 2. Frequently, the different RI values for the two eluents imply different eluent selectivity, strength, or both.

For well-resolved solutes in RPLC and NPLC systems, a statistically based correlation scheme was demonstrated in Chapter 3 for components in a sample which eluted differently in different eluents. For samples in which an unresolved distribution of solutes is present, such as crude oils, a more judicious choice of the two eluents must be made. In order to provide quantitative information using RPLC, NPLC, and SEC, eluent pairs for each type of chromatography must be closely matched in both selectivity and strength. This is not necessarily trivial, and without it there would be no correlation possible. The focus of this chapter will be to apply successively RPLC, NPLC, and SEC to the study of crude oils, to demonstrate that pairs of eluents can be chosen to obtain correlated chromatograms. The absolute quantitation scheme initially discussed in Chapter 2 can then be applied to these complex samples to derive useful information, even though the components are not well-resolved in the chromatograms.

Theory

The reader is referred to Chapters 2 and 4 for the mathematical derivations. To calibrate the detector response for each chromatographic system the two eluents can be injected into each other to determine their respective peak areas. For a given solute, its concentration (volume fraction), V_x, is related to the integrated areas in the chromatograms by

$$V_x = V\left(\frac{S_{x,A}}{S_{B,A}} + \frac{S_{x,B}}{S_{A,B}}\right) \tag{47}$$

V is the concentration of the eluents A and B used for calibration while $S_{B,A}$ is the peak area of B in A, and $S_{A,B}$ is the peak area of A in B. $S_{x,A}$ is the peak area of the solute x in A, and $S_{x,B}$ is the peak area of solute x in B. Notice that since the areas are originally collected at distinct integration intervals, the volume fraction V_x can be calculated for each interval or "slice" along the unresolved chromatogram. The RI value in each slice can be similarly calculated, since,

$$-\frac{(S_{x,A})(S_{A,B})}{(S_{x,B})(S_{B,A})} = \frac{F_x - F_A}{F_x - F_B} \tag{48}$$

with

$$F_i = \frac{n_i^2 - 1}{n_i^2 + 2} \tag{49}$$

Using the RI values of eluents A and B, n_x, the RI of the solute per integration slice can be calculated by combining Equations 48 and 49.

Similar to Equation 47, one can use two calibrating substances other than the eluents. The concentration of the solute, V_x, is then

$$V_x = V\left[\frac{S_{x,A} - S_{x,B}\left(\frac{K_2}{K_1}\right)}{S_{1,A} - S_{1,B}\left(\frac{K_2}{K_1}\right)}\right] \tag{50}$$

with

$$\frac{K_2}{K_1} = \frac{S_{1,A} - S_{2,A}}{S_{1,B} - S_{2,B}} \tag{51}$$

Everything is labeled the same way as in Equation 47 except subscripts 1 and 2 on the S's refer to the peak areas of the two calibrating substances in eluents A and B. It follows for the RI calculation that

$$\left(\frac{S_{x,A}}{S_{x,B}}\right)\left(\frac{K_1}{K_2}\right) = \frac{F_x - F_A}{F_x - F_B} \tag{52}$$

An RI for each slice can be calculated by combining Equations 49 and 52. Equations 47 through 52 form the basis for the concentration and RI chromatograms presented in the discussion section. The important point is that the chromatograms must be correlated. This then is the main reason for the following studies of chromatographic conditions, so that the proper conditions can be chosen for quantitation.

Experimental

All organic solvents used as either eluents or calibrants were from Burdick and Jackson (HPLC grade) except for dimethylformamide, hexane, and dodecylbromide, which were reagent grade materials. n-Alkanes used as retention time calibrants were at least 99% pure (Alfa Products, Danvers, MA). Two crude oil samples were studied: North slope crude (Tank:6000X1) and Arun condensate crude (Tank:1340X112), (Mobil Oil Corporation, Ferndale Refinery, Ferndale, WA). Water used as a modifier was deionized and distilled in the conventional way. The organic solvents were used without further purification.

Three different columns were used with two different eluents per column. The RPLC separation was provided by a 25 cm x 4.6mm I.D., 10 μm, C_{18} column (Anspec, Warrensville, IL) with either pure acetonitrile or 96.5% dimethylformamide, 3.5% H_2O (by volume) as eluents, at a flow rate of 0.76 mL/min. The NPLC separation was done on a 25 cm x 4.6 mm I.D., 5 μm, silica column (Anspec, Warrensville, IL) with either 2,2,4-trimethylpentane (iso-octane) or pentane as eluents, at 0.79 mL/min. For the SEC analyses, a 30 cm x 4.6 mm I.D., 100 Å, 5 μm, PL gel size-exclusion column was used (Anspec, Warrensville, IL) with either chloroform or toluene as eluents, at 0.80 mL/min.

The chromatography system was conventional and consisted of a reciprocating pump (Milton Roy, Riviera Beach, FL, Model 196-0066), and an injection loop of 10 μL connected to a conventional valve (Rheodyne, Berkeley, CA, Model 7010), which was connected to the

column. The outlet of the column was connected to a commercial absorbance detector (Rainin, Woburn, MA, Model 153-00) operated at 254 nm for the NP separations, and operated at 365 nm for the SEC and RP separations. From the absorbance detector the effluent was directed into a commercial RI detector (Waters Associates, Milford, MA, Model R401) with the reference cell operated in the static mode, being filled with the eluent in use. The time delay between the two detectors (in series) was approximately five seconds, and for this work is basically insignificant. The output of each detector was sent into a voltmeter (Keithley, Cleveland, OH, Model 160B), which provided an amplified analog output (± 1V) into a computer, which in turn performed real-time analog-to-digital conversion and data storage (Digital Equipment, Maynard, MA, Model PDP 11/10 with a LPS-11 laboratory interface). The data collection rate for the NPLC and SEC analyses was one point per 0.5 seconds, and was one point per second for RPLC analyses.

All injected solutions were diluted if necessary, before injection, to be within the linear range of the detectors. Then, all areas were adjusted to the same RI detector attenuation scale and normalized to the volume injected before any quantitation equations were applied. Multiple injections (2 or more for samples, 3 or more for calibrants) were made to ensure reproducibility.

Results and Discussion

Reverse-phase chromatography

Some knowledge of each crude oil is necessary in order to produce a useful chromatogram. By elemental analysis, the Arun condensate crude oil had an average formula of $(CH_{1.94})_n$ with 99.29% by weight of the crude composed of carbon and hydrogen. The North Slope crude oil had an average formula of $(CH_{1.71})_n$ with 99.07% carbon and hydrogen by weight. Thus, the samples are essentially hydrocarbon in nature with very few heteroatom containing compounds present. This is consistent with data for crude oils in general (80). Acetonitrile (CH_3CN, RI = 1.344) is chosen as one of the two eluents. A set of standard n-alkanes can then be eluted to form a yardstick in order to judge the performance of the other eluent. A consideration of the solubility parameter contributions (i.e., dispersion, dipole-dipole, hydrogen-bonding, etc.) implicit for interactions with the C18 column leads to the conclusion that the sample interacts primarily through dispersion interactions (86) since it is composed of hydrocarbons. It has been reported that hydrogen-bonding eluents in RPLC produce "non-ideal" interactions with solutes capable of such interactions (87). The quantitation method applied in this work should not be hindered by "non-ideal" behavior of the solute-eluent mixture passing through the detector, since dispersion interactions predominate, providing the required "ideal" behavior. Thus, it is necessary to find a second eluent in which contribution of the dispersion term to the solubility parameter closely matches that of CH_3CN. The two eluents will then

provide identical strength and selectivity towards the sample. The other requirement is that the second eluent must have a different RI than CH_3CN to ensure significance when applying the calculations. A difference of at least 0.05 RI units is desirable. Dimethylformamide (DMF, RI = 1.430) is a good initial choice for the second eluent. Pure DMF was found to be too strong a solvent for RPLC compared to CH_3CN. A common method to change the strength of an eluent in RPLC is to add water. The percent (H_2O) versus log (capacity factor) plot is linear (88) for a given solute over a small range of H_2O concentration. It was found that a good approximation for comparable chromatography for the n-alkanes is an eluent composition of 96.5% DMF to 3.5% H_2O. Using the same flow rate the measured retention times are shown in Table 10. These retention times correlate very well in the two eluents. Since crude oils are known to contain very similar materials, one can then assume that those chromatograms are also well matched.

The Arun condensate crude oil was eluted in these two eluents, and the chromatograms (raw data) are shown in Figure 7. Because the RI response is both solute RI and concentration dependent, the chromatograms look quite different. As they stand, individually, they are not suitable for quantitation. Using Equation 50, the data shown in Figure 7, and calibration given in Table 11, the concentration (V_x) chromatogram was calculated and shown in Figure 8(A), along with the absorbance (365 nm) chromatogram (Figure 8(B)). Note that some highly absorbing species elute well before any substantial concentration of

Table 10. Data for n-alkanes eluted using RPLC

	Retention Time[a] in CH_3CN (min.)	Retention Time[a] in DMF/H_2O (min.)
n-hexane	7.50	8.00
n-octane	9.75	10.50
n-decane	13.50	14.00
n-dodecane	19.75	19.50
n-tetradecane	29.75	29.00

[a]The same flow rate (0.76 mL/min), column (25 cm x 4.6 mm I.D., 10 μm, C18), etc., are used throughout. Times are ± 0.10 min.

Figure 7. Refractive index chromatograms of Arun crude oil
Column - C_{18} 10 μm reverse-phase; (A) - CH_3CN eluent;
(B) - DMF/H_2O eluent; flow rate - 0.76 mL/min.

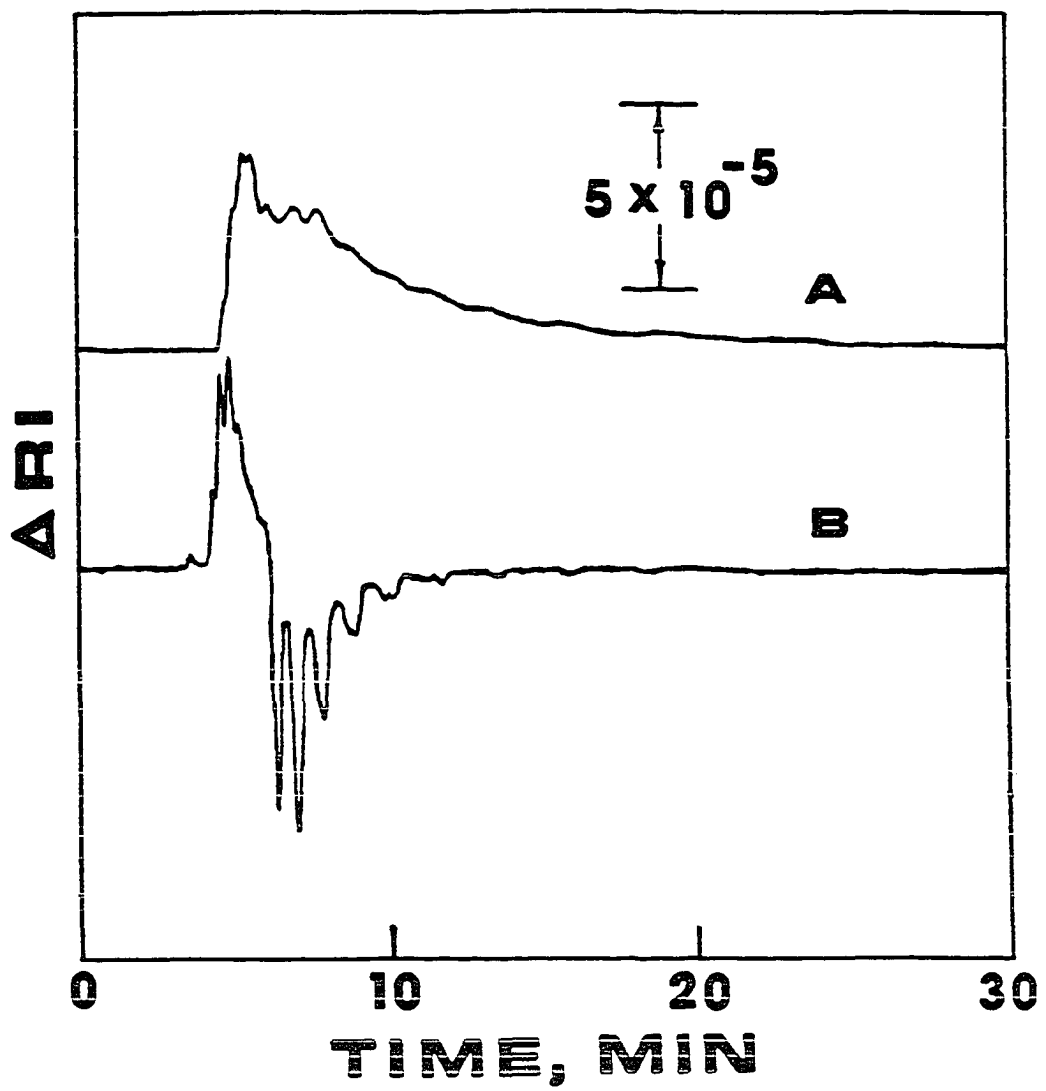
5 x 10⁻⁵
A
B
ΔRI
0
10
20
30
TIME, MIN

Table 11. Calibration data

Analyte	Eluent	Area[a] (x 10^3)	Relative Uncertainty (%)
Hexane	CH_3CN	364.0	3.7
Dodecylbromide	CH_3CN	1383.0	2.2
Hexane	DMF/H_2O	-531.1	3.2
Dodecylbromide	DMF/H_2O	275.9	3.9
Pentane	Iso-octane	-673.9	3.0
Iso-octane	Pentane	860.9	1.6
Chloroform	Toluene	-1231.6	3.1
Toluene	Chloroform	1036.3	0.4

[a]Adjusted from the original volume fraction and original detector attenuation to V = 1.00 and an attenuation of 16x.

Figure 8. Arun crude oil components as they elute from a reverse-phase chromatographic system
(A) - concentration (volume fraction) of materials eluted each second; (B) - absorbance of materials at 365 nm; (C) - RI of the materials; volume injected - 10 µL.

TIME, MIN
0
10
20
A
B
C
V_x $(\times 10^{-3})$
5.0
2.5
0.0
ΔABS
0.0
0.1
0.2
RI
1.55
1.50
1.45
1.40
1.35

the sample is seen. By applying Equation 52, the data in Figure 7, and calibration data of Table 11, the absolute RI chromatogram can be calculated. This is shown, with an arbitrary baseline of 1.35 RI units, in Figure 8(C). In this absolute RI chromatogram, as in the others to follow, an RI value is calculated only if the V_x of the interval is at least 2% of the maximum V_x in the entire V_x chromatogram. Otherwise, an arbitrary baseline value is used. The RI chromatogram suggests aromatics (RI ca. 1.50) elute first, followed by the smaller alkanes and then the larger alkanes. This is consistent with the n-alkane data of Table 10. A comparison of the V_x and RI chromatograms in Figures 8(A) and 8(C) shows that the Arun condensate contains alkanes primarily, and aromatic compounds make up only a small fraction of the whole sample. The absorbance chromatogram, then, is somewhat misleading. This emphasizes the need for this quantitation scheme, so that the chromatograms in Figure 7 and in Figure 8(B) will not be misinterpreted for the purpose of characterization.

Normal-phase chromatography

In NPLC, adsorption is the primary retention interaction. More polar compounds are eluted later due to stronger interactions with the silica stationary phase. Consideration of the crude oil samples, Arun and North Slope, requires the use of eluents with a very small elutropic value, ε^0, (ca 0.00), in order to achieve a good separation of crude oil components. 2,2,4-trimethylpentane (iso-octane) (RI = 1.392, ε^0 = 0.01) and pentane (RI = 1.385, ε^0 = 0.00) provide about

the same ε^0, an adequate RI difference, and the same selectivity towards solute separation. Slight differences in eluent strength were however observed. This is possibly due to differences in the residual water content or the inherent structural differences between iso-octane and pentane. Modification of one eluent in order to match the strength of the other eluent was not attempted because of the difficulty in reproducing the modified strength. Pentane was found to be stronger than iso-octane, producing a shorter chromatogram in time (at the same flow rate). Since the strength difference was very small, it was found that a chromatogram in pentane was predictable from the chromatogram in iso-octane. So, expanding the shorter chromatogram from its "chromatogram time domain" into the time domain of the longer chromatogram by a suitable transform will accurately relate the two. Using the same flow rate and column, the dead time and column efficiency were found to be the same. The peak variance due to extra-column effects and the contribution to broadening from injection were found to be insignificant when compared to the natural broadening due to retention. It can be shown that the retention time data of two chromatograms eluted in solvents of slightly different ε^0 values can be correlated in terms of retention time (89, 90). The result of this derivation is an approximate solution given by

$$\text{constant} = \frac{[T_A(T_A - T_0)]^{1/2}}{[T_B(T_B - T_0)]^{1/2}} \qquad (53)$$

T is the retention time, with the subscripts A, B and 0 denoting pentane, iso-octane, and the dead time, respectively. Using an eluent independent detector (e.g., the absorbance detector at 254 nm), retention times for the same features were taken from the chromatograms of Arun eluted in pentane and then in iso-octane. These points are labeled 1 through 7 in Figure 9. The raw data are given in Table 12. Fitting the Table 12 values to Equation 53, we find that the constant = 0.8945 with a correlation coefficient of 0.9996, and a y-intercept of -0.09. Using this information the pentane raw data were transformed into the chromatographic time domain of the iso-octane raw data. The effect can be seen in Figure 9, showing the retention times after adjustment. The chromatograms can be said to be well correlated. Note that the raw delta RI chromatograms for NPLC are not shown.

The correlated RI chromatograms for the Arun and North Slope crude oils are then obtained using Equation 53. Using Equation 47 and the calibration data in Table 11, the V_x chromatograms are calculated. Figure 10 shows these chromatograms. Note that the Arun and North Slope crude oils are very similar as far as functionality is concerned. This is consistent with elemental analysis as described earlier. It is also clear why the n-alkanes are not suitable as chromatographic retention-time calibrants for this case. All the alkanes elute in the first (large) peak in the V_x chromatograms. The absorbance (Figure 9) and V_x (Figure 10) chromatograms give quite a different picture of the crude oil sample composition. It is again

Figure 9. Comparison of absorbance chromatograms (254 nm) for Arun crude oil

(A) - iso-octane eluent, unadjusted; (B) - pentane eluent, after adjustment according to Equation 7; column - silica 5 μm normal-phase; amount injected - 40 nL.

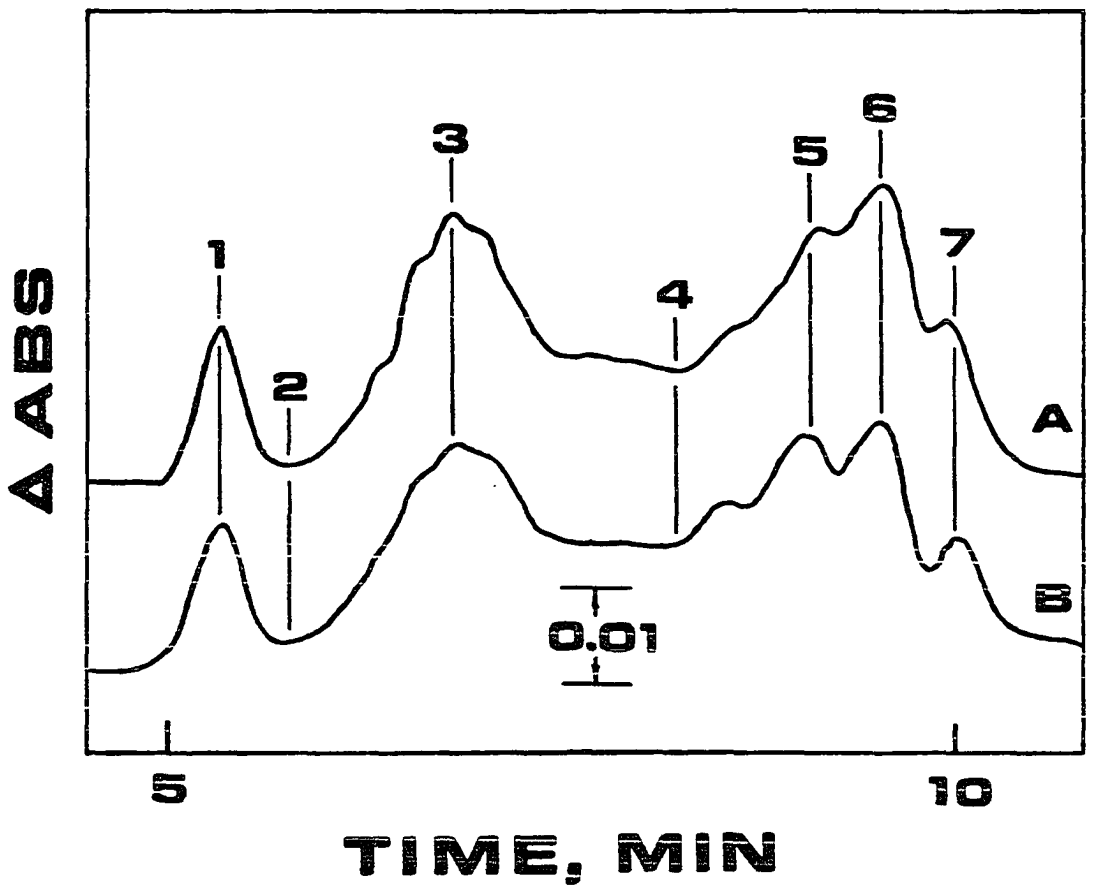
ΔABS
1
2
3
4
5
6
7
A
B
0.01
5
10
TIME, MIN

Table 12. Data for absorbance chromatograms used to correlate features for arun crude in NPLC

Point Number[a]	Retention Time[b] in Pentane (min.)	Retention Time[b] in Iso-octane (min.)
1	5.02	5.34
2	5.35	5.77
3	6.32	6.78
4	7.40	8.10
5	8.24	9.10
6	8.66	9.52
7	9.08	9.90

[a]Point Number as labeled in Figure 9.

[b]Both eluents were used with the same column providing the same dead time of T_0 = 3.75 min at the same flow rate of 0.79 mL/min.

clear, as in the RP chromatography of the Arun crude oil, that the highly absorbing components are present at a very low volume fraction.

Using Equation 49, the average RI and integrated concentrations for each of the numbered features in Figure 10 are also shown. The low RIs (feature 1) are indicative of alkane fractions and the high RIs (features 2 and 3) are indicative of aromatic or heteroatom fractions. It is important to note that the sums of the concentrations for each crude gives a volume fraction of 1.00. This then verifies that this absolute quantitative scheme is mathematically correct. This is then a convenient way to determine the aliphatic/aromatic ratios for such fossil fuel materials.

Size-exclusion chromatography

Correlation of chromatograms in two different eluents in SEC is much simpler than in either RPLC or NPLC. Using chloroform (RI = 1.4458) and toluene (RI = 1.4936) as eluents, a series of n-alkanes were eluted in both eluents at the same flow rate. These data are given in Table 13. Clearly, the SEC chromatographic systems are the same.

Using the same procedure as for the NPLC separation, and with calibration data from Table 11, V_x and absolute RI chromatograms for the North Slope crude oil were produced. Shown in Figure 11 are the V_x, absorbance (365 nm), and RI chromatograms for the North Slope crude oil. Since the separation is based on molecular size, no clear distinction between alkanes and aromatics can be seen in the RI

Figure 10. Concentrations of components as they elute per second in a normal-phase separation

(A) - Arun crude oil; (B) - North Slope crude oil. The inserted tables contain the values of the average RI and integrated concentrations for each of the number features.

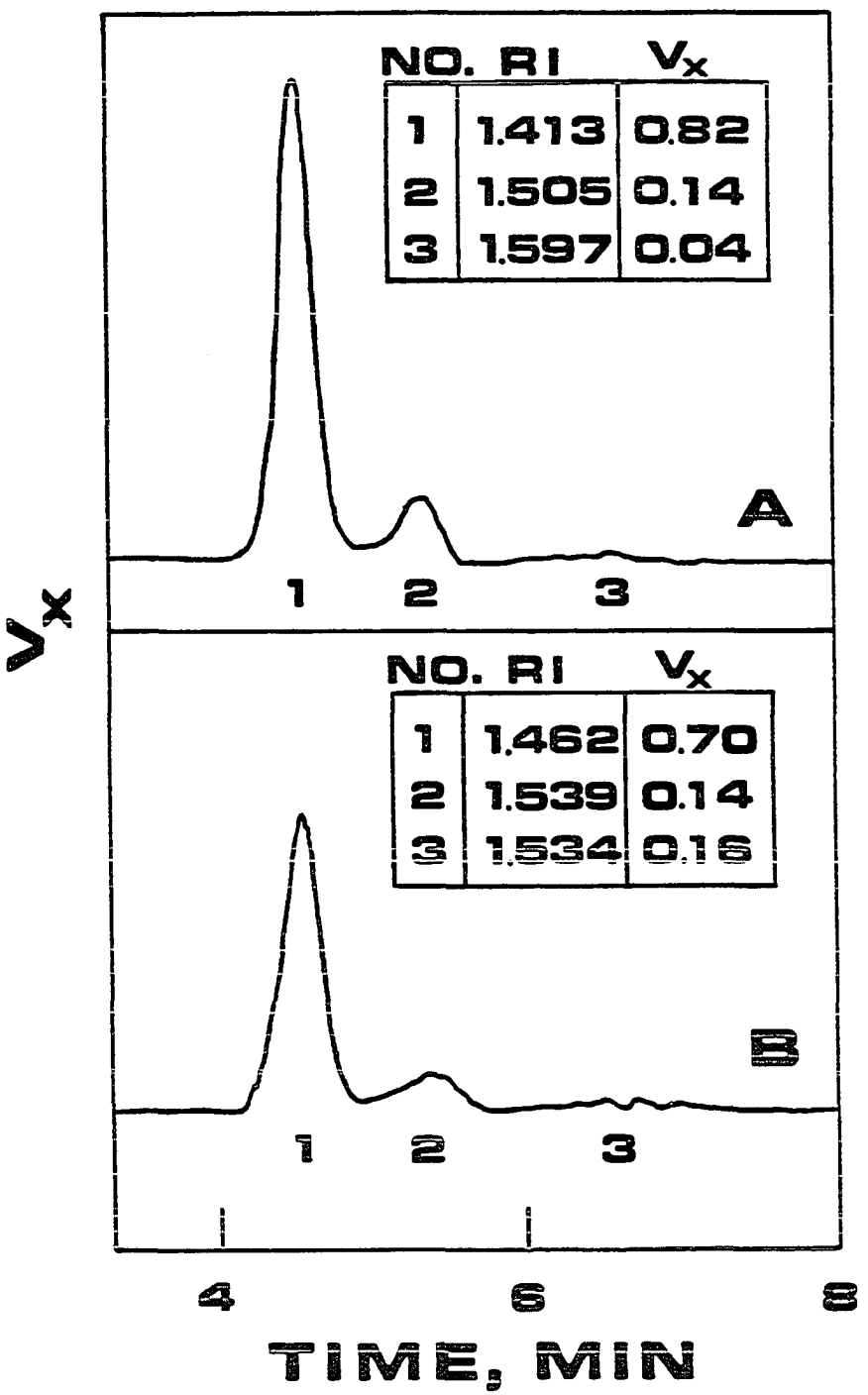
NO. RI Vx
1 1.413 0.82
2 1.505 0.14
3 1.597 0.04
A
1 2 3
NO. RI Vx
1 1.462 0.70
2 1.539 0.14
3 1.534 0.16
B
1 2 3
Vx
4 6 8
TIME, MIN

Table 13. SEC retention time data for n-alkanes

	Retention Time[a] (min.)		log V_m[b]
	$CHCl_3$	Toluene	
n-hexane	13.2	13.0	2.116
n-octane	12.6	12.4	2.211
n-decane	12.0	11.9	2.290
n-dodecane	11.6	11.5	2.357
n-tetradecane	11.2	11.2	2.415
n-hexadecane	10.9	10.9	2.467
n-eicosane	10.4	10.5	2.554
n-tetracosane	10.2	10.3	2.627
n-octacosane	9.8	9.9	2.690

[a]Retention times at a flow rate of 0.80 mL/min.

[b]Logarithm of the theoretical molar volume. Calculated using CRC values (55th ed.) for molecular weight and density (at 20°C).

Figure 11. North Slope crude oil components as they elute from a size-exclusion chromatographic system
(A) - concentration (volume fraction) of materials eluted each second; (B) - absorbance of materials at 365 nm; (C) - RI of the materials; volume injected - 10 µL.

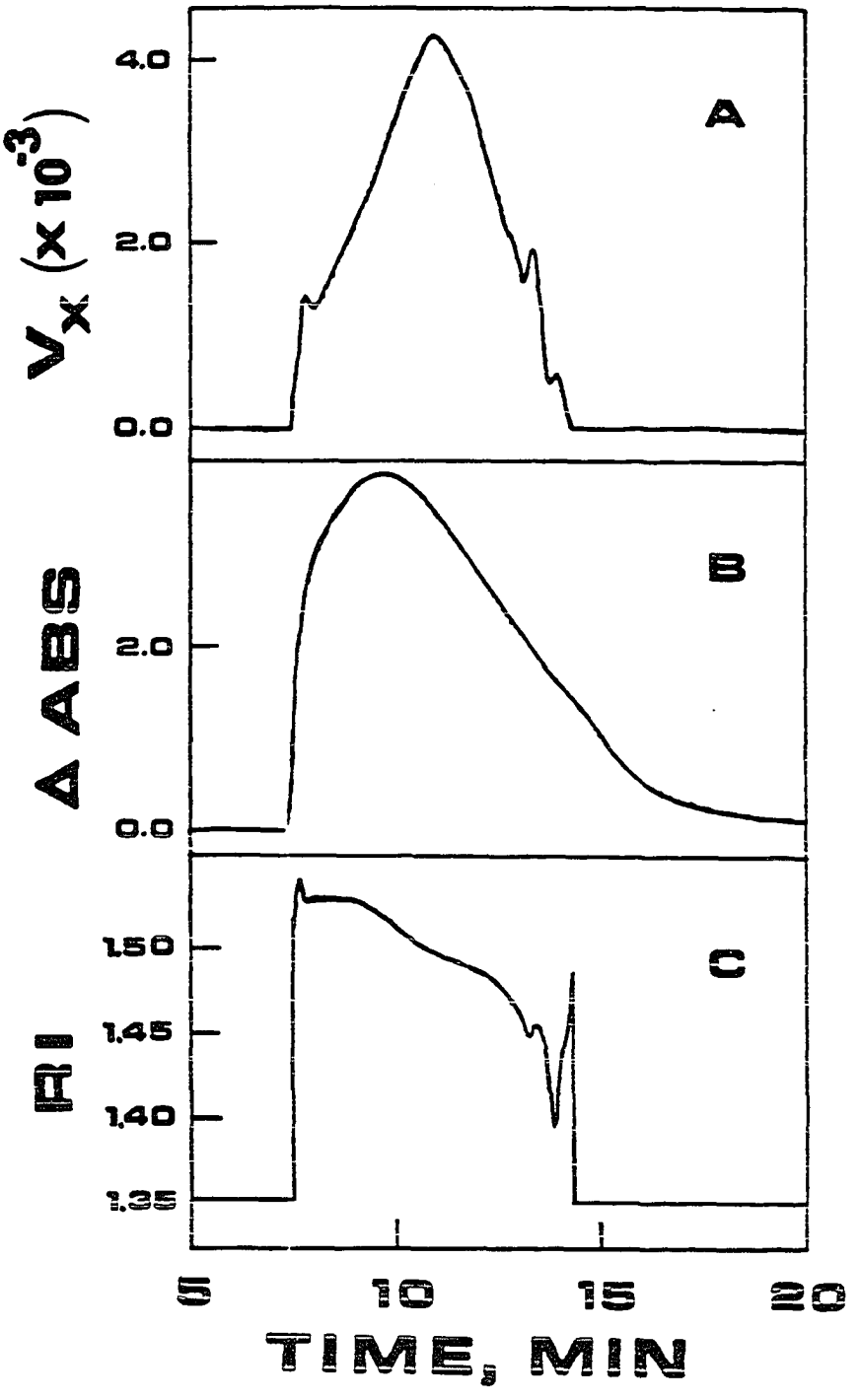
4.0
2.0
0.0
V_x ($\times 10^{-3}$)
A
2.0
0.0
Δ ABS
B
1.50
1.45
1.40
1.35
RI
C
5
10
15
20
TIME, MIN

chromatogram, although at longer retention times (smaller molecules) the RI values suggest that alkanes predominate.

By relating the n-alkane retention times (T, in seconds) to the logarithm of their molar volume (V_m, mL/mole), the data given in Table 13 produce the following linear relationship,

$$\log(V_m) = 0.002805\ (T) + 4.317 \tag{54}$$

A correlation coefficient of -0.9970 was obtained. V_x is the volume fraction (at time T) with respect to the injected volume. By multiplying V_x by the injection volume V_I and dividing by the effective molar volume of the solute (at time T) the moles of the solute per slice, C_x, are calculated by

$$C_x = \left(\frac{V_x}{V_m}\right)V_I \tag{55}$$

Summing up the moles for each slice yields the total moles of sample injected

$$\text{total moles sample} = \sum_{i=1}^{n} C_{x_i} \tag{56}$$

Thus, C_x chromatograms can be calculated from Equation 55 for the crude oils. Both the V_x and the C_x chromatograms for the North Slope and Arun crude oils are shown in Figure 12. It is interesting to note that while the two crude oils appeared similar in NPLC (Figure 10), they are quite different with respect to molecular size distributions (Figure 12). The C_x chromatogram is helpful in cases in which the

Figure 12. Concentrations of materials in crude oils as separated by size-exclusion chromatography

(A) - volume fractions eluted each second; (B) - moles eluted each second; 1 - Arun crude oil; 2 - North Slope crude oil.

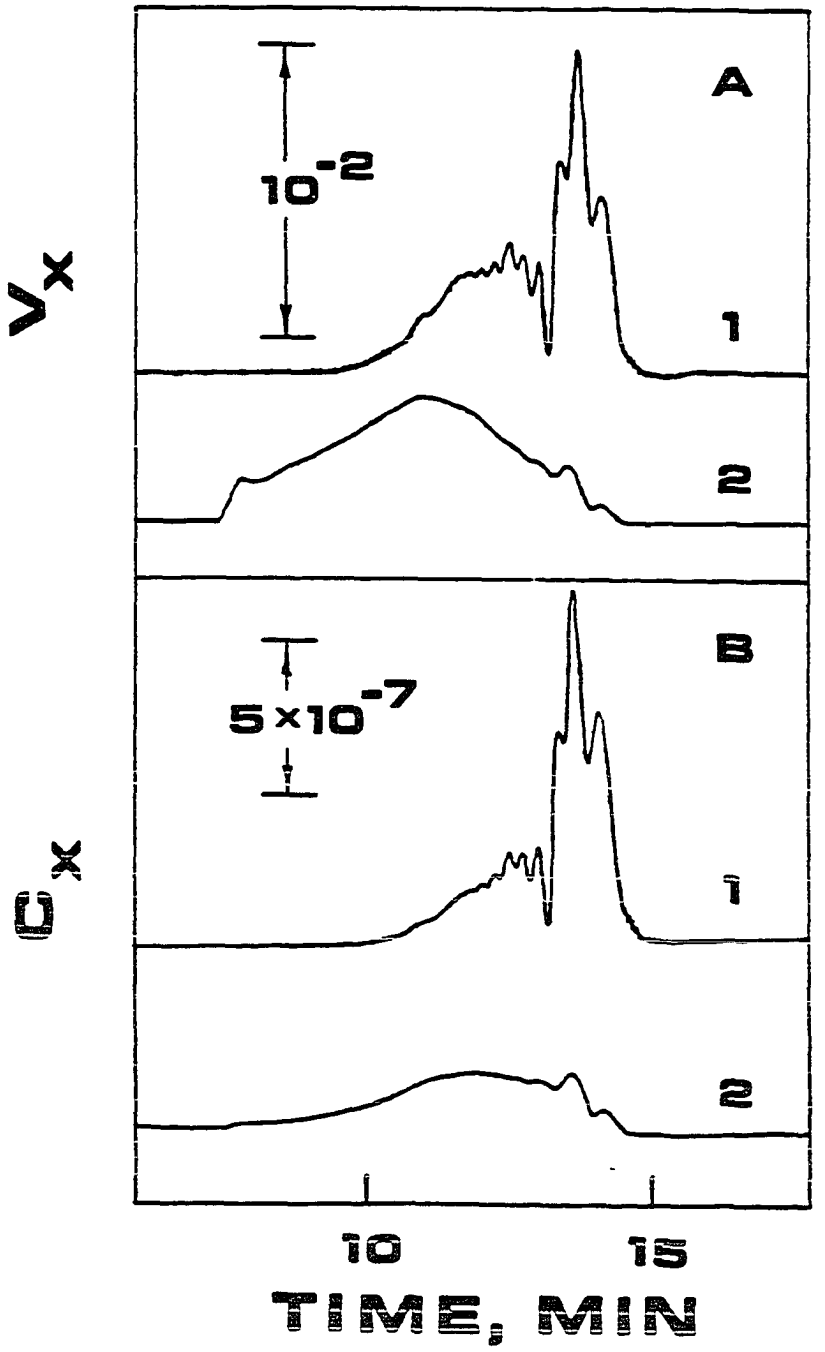
A
10^{-2}
1
2
B
5×10^{-7}
1
2
V_x
U_x
10
15
TIME, MIN

actual numbers of molecules at a particular size is of interest. For a 10 μL injection of crude oils, from Equation 56, 7.40×10^{-5} moles of molecules were calculated for the Arun crude oil, and 4.86×10^{-5} moles for the North Slope crude oil. This is consistent with the distributions shown in Figure 12. It is known that the Arun crude oil was a condensate (i.e., somewhat refined), and was sampled directly from an ocean tanker. The North Slope crude oil, on the other hand, was similar to a "true" crude oil in appearance, and was obtained by direct sampling from the Alaskan pipeline. Thus, it was expected that the Arun crude oil would contain fewer components, at higher number densities per component, and at molecular sizes somewhat smaller than the North Sloper crude oil due to the condensation processing.

Conclusion

It was shown that by choosing the appropriate solvent pairs in each case, one can get quantitative information (concentration chromatograms) and qualitative information (RI values) for complex samples like crude oils using RPLC, NPLC, or SEC. This is certainly much more efficient than collecting and weighing fractions (91). In contrast, similar studies by previous authors using RPLC (Figures 3 and 4 in (83)), NPLC (Figures 2 and 3 in (92)), or SEC (Figure 1 in (71)) did not produce quantitative information without assumptions about the response factors. The alternative is to assume that certain fractions are aromatic, polar aromatic, or aliphatic, and use empirical formulas relating the API gravity with the corresponding UV

response factors (93). Also, RI response factors have been used in similar studies (94, 95), and found to provide inadequate accuracy in quantitation. These methods depend on having a large number of truly representative samples to establish the empirical correlation. Even then, the predictions are unreliable because the major components in crude oils are saturates that can dominate the response factors used in the calculations. For crude oil characterization, the quantitative information and the RIs obtained from the procedure outlined in this chapter can be used to complement other analytical methods (96, 97, 98) to give a more comprehensive picture. When applying the quantitation method outlined in this chapter, an analyst must substantiate the selectivity matching between eluent pairs for a given chromatography system and the sample composition. This, however, does not limit the application of the method. Composition of a sample in general terms must be known, but specific assumptions about the sample composition are not required, such as response factors, etc.

Chapters 2 through 5 have dealt with a quantitation concept for LC, by optimizing the use of collected chromatographic data in order to provide novel information. It is also important to optimize the data collection process itself. This will be the subject of the next two chapters.

CHAPTER 6.

IMPROVEMENT OF THE LIMIT OF DETECTION IN CHROMATOGRAPHY BY AN INTEGRATION METHOD

Introduction

The limit of detection (LOD) in chemical analysis is an important parameter for many analytical methods. A recent review (4) dealt with the LOD concept, by objectively considering and providing recommendations for the use of statistics in determining the correct LOD for a given analysis. Application of static signal-to-noise theory to the detection and integration of dynamic (i.e. chromatographic) signals (99) provided good insight into understanding how the chromatographic process produces poorer LOD characteristics compared to static measurements due to peak broadening. Clarification of the LOD in chromatography has been analyzed concisely (100), with similar equations developed as in Ref. (99) for the effect of the chromatographic process on detection limits.

By considering the chromatographic peak height as the sole constituent for detectability, much of the "peak" information is wasted. Use of the entire peak area relative to the surrounding baseline may better provide a statistically satisfying and objectively determined LOD. According to the International Union of Pure and Applied Chemistry (IUPAC), the LOD is the lowest concentration (or mass) of a chemical species that can be determined to be statistically different from an analytical blank (101). What is truly important is

the statistical information (i.e. precision and accuracy) for the final quantitative result. The purpose of this work is to study and characterize an integration method in which dynamic signals can be objectively determined at a much better LOD than if determined from a static signal LOD model (99, 100). The basis of the improvement will depend upon the nature of the data, with the baseline behaving randomly (uncorrelated) and the eluting peaks behaving with an implicit non-random (correlated) behavior. Computer simulation will facilitate the development of this idea, while experimental data will be discussed afterward to compare with the simulation.

In its most basic form, the method requires three steps. First, chromatographic data from a detector are collected and stored for data processing. Next, the chromatogram is baseline adjusted so that the noise is centered (numerically) about zero. Finally, the chromatogram is integrated from beginning to end, point by point, to produce a secondary chromatogram. It was found that signal detectability is greatly enhanced in the integrated chromatogram relative to the original chromatogram. The method will be more rigorously developed and studied in this work.

Theory

Chromatographic peak model and relationships

First, it is important to relate the area of a chromatographic peak to the maximum height of the same chromatographic peak. A

Gaussian peak shape model is used here, but is applicable to other peak shapes. Each peak i in a chromatogram can be described by

$$S_i(t) = \frac{V_i R_i}{\sigma_i \sqrt{2\pi}} \exp \left\{ \frac{-(t - t_{R,i})^2}{2\sigma_i^2} \right\} \tag{57}$$

where $S_i(t)$ is the height of the peak i at time t, defined by the standard deviation of the peak (σ_i), retention time (t_R) at the maximum $S_i(t)$, volume fraction injected (V_i), and analyte detection response factor (R_i). Albeit, an exponentially modified Gaussian (EMG) function would be more rigorous in modeling a chromatographic system (102), but a Gaussian model will be adequate. The area of a chromatographic peak ($S_{i,AREA}$) can be calculated from Equation 57 by integrating,

$$S_{i,AREA} = \int_{-\infty}^{+\infty} S_i(t)dt = \int_{-\infty}^{+\infty} \frac{V_i R_i}{\sigma_i \sqrt{2\pi}} \exp \left\{ \frac{-(t - t_{R,i})^2}{2\sigma_i^2} \right\} dt \tag{58}$$

where integration from $(t_{R,i} - 3\sigma_i)$ to $(t_{R,i} + 3\sigma_i)$ is sufficient in recovering 99.74% of the total area. Note that

$$\int_{-\infty}^{+\infty} \frac{1}{\sigma_i \sqrt{2\pi}} \exp \left\{ \frac{-(t - t_{R,i})^2}{2\sigma_i^2} \right\} dt = 1 \tag{59}$$

Thus, since V_i and R_i are independent of time,

$$S_{i,AREA} = V_i R_i \tag{60}$$

Now, calculation of the maximum signal ($S_{i,MAX\ HT}$) of a chromatographic peak is facilitated by substituting $t = t_{R,i}$ into Equation 57,

$$S_{i,MAX\ HT} = \frac{V_i R_i}{\sigma_i \sqrt{2\pi}} \tag{61}$$

Conventionally, the maximum signal ($S_{i,MAX\ HT}$) is used to determine detectability. That is, $S_{i,MAX\ HT}$ must be greater than a confidence value determined by considering the noise of the background (4), in order for peak i to be detectable. By using only the $S_{i,MAX\ HT}$ of a peak for the purpose of deciding detectability, much of the "implicit" correlation about a chromatographic peak is wasted. The improvement in sensitivity by using the entire peak relative to using the maximum signal will be defined as the signal increase factor (SIF) and can be expressed by dividing Equation 60 by Equation 61,

$$SIF = \frac{S_{i,AREA}}{S_{i,MAX\ HT}} = \sigma_i \sqrt{2\pi} \tag{62}$$

It should be noted that no consideration of background noise has been incorporated into Equation 62.

For a typical chromatographic system (90), and for the purposes of simulation, the standard deviation of each peak (σ_i) can be related to retention by

$$\sigma_i = \left(\frac{t_0^2}{r}[k_i(1 + k_i)]\right)^{1/2} \tag{63}$$

for k_i > zero, where r is a constant for a given chromatographic system independent of analyte or retention time, and k_i is the capacity factor for peak i and is defined in the conventional way

$$k_i = \frac{t_{R,i} - t_0}{t_0} \tag{64}$$

with t_0 equal to the dead time, typically around 150 seconds. In Equation 63, r is on the order of 1000 to 2000 for liquid chromatography and σ_i calculated is in units of time (90). The result is that the SIF calculated in Equation 62, which is effectively the chromatographic dilution factor for a given peak, is also in units of time.

Chromatographic baseline model and relationships

A chromatographic baseline F(t) can be expressed as a linear combination by

$$F(t) = mt + b + D(t) + R(t) + N_t \tag{65}$$

where m is the slope of linear baseline drift, t is the time, b is the y-intercept of a baseline chosen at $t = 0(t_{inject})$, D(t) is any non-linear and essentially non-repeating baseline fluctuation such as temperature effects, R(t) is any non-linear yet repeating baseline fluctuation such as electronic ringing or pump pulsation effects, and N_t is the random noise associated with a physical measurement that can be statistically treated. Sampling a large population of N_t values should yield Gaussian statistics for Gaussian experimental noise (which is frequently observed for chromatography detectors).

Through proper experimental consideration and procedure, both D(t) and R(t) in Equation 65 can be reduced to near zero so they can be neglected. For any chromatographic system there is a portion of time before any material will elute (ca K' > 7 or so). By doing a linear least-squares fit to these two portions of a chromatogram, the slope (m*) and y-intercept (b*) (at $t = t_{inject}$) can be calculated to good precision. Thus, a baseline adjusted (BLA) chromatogram can be calculated by considering Equation 65 (neglecting D(t) and R(t)) and sequentially subtracting the slope-intercept contribution,

$$F^*(t) = F(t) = m^*t - b^* = N_t \qquad (66)$$

for t = 1, 2, 3..., n-1, n for a n-point chromatogram. For the purpose of the present study, n will equal 1200, and each increment of t denotes one second in time. Note that there is nothing magical about using 1200 as the number of data points. It is a convenient value that provides a 20 minute chromatogram from a detector with a 1 second time constant.

The concept of integrating baseline noise has been studied to understand the effect of various types of noise on commonly used integration techniques in chromatography (103). Maximizing the precision of quantitation was the goal in that study. Intuitively, if noise is truly random, the integration (i.e., addition) of noise should produce a value that remains close to the mean value of F*(t) before integration, which should be approximately equal to zero (103). What one is concerned with here is how a chromatographic peak

behaves relative to the background noise in both the normal and integrated time domains, for the purpose of improving detectability. One can introduce the idea of an integrated baseline (IBL) at each time interval t (i.e., data point) in a chromatogram,

$$IBL(t) = \sum_{t=1}^{t} F^*(t) = \sum_{t=1}^{t} N_t \qquad (67)$$

where IBL(t) is the running-total integration of F*(t). Figure 13 displays an example of Equations 65, 66 and 67. It is important to note that a baseline adjusted to be centered about zero is necessary to have the IBL stay close to zero. Although the noise appears larger in the IBL compared to the normal baseline in Figure 13, it will be shown later that the signal in an integrated chromatogram relative to a normal chromatogram more than compensates for this increase. For the IBL, the units for the vertical scale are "Relative Signal x Time" and not just the "Relative Signal", as is the case for the normal baseline. Notice that Equation 67 (and some others to follow) is a running-total expression and not a running-average. Using a running-total will not decrease the resolution (i.e., separation information) of closely eluting chromatographic peaks, since no averaging of information is done, whatsoever.

Objective determination of confidence limits for the IBL chromatogram must be considered. Calculation of the standard deviation of the baseline fluctuations for any baseline (IBL or otherwise) will be made by considering the time span of an "event" of chromatographic elution (4). The chosen event time-span will be 60

Figure 13. Typical and integrated baseline noise

(A) Typical baseline noise, not BLA (Equation 65).

(B) BLA noise (Equation 66).

(C) Integrated BLA noise (Equation 67).

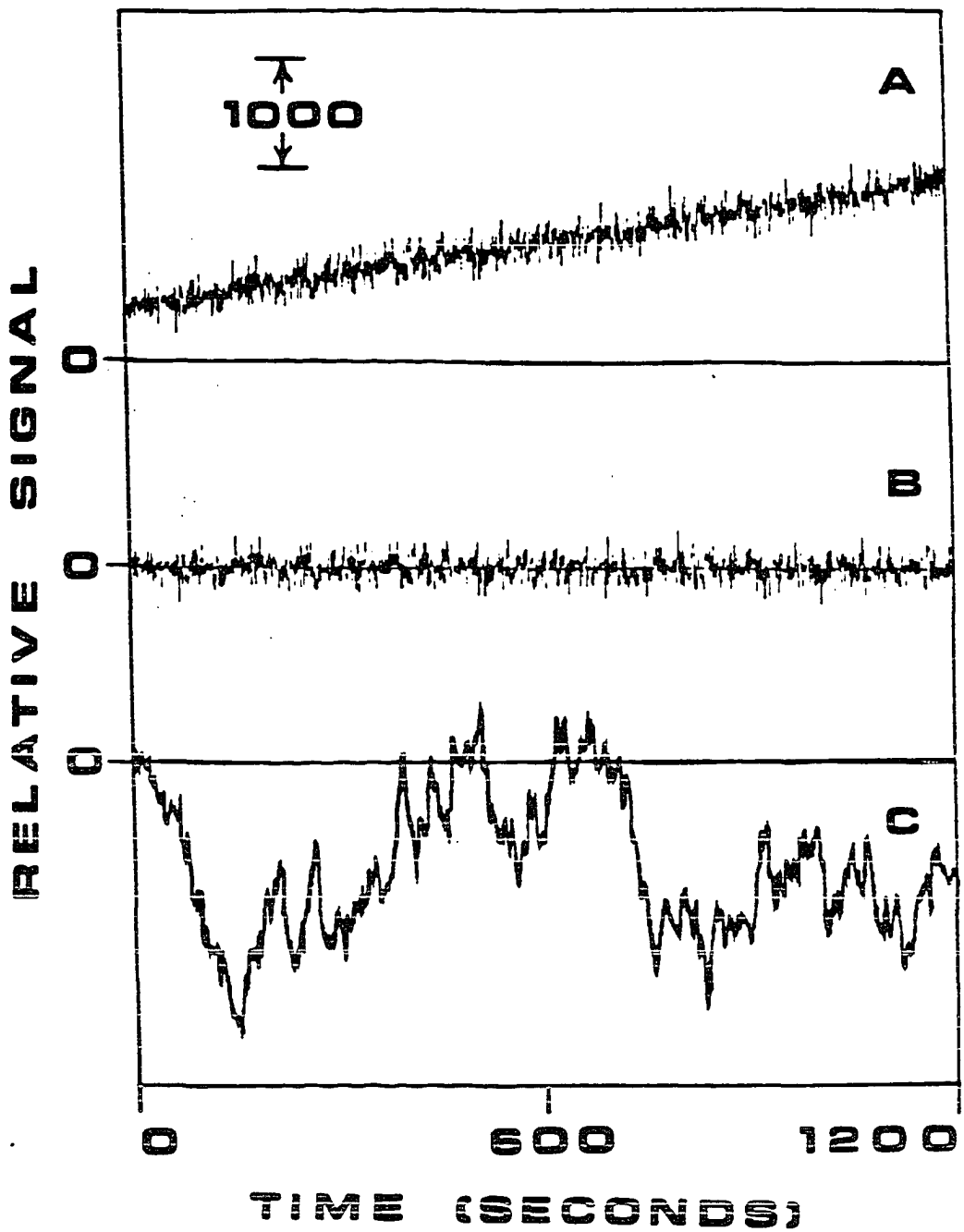
1000
A
B
C
0
0
0
RELATIVE SIGNAL
0
600
1200
TIME (SECONDS)

data points (i.e., seconds) for this simulation. Going back to Equation 63 it can be seen that 60 points should be adequate for most k values in a realistic separation. Thus, the average value (u) of a section j of a baseline can be calculated by,

$$u_j = \frac{\sum_{t=t_b}^{t_f} X(t)}{p} \tag{68}$$

with j = 1, 2, 3, 4...., m-1, m, and p=60 such that mxp = 1200, and with $t_b = 1 + ((j - 1)p)$ and $t_f = p + ((j - 1)p)$. Then, the standard deviation (σ) for each baseline section can be calculated by,

$$\sigma_j = \left(\frac{\sum_{t=t_b}^{t_f} (X_t - u_j)^2}{p - 1} \right)^{1/2} \tag{69}$$

for j = 1, 2, 3...., m-1, m, and with t_b and t_f as in Equation 68, and

$$\bar{\sigma}_X = \frac{(\sum_{j=1}^{\bar{m}} \sigma_j)}{m} \tag{70}$$

for m sections of length p, were t is the index synonymous with time. From Equation 70, $\bar{\sigma}_X$ is the average standard deviation of a "series" of blank or background measurements in general form. For a BLA chromatogram, $\bar{\sigma}_X = \sigma_N$ is calculated using Equations 68 through 70 with X(t) = F*(t). For the integrated BLA chromatogram, $\bar{\sigma}_X = \sigma_I$ is calculated similarly with X(t) = IBL(t).

Thus, in the absence of any peaks, a comparison of the baseline noise for a normal chromatographic baseline and an integrated chromatographic baseline can be made by relating σ_N and σ_I. Assuming the same number of standard deviations is used in defining detectability, a noise increase factor (NIF) can be defined as

$$NIF = \frac{\sigma_I}{\sigma_N} \tag{71}$$

Equation 71 should adequately describe the theoretical relationship between the noise in a normal chromatogram and the noise in the integrated chromatogram. It is anticipated that the NIF of Equation 71 will be greater than one.

Combining the chromatographic peak and baseline models

For the simulation of a "real" chromatogram containing peaks and baseline noise, a convolution of both of these features must be made. A convolution of chromatographic peaks with baseline noise to form a chromatogram is made by combining Equations 57 and 65. A simulated normal chromatogram C(t) is produced by,

$$C(t) = S(t) + F(t) \tag{72}$$

C(t) is a sequential array of elements with several peaks. Each peak (indexed by i) is defined by a retention time ($t_{R,i}$) and a peak width (σ_i, Equations 63 and 64). For a BLA chromatogram, Equation 72 will be

$$C(t) = \left[\frac{V_i R_i}{\sigma_i \sqrt{2\pi}} \exp \left\{ \frac{-(t-t_{R,i})^2}{2\sigma_i^2} \right\} \right] + N_t \tag{73}$$

The exponential part essentially vanishes for $|t - t_{R,i}| > 3\sigma_i$. Also, N_t represents the random baseline noise. Also an integrated chromatogram I(t) can be calculated using Equation 73

$$I(t) = \sum_{t=1}^{t} C(t) \tag{74}$$

where I(t) is the running-total integration of C(t).

The comparison in detectability between C(t) and I(t) is the main concern. It is observed from Equation 62 alone that one has a better detectability in the integrated chromatogram, while Equation 71 alone suggests a better detectability in the normal chromatogram. An improvement factor (IMP), for the integrated chromatogram relative to the normal chromatogram can be calculated using Equations 62, 63, 64, and 71 as follows,

$$IMP = \frac{SIF}{NIF} = \frac{\sigma_N}{\sigma_I} \left[\frac{2\pi}{r}(t_{R,i}^2 - t_0 t_{R,i}) \right]^{1/2} \tag{75}$$

The value of IMP increases as the retention time increases, showing greater improvement for later eluting peaks compared to earlier eluting peaks. The constant r decreases as the efficiency of a column decreases, suggesting that the poorer the column, the better the improvement (larger IMP). The value of IMP is independent of any data averaging that might be applied to a chromatogram. However, it is important to have a chromatogram that has enough points to maintain the chromatographic information for the resolution of closely eluting

species, and to achieve good precision in the final quantitation. This is realized experimentally by detecting the event with an instrument that has an appropriate time constant. As a suggested minimum, the width (σ) of the earliest chromatographic peak should be at least 10 time constant intervals. Then, a data collection rate the same as the detector time constant will produce the optimum IMP possible for a given detector time constant. The ratio σ_N/σ_I is determined empirically by characterizing the detected background noise (without injection).

Experimental

Chromatographic simulation, quantitation and statistical calculations were all done on a PDP 11/10 minicomputer (Digital Equipment Corp., Maynard, MA). All software was written in-house except for the utilization of a pseudo-random number generator designed specifically for a 16-bit computer (104). The pseudo-random number generator produces numbers evenly distributed between 0 and 1, so the distribution was transformed into a normal distribution (Gaussian) by a suitable method (105). The noise generated was treated statistically, and the distribution was found to be Gaussian by calculating the fraction of noise for a population between one, two, and three standard deviations. All equations pertaining to the chromatographic simulation are given in the Theory section.

Experimental noise was collected for two sets of conditions. To ensure that problems due to long-term fluctuations would not affect

the data, a 10 ms data collection rate (to produce a 1200 point data set) was used. A 12 second baseline was produced. An Amperex (North American Philips), 56-DVP photomultiplier tube was operated at either 1500 Volts (room lights on) or 2100 Volts (room lights off) with a Hamner (Princeton, N.J.), Model NV-13-P, high voltage power supply. The photomultiplier tube output signal was sent into a Princeton Applied Research (Princeton, N.J.), Model HR-8 lock-in amplifier with termination at 100 kΩ. A 10 ms output time constant was used with a 100 kHz measurement lock-in frequency supplied by a Wavetek (San Diego, California) Model 162 wave generator. The signal output from the lock-in amplifier was collected by the computer with a LPS-11 laboratory interface at a 10 ms data collection rate. The resulting data files were analyzed as before and found to also show a Gaussian distribution.

Results and Discussion

To this point, equations have been left in general terms, except for defining the data arrays to be 1200 points. For the simulated data to be presented it is important to note that what is important is the relative values in comparing a normal chromatogram to an integrated chromatogram.

Calculation of a "working" NIF (Equation 71) is facilitated by statistical analysis of three baseline noise chromatograms (without peaks). Table 14 contains the results of applying Equations 68, 69, and 70 to the normal and the integrated chromatograms for typical

Table 14. Typical baseline noise data

Interval (s)	Normal Chrom. u_j[a]	Normal Chrom. σ_j[b]	Int. Chrom. u_j[c]	Int. Chrom. σ_j[d]
1 - 60	-7.61	73.51	-231.72	199.34
61 - 120	-21.08	96.30	-1190.20	448.92
121 - 180	1.05	98.66	-2046.08	248.78
181 - 240	-1.49	95.48	-1415.66	299.04
241 - 300	3.93	108.55	-1420.20	295.80
301 - 360	5.66	105.40	-1307.92	230.81
361 - 420	11.57	100.48	-729.67	396.52
421 - 480	6.98	105.72	-290.26	280.69
481 - 540	-8.37	100.44	-150.69	394.25
541 - 600	-2.93	101.99	-700.70	210.88
601 - 660	16.55	99.63	23.39	239.18
661 - 720	-7.30	104.04	-20.96	189.35
721 - 780	-21.41	96.21	-1247.43	392.38
781 - 840	-1.52	107.97	-1556.82	253.66
841 - 900	1.05	85.03	-1495.66	102.61
901 - 960	8.01	102.39	-1004.27	207.81
961 - 1020	-2.91	113.15	-1024.23	302.38
1021 - 1080	-4.07	106.42	-1069.80	196.50
1081 - 1140	2.48	92.39	-1517.20	195.25
1141 - 1200	0.73	90.25	-1052.04	150.25
AVE = $\bar{\sigma}_x$[e]		99.20		261.72

[a]Equation 68, X(i) = F*(t).

[b]Equation 69, X(i) = F*(t).

[c]Equation 68, X(i) = IBL(t).

[d]Equation 69, X(i) = IBL(t).

[e]Equation 70.

baseline noise, that is Gaussian noise in the normal chromatogram. A normal baseline should be BLA and appears like Figure 13(B), while the integrated baseline appears as in Figure 13(C). By analyzing two more baselines similar to the one in Table 14, σ_N was found to be 98.67 (±0.38) and σ_I was 274.13 (±31.82). The important quantity is the ratio σ_I/σ_N, namely, NIF = 2.78.

Simulation of chromatographic peaks should suggest realistic column performance. A typical value for the column performance constant in Equation 63 and Equation 75 is r = 1500, along with t_0 = 150 seconds. Simulated chromatographic peak data were calculated using Equations 57 through 61 to form "noise-free" chromatograms (Table 15). Five, well-resolved peaks were generated such that each analyte has the same detector response factor (R_i), such as with an indirect mode detector. Volume fractions are chosen for the purpose of discussion, and should be used only to compare the normal and integrated chromatograms. The theoretical IMP factors are shown in Table 15, suggesting a marked improvement in detectability in the integrated chromatogram. Notice that the improvement increases with increased retention time. This is because the integration method compensates for the band broadening effect due to chromatographic retention.

Now it is possible to combine both baseline noise and chromatographic peak data to produce a simulated "real-life" chromatogram, via Equation 73. This is shown for successive dilutions in Figure 14. The peak data given in Table 15 correspond to the BLA

Table 15. True data and theoretical improvement factor (IMP) for simulated chromatograms

Peak Number	Peak t_R (s)	Max Height[a]	Area[b]	IMP (theoretical)(s)[c]
1	300	364.2	5000.0	4.94
2	450	210.3	5000.0	8.55
3	600	148.7	5000.0	12.10
4	750	115.2	5000.0	15.62
5	900	94.0	5000.0	19.13

[a]Equation 61 and Equation 63 with t_0 = 150 s, $R_i = 5 \times 10^6$, $V_i = 1.0 \times 10^{-3}$.

[b]Equation 60 with $R_i = 5 \times 10^6$, $V_i = 1.0 \times 10^{-3}$.

[c]Equation 75 using $\sigma_I/\sigma_N = 2.78$, t_0 = 150 s and r = 1500.

Figure 14. Simulated chromatograms at three different volume fractions

(A) Simulated chromatogram, with $V_i = 9 \times 10^{-3}$ and $R_i = 5 \times 10^6$ for all 5 peaks (Equation 73).

(B) Simulated chromatogram, with $V_i = 3 \times 10^{-3}$ and $R_i = 5 \times 10^6$ for all 5 peaks (Equation 73).

(C) Simulated chromatogram, with $V_i = 1 \times 10^{-3}$ and $R_i = 5 \times 10^6$ for all 5 peaks (Equation 73).

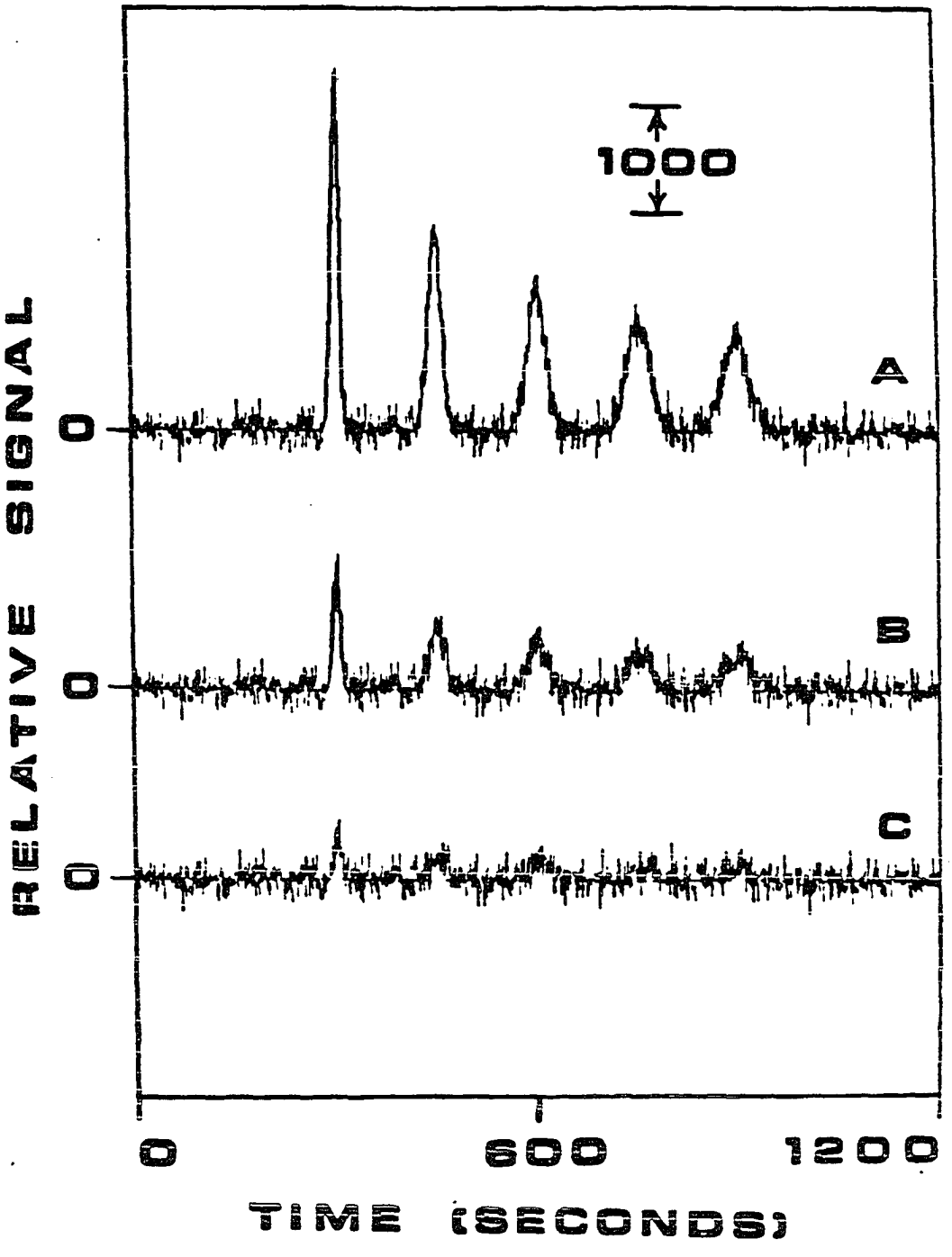
1000
A
B
C
0
0
0
RELATIVE SIGNAL
0
600
1200
TIME (SECONDS)

Figure 15. Integrated chromatograms at three different volume fractions

(A) Integrated chromatogram, integration of Figure 14(A) (Equation 74).

(B) Integrated chromatogram, integration of Figure 14(B) (Equation 74).

(C) Integrated chromatogram, integration of Figure 14(C) (Equation 74).

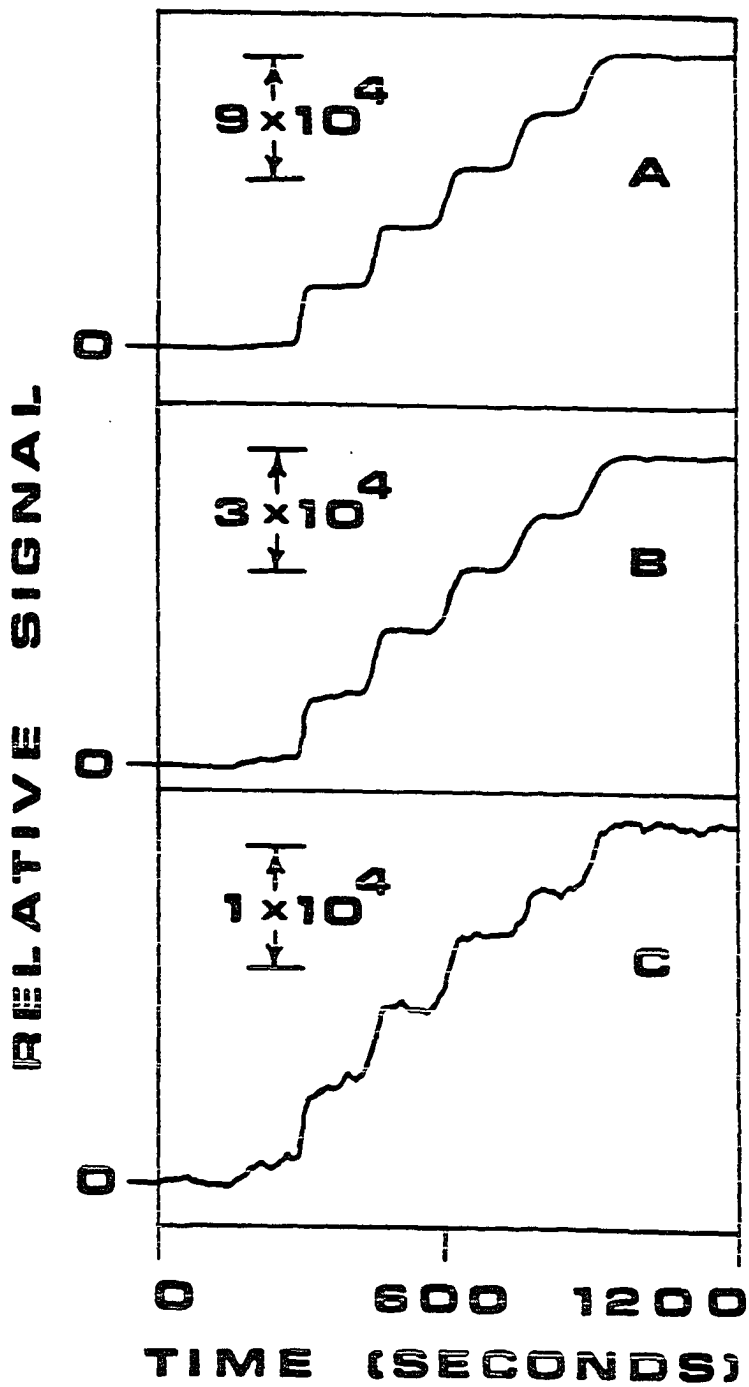
9x10^4
A
0
3x10^4
B
0
1x10^4
C
0
RELATIVE SIGNAL
0
600
1200
TIME (SECONDS)

chromatogram shown in Figure 13(C). Note that the detectability does not appear very favorable, especially for the later eluting peaks in Figure 14(C). By performing the running-total integration of the data in Figures 14(A)-14(C), using Equation 74, integrated chromatograms are obtained. The results are shown in Figure 15. Note the vertical scale used for each integrated chromatogram relative to the scale used in Figure 14. The improvement in detectability in the integrated chromatograms relative to the normal chromatogram is quite obvious.

It is necessary to study the precision and accuracy that this integration method provides, as compared to conventional approaches. Statistics concerning precision and accuracy can be addressed by simulating multiple injections via a fixed S(t) in Equation 72, but varying the baseline noise function F(t). Thus, it is assumed that no uncertainty in V_i exists, so the uncertainties in quantitation due only to the data handling can be studied. Three integrated chromatograms using Equation 74 on three different C(t) arrays for the same "sample" are shown in Figure 16. Note that Figure 16(A) is for the same sample as Figure 15(C). Determining the statistics of precision and accuracy in the quantitation of each signal will provide insight into reproducibility, but first, an explanation on how the signal is determined in this integration method is required.

Earlier, a σ_I value was stated. From this value a LOD for the integrated domain can be calculated as some number (typically 5) multiplied by σ_I. Deflections in an integrated chromatogram exceeding this LOD constitute an analytical signal. For a given analytical

Figure 16. Integrated chromatograms (Equation 74) of same peak data but different noise data in Equation 73, for $V_i = 1 \times 10^{-3}$, $R_i = 5 \times 10^6$

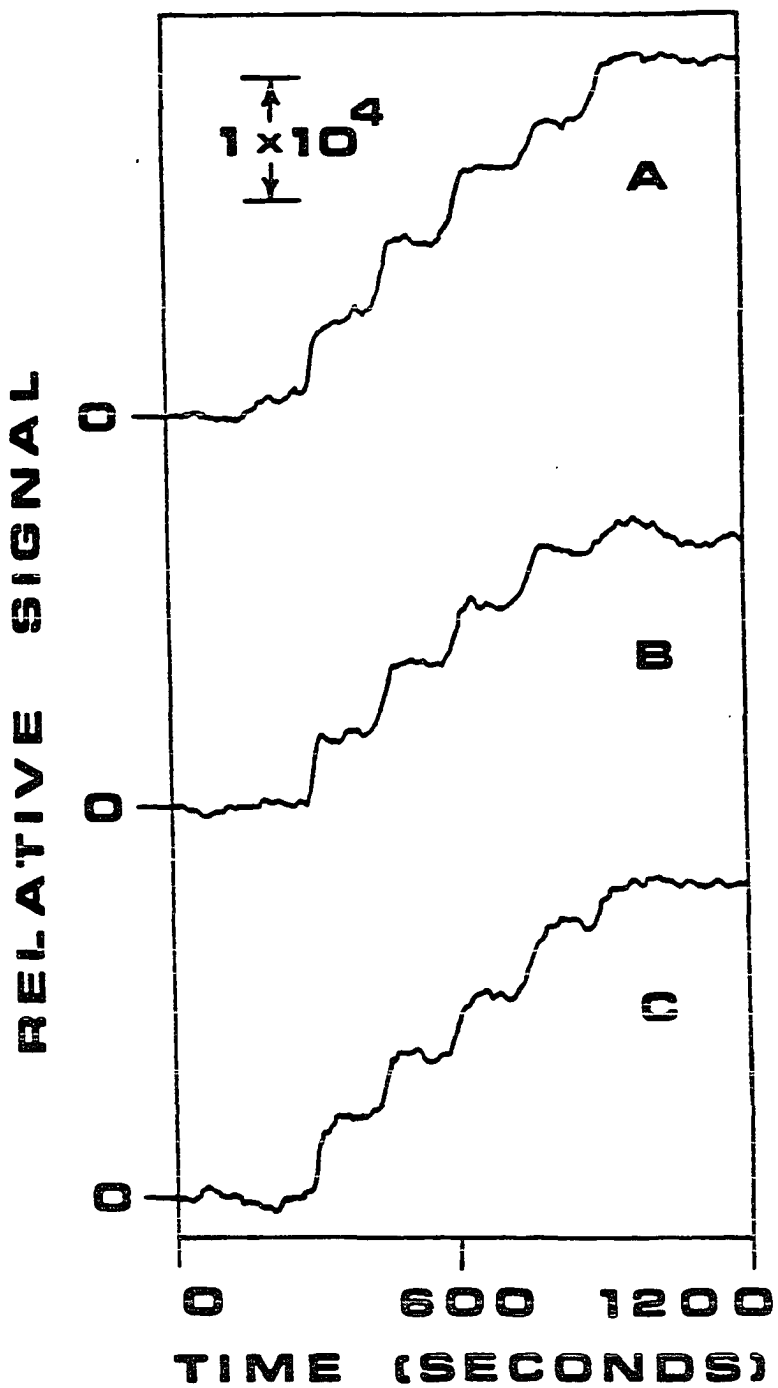
1×10⁴
A
B
C
0
0
0
RELATIVE SIGNAL
0
600
1200
TIME (SECONDS)

signal, a region on each side of the signal relatively close to having a slope of zero will be observed as can be seen in Figure 17. The quantity corresponding to the LOD, $5\sigma_I$, is shown for convenience. Since the slope may not be exactly zero in the two regions on either side of the signal, a least-squares linear regression is calculated for each section. The extrapolated linear regression lines are shown for the signal in Figure 17. The distance between the two lines at the inflection point of the analytical signal curve is the area of the original chromatographic peak, and thus, the signal of the analyte in the integrated chromatogram.

Precision of an analytical method can be discussed using the relative standard deviation. The standard deviation for the quantitation of three trials (σ_Q) relative to the average for the three trials (Q), multiplied by 100, will be used,

$$RSD\% = (\frac{\sigma_Q}{Q})100\% \tag{76}$$

Accuracy, likewise, is discussed by comparing the true value (T), given in Table 15, relative to the average of three trials (Q). A relative difference of these two quantities can be calculated by,

$$RD\% = (\frac{Q - T}{T})100\% \tag{77}$$

Note that the sign is important for this quantity in comparing analytical methods.

Three other analytical methods used to quantitate chromatographic data can be compared to this integration method. Method I employs

Figure 17. Demonstration of the quantitation of a signal in an integrated chromatogram; $V_i = 1 \times 10^{-3}$, $R_i = 5 \times 10^6$, and $t_R = 600$ s

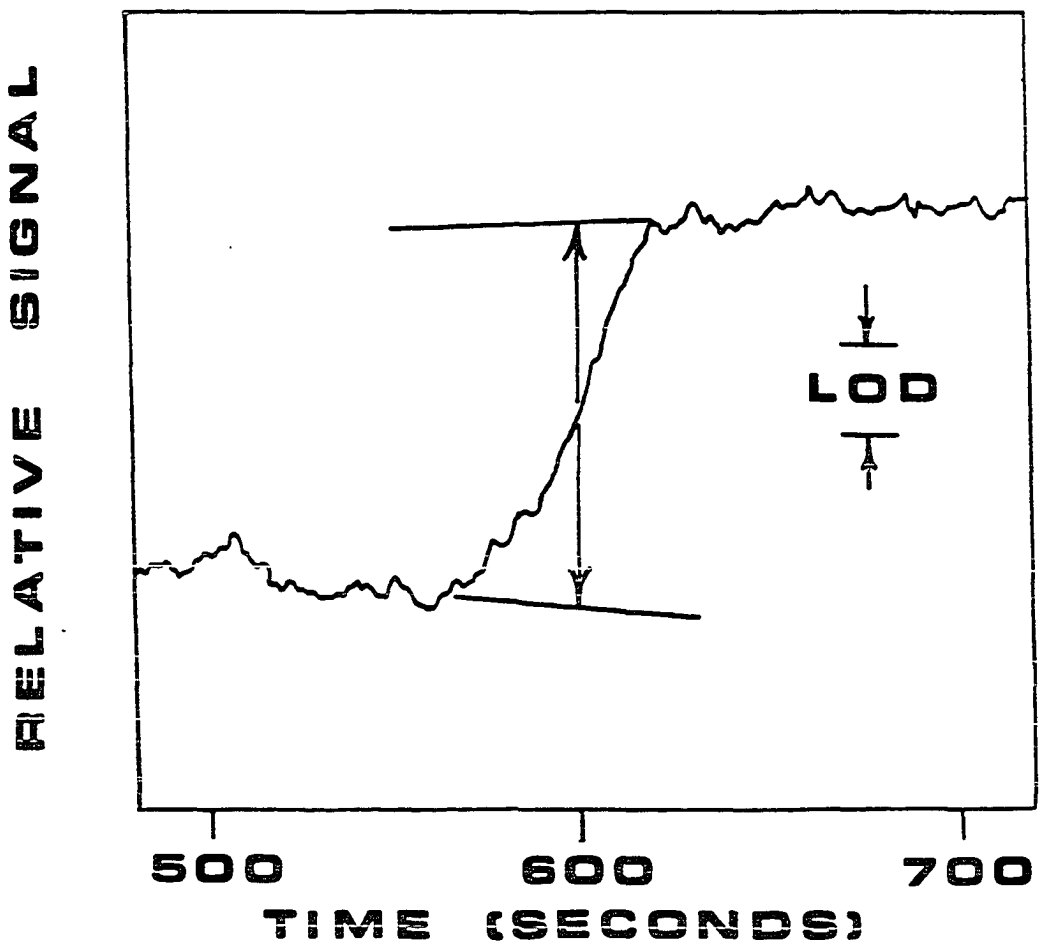
RELATIVE SIGNAL
LOD
500
600
700
TIME (SECONDS)

defining the peak height as the measurement of the largest signal on an interval in a normal chromatogram known to contain a peak, but exact knowledge of the retention time is not known. Method II also determines the peak height in a normal chromatogram, but the retention time must be known to the same precision as the data acquisition rate. In Method II the peak height is measured at precisely the retention time, thus, not necessarily providing the largest signal for a given peak. Method III provides the peak area by summing the signals in a normal chromatogram, but only those signals greater than or equal to some confidence level (99). This method, in essence, treats each data point as a separate event, and suggests no implicit correlation of the data for an eluting chromatographic peak. For Method III, only those data points greater than $3\sigma_N$ are added to the total for a given peak. The integration method described in this work will be labeled Method IV.

Results were obtained for the application of the four quantitation methods for the three samples shown in Figure 14, using three arbitrarily chosen baseline noise arrays. The standard deviation (σ_Q) of the three signals obtained for a given peak were calculated, and the "true" values were known (Table 15) so Equations 76 and 77 could be applied. The results for studying precision are given in Table 16, while the accuracy data are given in Table 17. The following comparisons relative to Method IV can be made from the data of these two tables. Method I clearly produces a signal that is very inaccurate, biased to higher values compared to the true values,

Table 16. Precision (RSD%) for average of three trials

Peak Number	Max Ht[a] (t_R Not Assumed)	Height[b] @ t^R	Peak Area[c]	This Work[d]
Sample 1[e]				
1	7.4	14.0	3.4	8.3
2	6.4	59.5	19.1	6.8
3	11.7	46.6	39.2	8.6
4	_f	_f	_f	18.8
5	_f	_f	_f	20.8
Sample 2[e]				
1	3.9	4.5	5.5	2.8
2	7.5	18.2	4.4	2.4
3	6.0	12.0	4.3	3.0
4	5.4	45.1	6.4	6.4
5	8.7	16.3	32.5	6.2
Sample 3[e]				
1	1.4	1.5	0.68	0.94
2	2.8	5.9	1.3	0.83
3	2.4	3.7	2.4	1.0
4	0.47	10.6	2.5	2.1
5	8.5	6.2	1.9	2.0

[a]Method I.

[b]Method II.

[c]Method III.

[d]Method IV.

[e]Peak number as in Table 15.

Sample 1: $V_i = 1 \times 10^{-3}$; Sample 2: $V_i = 3 \times 10^{-3}$.

Sample 3: $V_i = 9 \times 10^{-3}$; Samples 1, 2, and 3: $R_i = 5 \times 10^{6}$.

[f]Undefined, since $\sigma_Q > Q$.

Table 17. Relative % difference (RD%) from true value for average of three trials

Peak Number	Max Ht[a] (t_R Not Assumed)	Height[b] @ t^R	Peak Area[c]	This Work[d]
Sample 1[e]				
1	+38.4	-4.2	-53.0	+1.3
2	+82.1	-12.0	-84.1	+11.8
3	+134.7	-30.7	-86.6	+9.8
4	_[f]	_[f]	_[f]	+2.8
5	_[f]	_[f]	_[f]	-14.2
Sample 2[e]				
1	+10.3	-1.3	-6.8	+0.43
2	+22.7	-3.9	-15.9	+3.9
3	+43.0	-10.3	-30.8	+3.3
4	+50.8	-38.4	-50.0	+0.92
5	+62.7	+24.1	-71.1	-4.7
Sample 3[e]				
1	+2.3	-0.45	-0.91	+0.14
2	+6.7	-1.3	-3.9	+1.3
3	+12.3	-3.4	-5.8	+1.1
4	+14.0	-12.8	-8.4	+0.31
5	+16.7	+8.0	-16.3	+1.6

[a]Method I.

[b]Method II.

[c]Method III.

[d]Method IV.

[e]Peak number as in Table 15.

Sample 1: $V_i = 1 \times 10^{-3}$; Sample 2: $V_i = 3 \times 10^{-3}$.

Sample 3: $V_i = 9 \times 10^{-3}$; Samples 1, 2, and 3: $R_i = 5 \times 10^{6}$.

[f]Undefined, since $\sigma_Q > Q$.

although the precision is reasonably good. Method II has no expected bias, but the precision and the accuracy are both relatively poor. Because of the confidence level criterion imposed upon Method III, the peak area is substantially less than the true values, as previously reported (99). The precision of Method III is comparable to Method IV, except at low volume fractions. In general, the predicted improvement in detectability (IMP, Equation 75) is substantiated by the observations made from Tables 16 and 17. For Sample 1, the peaks at 750 and 900 seconds cannot be quantitated by Methods I through III, while the new integration method (Method IV) works quite well. It is interesting to note that the signals shown in Figure 16, together with statistics given in Tables 16 and 17 (Sample 1, Method IV), are at an average signal-to-noise (S/N) of 7.30. For this system at the LOD (S/N=2), a volume fraction of 2.74×10^{-4} is calculated. Comparatively, the other three methods are essentially useless even at a volume fraction of 1×10^{-3}.

Conclusion

Because the success of this integration method is strongly dependent upon the behavior of the original baseline, it is worthwhile to study a few experimentally obtained "real" noise arrays. A few typical detection systems were studied and the results supported the data previously provided by the simulation. One of the detection systems studied is described in the Experimental section. The importance of minimizing the effects of D(t) and R(t) in Equation 65

through proper experimental considerations can not be emphasized enough. In applying this integration method, it is essential to use the baseline adjustment procedure as discussed in the Theory section. Once baseline adjusted, it is a simple task to generate the running-total integrated chromatogram from a normal chromatogram. Similar to any other quantitative method, rejection of spurious results can be made by proper statistical tests. That is, anomalous features in an integrated chromatogram can be dealt with just as is conventionally done in a normal chromatogram for such things as glitches, pseudo-peaks, impurity peaks, etc. This integration method should give better LOD values, that are essentially independent of chromatographic dilution effects. Furthermore, this method can be readily incorporated into typical data handling systems currently in use for chromatography. Finally, the method should have general applicability for any data set in which the experimental noise, be it Gaussian or otherwise, is uncorrelated along a given abscissa and an analytical signal is correlated along the same abscissa. The abscissa may be time, wavelength, frequency, etc.

CHAPTER 7.

COMPARISON OF AN INTEGRATION PROCEDURE TO FOURIER TRANSFORM AND DATA AVERAGING PROCEDURES IN CHROMATOGRAPHIC DATA ANALYSIS

Introduction

In the last chapter an integration procedure for improving the limit of detection (LOD) in chromatographic systems was presented. The integration procedure, though not a data averaging procedure or a simple data frequency filtering procedure, is a technique that suggests data smoothing has occurred in some way. This aspect of the integration procedure was not previously discussed in sufficient detail, within the context of other data "enhancing" procedures. Presented here are some of the key differences between integration and other common data smoothing procedures, as applied to chromatographic data.

Fourier Transform Concepts Applied to Integration

Fourier transform (FT) concepts are readily available in the literature, and will be the basis of this presentation. For this purpose a general review of the application of FT concepts is quite useful (106). If $f(t)$ is a data array originating in the time domain, then $F(\omega)$ is a data array in the frequency domain obtained via a suitable FT. Further, a mathematical relationship exists for the calculation of the nth derivative of the time domain array, by manipulation of the frequency domain array (106),

$$\frac{d^n f(t)}{dt^n} \overset{\rightarrow}{\leftarrow} (i\omega)^n F(\omega) \tag{78}$$

where the symbol $\overset{\rightarrow}{\leftarrow}$ indicates the reversible nature of the FT, t is time, ω is angular frequency, and $i = \sqrt{-1}$. The FT from the time domain to the frequency domain is given by

$$F(\omega) = \int_{-\infty}^{+\infty} f(t)\cos(\omega t)dt \tag{79}$$

The reversible nature of the FT allows, also

$$f(t) = \int_{-\infty}^{+\infty} F(\omega)\cos(\omega t)d\omega \tag{80}$$

The calculations are typically done on a computer, so data arrays are employed, with indexing, and the integral is replaced by an approximated summation of differential elements. So, Equation 79 is calculated as

$$F(\omega_j) = 2 \sum_{i=1}^{N} f(t_i)\cos\{\omega_j t_i\} \tag{81}$$

where each element in the frequency domain, ω_j, is calculated on an individual basis from the entire time domain array, of elements t_i. A similar expression can be written for the inverse FT back to the time domain. From Equation 80 is derived,

$$f(t_i) = 2 \sum_{j=1}^{N} F(\omega_j)\cos\{\omega_j t_i\} \tag{82}$$

In the calculations to follow, the indexing of i and j were performed with the same N value. Equations 81 and 82 were tested and the computer program used preserved the identity of the simulated chromatographic noise and peak data.

For a typical chromatographic system with a detection time constant and data collection of 1 second, all frequency information within a chromatogram is contained between 0 and 1 Hz. The FT (into the frequency domain) of "white" noise, such as that used in the last chapter, produces a distribution of data, uniform in amplitude and frequency, between 0 and 1 Hz. For a chromatographic peak, without noise, the FT into the frequency domain produces a spectrum that contains most of the peak information at the lower frequency end. The extreme limit of this result, is that for an infinitely wide peak in the time domain, the FT into the frequency domain is defined by only the zero point value. An offset baseline in the time domain can be thought of as an infinitely wide peak.

It is interesting to describe the integration procedure in the context of Equation 78. Collecting the entire chromatogram prior to any integration allows for an objective baseline adjustment (BLA) procedure, as described earlier. Any baseline offset or long-term drift in the time domain will be observed as extremely low-frequency data in the frequency domain via a FT. The BLA procedure, prior to integration, effectively reduces much of this kind of "noise" in the original chromatographic data array, and is equivalent to introducing a very low frequency cut-off in the FT frequency spectrum. In

principle, BLA can also be achieved by an analog high-pass filter with a frequency much lower than that of any chromatographic event.

Upon applying running-total integration to the BLA data array an integrated chromatogram is obtained. According to Equation 78 this operation is equivalent to substituting n = -1. An important observation is that integration in the time domain manifests itself as division by $i\omega$ in the frequency domain. Thus, higher frequency components of the data are attenuated, while lower frequency components are accentuated. Since most of the original peak information is at lower frequencies, and noise is spread throughout the frequency domain, the implication of Equation 78 for integration is enhanced detectability in the integrated chromatogram relative to the original chromatogram. Some of these points can be seen after consideration of Figure 18. The FT from the time domain to the frequency domain (Figures 18(B) and 18(D)) was accomplished with Equation 81. Another feature is the use of the whole peak, or peak area, instead of just the peak height for determining detectability. In terms of Equation 78, the shape of an integrated peak, as compared to the original peak, produces frequency domain data that favor the former in S/N. This concept has seemingly been overlooked, or at least not effectively applied in chromatography. The observation that integrated data provide better LOD values as compared to peak height data in graphite furnace/atomic absorbance work (107) means that other fields of study have incorporated this point. Yet, the integration procedure outlined in the last chapter goes further and suggests that

Figure 18. Comparison of a typical and integrated peak in time and frequency domains

(A) Typical peak in time domain with the horizontal scale only 80 data index units, in (A) only.

(B) FT into the frequency domain of (A).

(C) Running-total integration of (A).

(D) FT into the frequency domain of (C).

Note that the vertical axes are not at the same scale. (A) and (C) are compared to each other, while (B) and (D) are to be compared relative to each other. That is, the signal in (C) is roughly 5 times that of the peak height in (A).

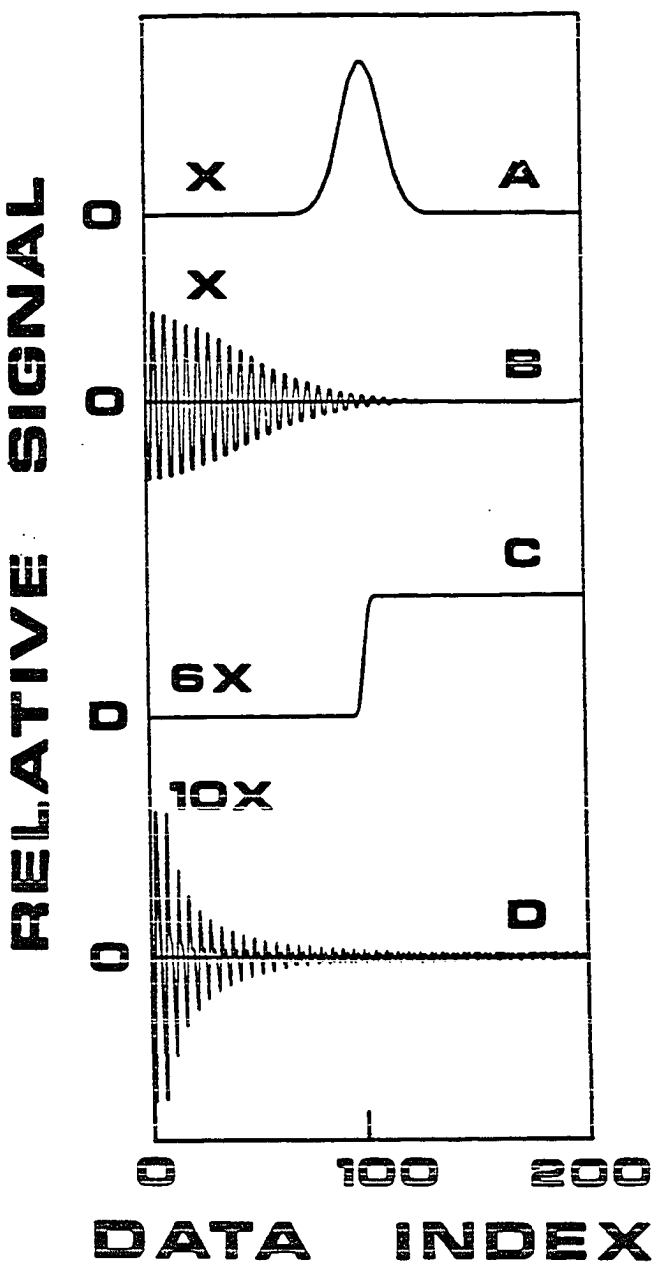
RELATIVE SIGNAL
X
A
0
X
B
0
C
6X
0
10X
D
0
0
100
200
DATA INDEX

detection is possible even if the original data do not provide peak heights that are above the "detection limit". It is also suggested that the temporal information for a series of events (chromatographic resolution) need not be degraded while noise is reduced.

General Comparison of Techniques

A comparison can be made between the integration procedure proposed earlier (Chapter 6) and both a FT procedure and a data averaging procedure. The FT and data averaging procedures are outlined in the literature (106). This comparison is made for procedures that do not significantly broaden chromatographic peak widths by loss of pertinent frequency information within the data. The integration procedure inherently provides integrated signals that are identical in width as the original chromatographic data. This is obvious in Equation 78 with $n = -1$. Even though the high frequency components are attenuated by $i\omega$, they are never discarded, as shown in Figure 18. One can always get back the original chromatogram from the integrated chromatogram by doing a formal differentiation (Equation 78 with $n = 1$). The exact same number of data points describe the chromatographic event before or after integration, so no loss in <u>real</u> chromatographic resolution results. There is, however, a loss in <u>apparent</u> resolution. This is because visual perception is better adapted to distinguish large changes in slopes (differentiated chromatograms) versus small changes in slopes (integrated chromatograms). The important point is that resolution also depends

on S/N. While differentiated (108) or unintegrated chromatograms emphasize the inflection points more, they are also more noisy, compared to integrated chromatograms.

A FT procedure based upon truncation in the frequency domain provides smoothing that translates into increased S/N upon taking the inverse FT back to the time domain (106). In this procedure, knowledge of chromatographic peak frequency components allows one to truncate the FT in the frequency domain at frequencies above the point where the peaks no longer contribute. For this method, there is a trade-off in the process of improving the S/N. By lowering the frequency of truncation, integrity (i.e., peak width, resolution, and height information) of the chromatographic data will decrease while the S/N increases. Note that the high frequency components are lost forever, and indeed there is a real loss of resolution. Demonstration of this FT-truncation procedure can be seen in Figure 19. The original "white" noise is shown in Figure 19(B), while the FT into the frequency domain (Equation 81) is Figure 19(A). Setting to zero all points above a threshold frequency and subsequent inverse FT (Equation 82) back to the time domain produces the observed smoothing pattern in Figures 19(B) through 19(E).

A data averaging procedure is essentially taking the original data and applying a running-average (or a time constant) to the data. For data limited by "white" noise, the theoretical improvement in S/N by data averaging is $\sqrt{N}$ were N is the number of points used to calculate the average value at a given point in the chromatogram.

Figure 19. "White" noise study

(A) "White" noise in the frequency domain.

(B) "White" noise in the (original) time domain.

(C) Noise in time domain after truncation (set to zero) of frequency indices 101 to 200 and subsequent inverse FT.

(D) Same method as (C), with indices 41 to 200 truncated.

(E) Same method as (C), with indices 21 to 200 truncated.

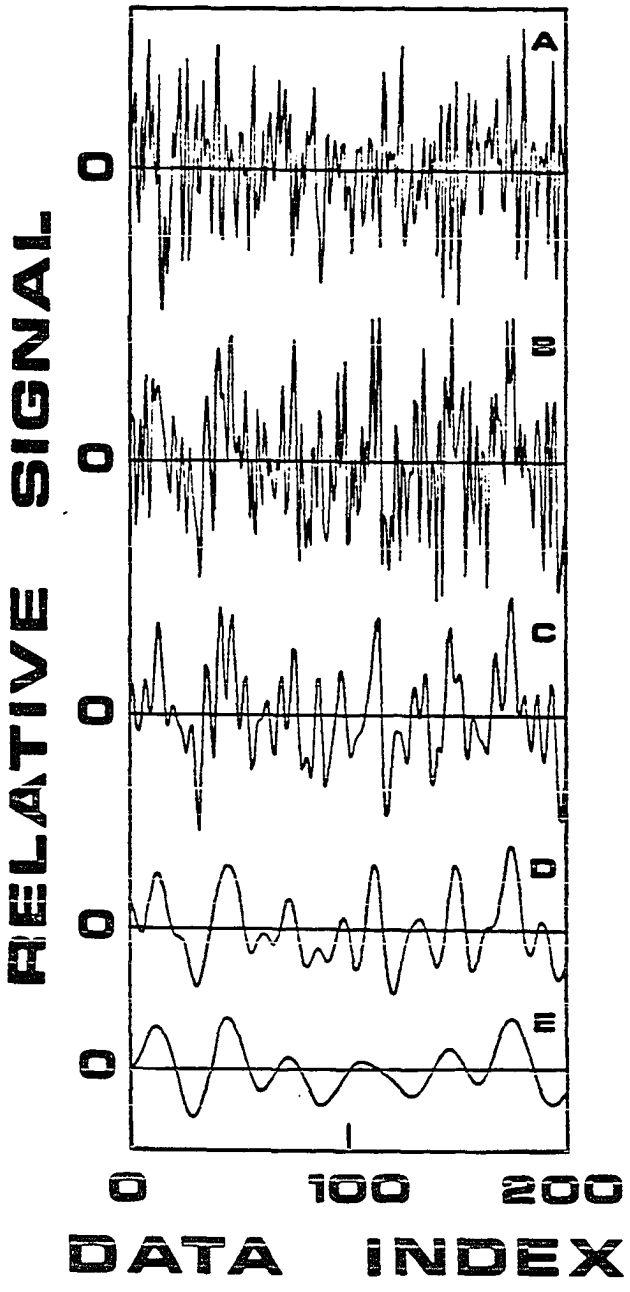
A
B
C
D
E
0
0
0
0
0
RELATIVE SIGNAL
0
100
200
DATA INDEX

Thus, if the data were originally collected with a 1-second time constant, the data averaging procedure effectively provides a N-second time constant. It is anticipated that data averaging will improve the S/N and ultimately the LOD at the expense of broadening the chromatographic peak data. This is because once again the high frequency components are lost forever. Also, the number of significant points is reduced by 1/N. The smoothing of noise, as shown in Figure 19 for the FT method, is similar in appearance to data averaging.

The chromatographic detector noise and peak simulation utilized in Chapter 6 provided data that were subjected to each of the three procedures outlined. Upon treating a given data array the signal and the resulting noise must be measured for each procedure. For the data averaging and FT procedure, the signal is the peak height. The signal for the integration procedure is determined, as the height of the inflection in the integrated data array. The noise is determined statistically as 5σ noise. The S/N value determined from the original data array acts as a reference point for the three procedures. Other researchers found that integration of noise produces increased uncertainty in quantitation with increased integration time (109). Effectively, the larger the number of points that must be integrated to define a peak, the larger the uncertainty in the quantitative results. This suggests that the use of a fixed "event" width, as used in Chapter 6, is not adequate in providing the noise value for the integrated baseline. One can instead use a slowly increasing "event"

width to define the LOD for the integrated data file. This slowly increasing "event" width is similar in essence as the idea of slowly increasing the time constant applied to the data in the original chromatogram (110). For the results obtained, using Gaussian peaks, the event width is equal to $2.55(W_{\frac{1}{2}})$, where $W_{\frac{1}{2}}$ is the width of the peak at half height. This is equivalent to $\pm 3\ \sigma_p$, where σ_p is the peak standard deviation. Accordingly, σ is linearly related to retention by (90)

$$\sigma_p = \left(\frac{t_o}{r}[k(1+k)]\right)^{1/2} \tag{83}$$

for k > zero, where t_o is the dead time, r is the column efficiency (a constant for similar analytes), and k is the solute capacity factor, which is defined in the conventional way. By varying the $W_{\frac{1}{2}}$ for the peak data, the relative S/N values for the three procedures (integration, FT-truncation, data averaging) were calculated. The results of these calculations are shown in Figure 20. Note that the data averaging procedure was facilitated using N = 4 (4-second time constant). For visual reference in Figure 21, the results of applying the integration and FT procedures can be compared to the original data for a peak width $W_{\frac{1}{2}}$ = 31.1 data units. Some general trends concerning Figures 20 and 21 can be made. The data averaging procedure does not provide a full factor of 2 improvement in S/N as suggested by theory for a 4-point average. This is due to loss of peak height in the averaging process. FT followed by truncation of frequency components that do not contain signal information, and subsequent inverse FT,

produces an improved S/N as compared to data averaging. The concern with FT "filtering" procedures is in throwing away frequency information pertaining to the analytical signal. The data in Figures 20 and 21 for the FT procedure were calculated at the limit before peak distortion occurs due to over-filtering in the frequency domain, thus obtaining the best S/N possible without severe peak distortion. The integration procedure was applied as reported in Chapter 6. For chromatographic detection systems limited to a great extent by "white" noise, it is clear both graphically (Figure 20) and visually (Figure 21) that the integration procedure provides the greatest improvement in S/N relative to the original data array.

Application of the integration procedure would allow quantitation of unresolved peaks that may be impossible to quantitate, or even to "detect", in the original data array. Once quantitated, the signal width in the integrated time domain can be compared via Equation 83 to diagnose, for a given chromatographic system, the presence of peak overlap and to what extent. Thus, the integration procedure may provide the means to quantitate unresolved peaks that could not be quantitated initially in the original data.

Application of Integration Procedure with Real Chromatographic Data

Up to this point, the discussion has dealt with simulated noise and peak data. The assumption was made that chromatographic detector noise is often randomly distributed, in time, about a mean value, such as with "white" noise. An example of real data from an ion

Figure 20. S/N relative to the original data as a function of chromatographic peak width a half height, $W_{\frac{1}{2}}$
(A) Integration procedure, (B) FT procedure, (C) data averaging procedure.

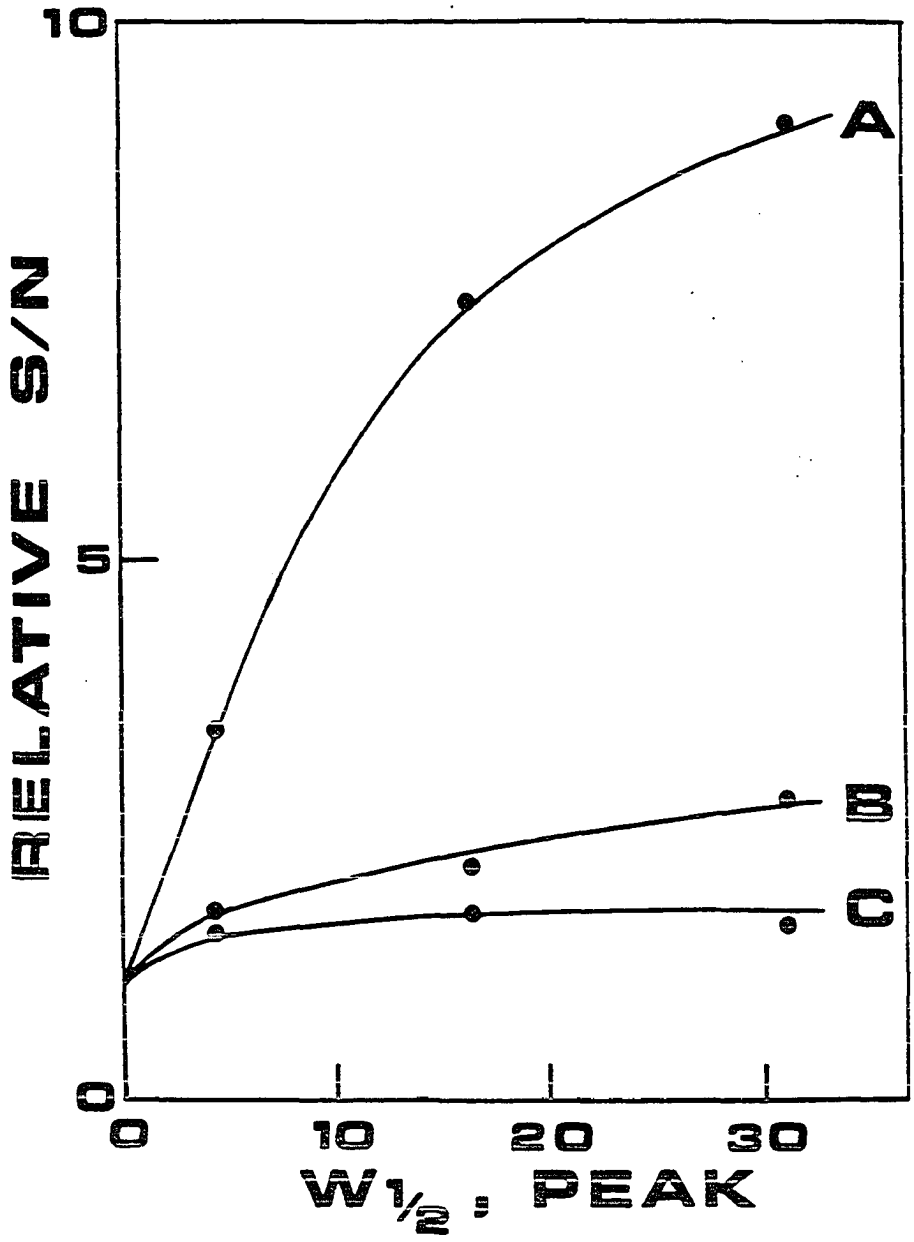
10
5
0
RELATIVE S/N
A
B
C
0
10
20
30
W1/2 : PEAK

Figure 21. Comparison of the original data (A), applying integration procedure to A (B), and applying FT-truncation procedure to A (C)

Scale for each curve is relative and is designated in terms of X. So, the height of B is about 25X the height of A.

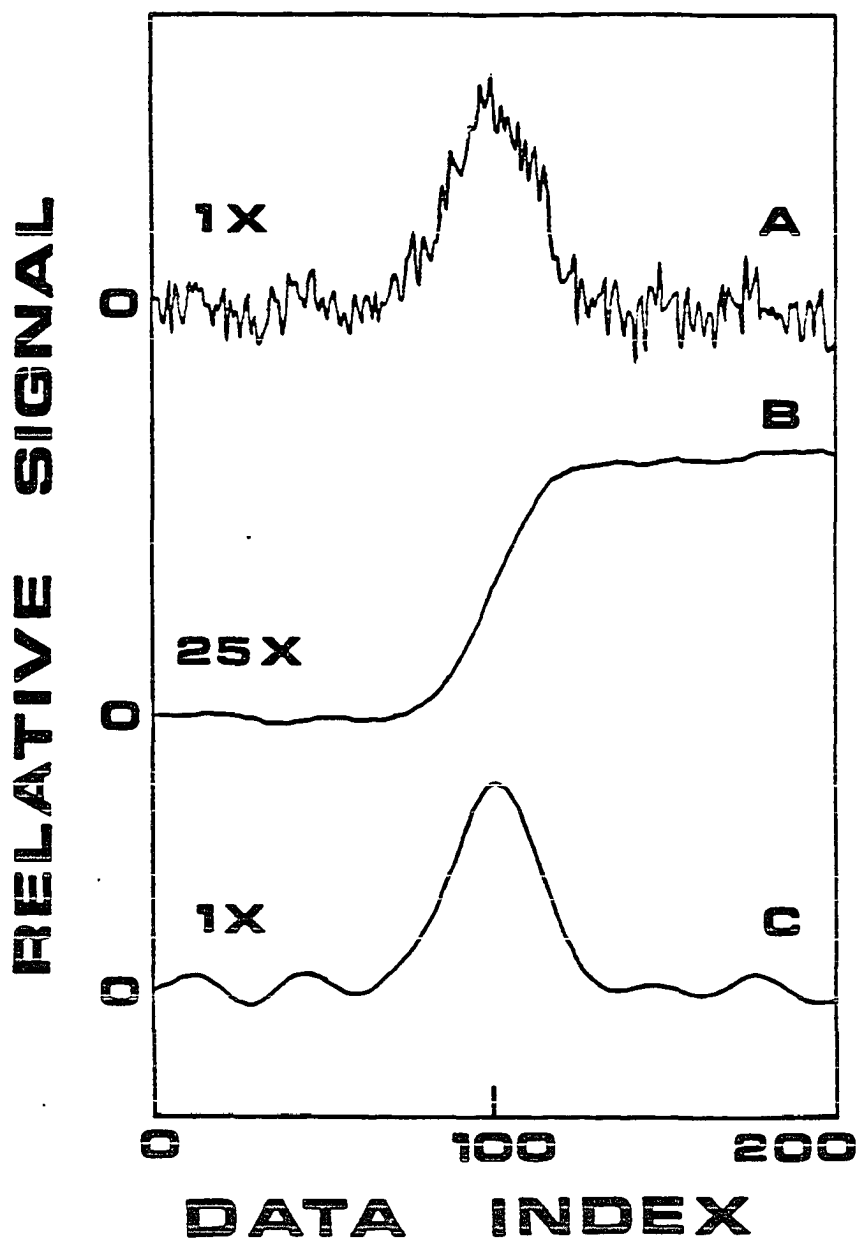
RELATIVE SIGNAL
1X
A
0
B
25X
0
1X
C
0
0
100
200
DATA INDEX

chromatography separation followed by UV absorbance detection was studied with the integration procedure. The chromatogram studied recently appeared in the literature (right side of Figure 2, page 59) (11). Applying the integration procedure to this chromatogram produced an integrated noise value 4.3 times that of the noise in the original chromatogram for an event width of 120 data collection units. This is roughly 1.5 times larger than the value obtained in the simulations of Chapter 6, suggesting that the real-life detector is not exhibiting "white" noise exclusively, but contains some long-term drift components. However, the factor of 1.5 also suggests that white noise is not a bad approximation to the real noise. Figure 22 contains both the original and integrated data for the peak in the chromatogram that elutes at approximately 13.3 minutes. By establishing confidence limits in both the original and integrated time domains, and measuring the peak signal in each, an improvement in the LOD of 11.6 was determined. In the context of absorbance detection in chromatography this corresponds to an extension in absorbance detectability from 2×10^{-4} AU to 1.7×10^{-5} AU. The integration procedure may also be quite useful when coupled with other commercially available detectors. One expects that fluorescence detectors will behave quite similarly as absorption detectors. However, refractive index detectors are much more sensitive to changes in temperature, pressure, solvent composition, etc., so that white

Figure 22. Application of integration procedure with real chromatographic data

(A) Section of original data from Figure 2, page 59 (11).

(B) Same section of data as in A after integration procedure was applied to the entire chromatogram. Scale for each is in terms of X. So, the height of B is about 50X the height of A. The peak in A is the ion chromatography separation/UV absorbance detection of SO_4^{2-} from 20 uL injected amount of 1.2×10^{-3} N solution, using 1×10^{-3} M potassium citrate eluent.

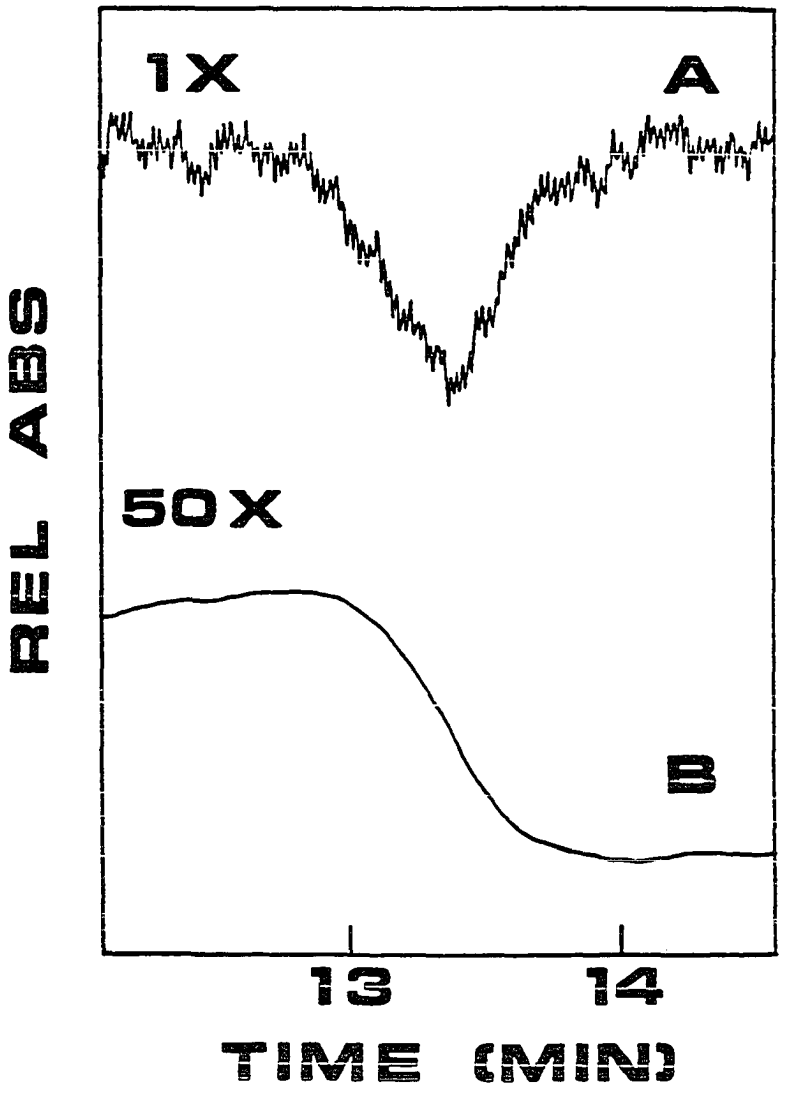
1X
A
50X
B
REL ABS
13
14
TIME (MIN)

noise may not be a good approximation. But then all data smoothing routines will fail when noise has frequency components similar to those of the signal.

Conclusion

The integration method is fully equivalent to the FT representation of Equation 78 with n = -1. However, since integration can be done in real time by summation (running total), there is no need to perform the forward FT, division by $i\omega$ in the frequency domain, followed by the inverse FT. The integration method is more effective than most frequency based filters, as shown by Figures 20 and 21. This is concurrent with preserving the integrity of the chromatographic resolution information, which the integration method does easily since no loss of resolution occurs during the application of the method. Other S/N improvement filters should be compared according. For cases where standard chromatographic software will not even recognize the existence of "peaks" because of poor S/N, the integration procedure may still be able to provide peak recognition and some quantitative information. After such a recognition, one may then use chromatographic information (σ_p) to refine the quantitation by defining the limits of integration and to test for unresolved peaks. The application of FT concepts (106) has been useful in this study, and compliments similar studies and applications, such as a LC band broadening study using FT techniques (111), and the use of cross-correlation techniques in S/N enhancement (112). The FT approach may

be useful in the analysis of chromatographic noise exhibited by different detectors. From this, the feasibility of using integration to improve detectability can be decided.

CHAPTER 8.

LASER-BASED CIRCULAR DICHROISM DETECTOR FOR CONVENTIONAL AND MICROBORE LIQUID CHROMATOGRAPHY

Introduction

Selective detection and study of optically active chemical species has developed into an important area of analytical research. Circular dichroism (CD) has shown good promise in this area of research (113-116), while nuclear magnetic resonance and optical activity detection have also been very useful (117). Since CD is inherently a "second order" absorbance measurement, many investigations have been in the area of CD instrument calibration and performance improvement (113, 118, 119). The ability of CD to provide valuable structural information about chemical species in a variety of matrices has driven researchers to attempt to overcome instrumental difficulties. Many interesting CD applications have been reported, such as a chiral metal complex inversion study (120), a critical micelle concentration determination (121), solute-induced drug discrimination (122), nicotine analysis in real samples (123), and opium alkaloid determinations (124), to name a few. These studies all employ CD as a wavelength-scanning spectrometric technique, for a sample measured in a "static" mode. This is in contrast to measuring a sample in a "dynamic" mode, in which the sample concentration changes with time, such as chromatography coupled with CD detection.

A gas chromatography-CD system provided detectability down to roughly 10 to 50 micrograms (125). High performance liquid chromatography coupled with circular dichroism detection (HPLC-CD) was demonstrated by interfacing an LC system to a CD spectrometer originally designed for static mode operation (126, 127). A 3 μg limit of detection (LOD) for L-tryptophan using HPLC-CD was reported (127). Urless stopped-flow techniques are used, single wavelength detection is employed to provide a selective detection system for either a single species or a certain class of CD active compounds.

While the original work in HPLC-CD provides ample selectivity (126, 127), a future direction in HPLC is towards microbore chromatography (2, 6, 7). The inference is that the detection system, be it CD or otherwise, must be compatible with the rest of the microbore system. Thus, it is essential to move away from using a CD spectrometer that has been converted into an LC detector, and move towards a detector designed for a smaller volume simultaneous with either maintaining or, preferably, improving analyte detectability (128). This direction is most easily taken by designing a laser-based detector that provides better power throughput, collimation and focusing superiority, along with spectral and polarization purity, as compared to conventional light sources. These characteristics afforded by a laser-based system are essential in optimizing small volume detection for microbore chromatography (2, 128) using CD detection, which is facilitated by polarization techniques and optics (114).

An improvement in mass and differential absorbance detectability must be demonstrated in order to justify the development of a laser-based CD detector. Since the laser is known to operate at relatively high flicker noise levels at lower frequencies (129), the goal of this research was to overcome this difficulty by polarization modulation of the laser light at higher and higher frequencies (ca 100 kHz to 10 MHz) until an optimum signal-to-noise ratio for the CD detection system was obtained. The results will be reported here and compared to previous work in the area of HPLC-CD analysis. A HPLC-CD system would find good utility in the analysis of complex mixtures of either optically-active metal complexes (130) or amino acids (131), for example. Because interest in the HPLC analysis of metal complexes has grown recently (132-134), the detection system reported here will be demonstrated with a reversed-phase (RP) ion-pair HPLC separation of metal complexes outlined in one of the earlier papers (134). Both conventional and microbore HPLC-CD will be investigated.

Theory

CD is defined as the difference in absorbance of left-circularly polarized light (LCPL) and right-circularly polarized light (RCPL). The CD quantity, $\Delta\varepsilon$, can be related to the molar absorptivities of LCPL and RCPL as

$$\Delta\varepsilon = \varepsilon_L - \varepsilon_R \tag{84}$$

where L denotes LCPL and R denotes RCPL. Multiplication of both sides of Equation 84 by pathlength (b, in cm) and concentration (C, in M) yields

$$\Delta A = \Delta\varepsilon bC = \varepsilon_L bC - \varepsilon_R bC = A_L - A_R \tag{85}$$

where absorbance, A_i, is defined in the conventional way, for the arbitrary subscript i,

$$A_i = \log\left(\frac{I_{o,i}}{I_i}\right) = \varepsilon_i bC \tag{86}$$

with $I_{o,i}$ the incident beam intensity and I_i the transmitted beam intensity, using the base ten logarithm. Substituting into Equation 85 using Equation 86 for i=L for LCPL and i=R for RCPL.

$$\Delta A = \log\left[\frac{I_{o,L}}{I_L}\right] - \log\left[\frac{I_{o,R}}{I_R}\right] \tag{87}$$

Since Equation 84 dictates that $\varepsilon_L > \varepsilon_R$ for $\Delta\varepsilon$ to be positive, this requires $I_L < I_R$ (for $I_{o,L} = I_{o,R}$), or,

$$\Delta I = I_R - I_L \tag{88}$$

Since $I_{o,L}$ and $I_{o,R}$ are not exactly the same in practice (due to slight imbalance in the modulation), the difference can be arbitrarily expressed as

$$\Delta I_o = I_{o,L} - I_{o,R} \tag{89}$$

This represents the offset from true null. Rearrangement of Equation 87, substitution of Equation 88 and Equation 89, and conversion to the natural logarithm gives,

$$\Delta A = [\frac{1}{2.303}]\ln[(1 + \frac{\Delta I_o}{I_{o,R}})(1 + \frac{\Delta I}{I_R})] \tag{90}$$

Taking the exponential of both sides, assuming $\Delta A << 1$, and multiplication of the right side of Equation 90 yields,

$$\Delta A = [\frac{1}{2.303}][\frac{\Delta I}{I_R} + \frac{\Delta I_o}{I_{o,R}} + \frac{\Delta I_o \Delta I}{I_R I_{o,R}}] \tag{91}$$

Using Equation 86 and solving for I_R provides

$$I_R = [\frac{I_{o,R}}{1 + 2.303A_R}] \tag{92}$$

Substituting Equation 92 into Equation 91 while neglecting the insignificant term $(\frac{\Delta I_o \Delta I}{I_R I_{o,R}})$, and solving for ΔI yields,

$$\Delta I = \frac{2.303\Delta A I_{o,R} - \Delta I_o}{1 + 2.303A_R} \tag{93}$$

The definition of ΔI_o in Equation 89 was arbitrary, experimentally the sign can be either positive or negative. Also, for the purpose of Equation 93 the subscript R can be neglected and absorbance "average" can be employed. These factors will allow Equation 93 to be expressed as

$$\Delta I = \frac{2.303\Delta A I_0}{1 + 2.303A} \pm \Delta I_0(1 - 2.303A) \qquad (94)$$

This, then, is the complete description of the observed signal, ΔI, as it relates to the experimental parameters. Note that the signal, ΔI, is affected by the background absorbance (i.e., is attenuated) by the term, $1 + 2.303A$. Also note that the second term, containing ΔI_0, can have a marked affect if the background absorbance is large and changing with time. That is, it is the dynamic, concentration dependent, part of the second term, $2.303A\ \Delta I_0$, that will affect the signal, ΔI, in a chromatography context. By dividing the concentration dependent ΔI_0 term, or "I_0 offset effect", by the numerator of the CD effect term, the ratio R can be calculated.

$$R = \frac{\Delta I_0 \varepsilon}{I_0 \Delta\varepsilon} \qquad (95)$$

R is an indication of the error introduced into the CD measurement. An example of what Equation 95 implies follows. In order for the CD measurement to be in error by only 1% due to the "I_0 offset effect", for $\varepsilon/\Delta\varepsilon = 10^3$, the modulation of the beams $I_{0,R}$ and $I_{0,L}$ must be able to maintain the power of these two beams to at least 1 part in 10^5 relative to true null. This includes the initial balancing of the beams or any subsequent "detector drift". Clearly, this is not an instrumental hardship for many inorganic complexes (130), but would be quite challenging for organic species that have a $\varepsilon/\Delta\varepsilon$ ratio typically

near 1×10^5. It should be emphasized that the offset affects the accuracy but not necessarily the detectability of the measurement.

For conditions in which $2.303A \leq 1 \times 10^{-2}$, that term can be neglected with a maximum of only 1% error in the accuracy of the measurement of ΔI in Equation 94. Assuming that ΔI_o term and the 2.303A term can be neglected in Equation 94 and substituting in $\Delta A = \Delta \varepsilon bC$, a simple expression for the detected CD signal is obtained,

$$\Delta I = 2.303 \Delta \varepsilon b C I_o \tag{96}$$

with the variables as defined earlier. Note that the concentration, C, in Equation 96 is the detected concentration and not the injected concentration. Equation 96, then, predicts a linear signal, ΔI, with concentration, C, and light intensity, I_o. Equation 96 will be confirmed in this work, while Equations 94 and 95 will be discussed in more detail.

Experimental

Detection system

The detection system was laser-based, modulated using polarization techniques, and can be seen in Figure 23. The 488 nm light from the argon ion laser (Control Laser, Orlando, FL, Model 554A) was directed to an optical flat in which only the reflected portion of the beam was used. This beam was further reflected from a mirror, through a pin-hole spatial filter, and sent through the center of a 33 cm focal length lens. For CD measurements in conventional

Figure 23. CD experimental configuration for conventional HPLC

(AR) argon ion (488 nm) cw laser; (OF) optical flat; (S) beam stop; (M) mirror; (SF) pin-hole spatial filter; (FL) 33-cm focal-length lens; (PC) Pockels cell; (MD) modulation drive; (WG) wave form generator; (R) rhomb prism; (C) detection cell; (D) photodetector; (LA) lock-in amplifier; (CR) chart recorder; (CS) chromatography system; (W) waste. Insert - Absorbance experimental configuration (GT) Glan-Thompson prism; (M) mirror.

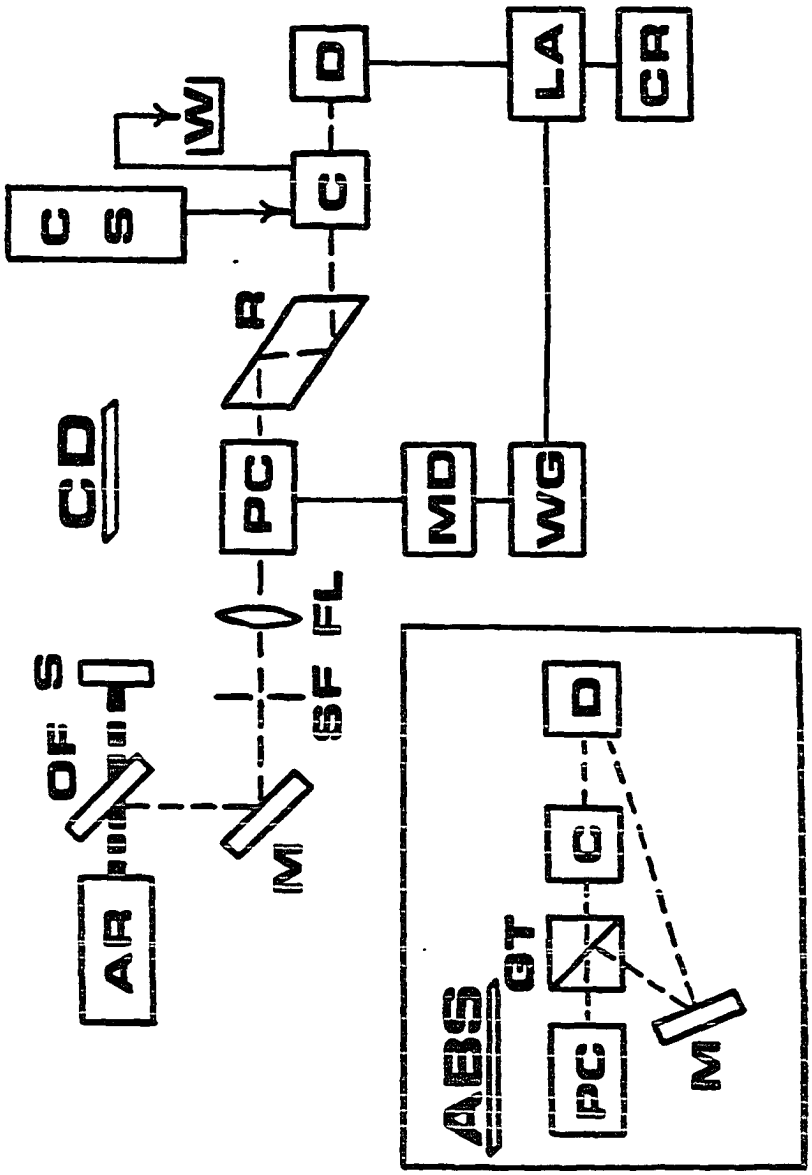
D
LA
CR
W
C
C S
R
CD
PC
MD
WG
FL
SF
S
OF
AIR
M
D
C
GT
ABS
PC
M

chromatography, the light from the lens was sent through an electro-optic modulator (Lasermetric Inc., Teaneck, NJ, Model 3030), through a Fresnel rhomb prism (Karl Lambrecht Corp., Chicago, IL, Model FR4-25-580), came to a focus in the detection cell, and finally diverged to a larger diameter at the detector (Hamamatsu Corporation, Middlesex, NJ, Model S1790), where the laser power measured was typically near 20 mW. The signal from the detector was sent to a high-frequency lock-in amplifier (Princeton Applied Research, Princeton, NJ, Model 5202), and the lock-in amplifier output was sent to a chart recorder that operated at 1 volt fullscale. The electro-optic modulator (i.e., Pockels cell) functioned via a modulation driver (Conoptics Inc., Danbury, CT, Model 25), which in turn was synchronized with the lock-in amplifier via a wave generator (Wavetek, San Diego, CA, Model 162). The polarization of the light exiting the laser was vertical to the plane of the optical table. This polarization produced RCPL as determined from the arrangement of the rhomb prism. By modulating the Pockels cell appropriately (135), on the first half cycle of the modulation frequency, RCPL was produced, and on the second half cycle, the polarization of the laser light was rotated 90° through the Pockels cell and the rhomb prism then produced LCPL. Note that the system described was modulated at very high frequencies (ca 100 kHz to 10 MHz), yet a square-wave was obtained up to roughly 6 MHz. Thus, the entire modulation time can be employed to derive the signal. This is in contrast to other experimental designs reported (118). For microbore chromatography, at the expense of losing some S/N through

the Pockels cell, the 33 cm focal length lens before the Pockels cell was removed and replaced with a 10 cm focal length lens positioned after the rhomb prism so the focus was directly at the center of the microbore cell.

An absorbance detector can be put together quite easily by replacing the rhomb prism in the CD experiment with a Glan-Thompson prism (Karl Lambrecht Corp., Chicago, IL, Model MGLA-SW-8) and a mirror as shown in the insert of Figure 23. Note that the S/N obtainable with this arrangement is not intended to be optimized, but rather, the arrangement is used merely as a quick way to obtain an absorbance measurement (i.e., chromatogram) from essentially the same experimental configuration.

Chromatography system

The eluent consisted of 20% acetonitrile (Burdick and Jackson, Muskegon, MI, HPLC grade) and 80%, by volume, of an H_2O solution, initially deionized and purified with a commercial system (Millipore, Bedford, MA, Milli-Q System), containing 25 mM p-toluenesulfonic acid (J.T. Baker Chemical Co., Phillipsburg, NJ, practical grade) adjusted to pH=3.50 as suggested in the literature (134). The conventional chromatography system consisted of a syringe pump (ISCO, Lincoln, NB, Model 314), an injection valve (Rheodyne, Berkeley, CA, Model 7010) with a 10-μL sample loop, and 25 cm x 4.6 mm i.d. 5-μm C_{18} chromatography column (Regis Chemical, Morton Grove, IL) connected to the detector cell, which was made in-house and was 2.0 cm in length with a volume of 40 μL. The microbore chromatography system used the

same pump with a 0.5-μL sample loop coupled to an internal loop injection valve (Rheodyne, Berkeley, CA, Model 7410) and a 25 cm x 1 mm i.d. 5-μm microsphere C_{18} connected to a cell (also made in-house) that was 1.0 cm in length with a volume of 2.6 μL.

Samples studied

Inorganic complexes were prepared by standard methods (136). Four different species were used: (+)-$Co(en)_3^{3+}$, (-)-$Co(en)_3^{3+}$, $Co(NH_3)_5Cl^{2+}$, and $Cr(NH_3)_6^{3+}$. For (+)-$Co(en)_3^{3+}$, ε_{max}(469 nm) = 84 L $cm^{-1}mol^{-1}$, and $\Delta\varepsilon_{max}$(493 nm) = +1.89 L $cm^{-1}mol^{-1}$ [22]. Only the enantiomerically pure $Co(en)_3^{+}$ complexes are CD active at 488 nm, while all the complexes show an appreciable absorbance at that wavelength.

S/N optimization

The high frequency lock-amplifier previously mentioned operated down to 100 kHz as the minimum frequency. To study the laser "flicker noise" over a broader range of modulation frequencies, S/N data were collected using another lock-in amplifier (Princeton Applied Research, Princeton, NJ, Model HR-8) for 1 kHz to 100 kHz. The results for the two lock-in amplifiers at 100 kHz were nearly identical so the data could be easily compared. Use of an oscilloscope (Tektronics, Inc., Beaverton, OR, Model 7904) aided in signal balancing and in optimizing the depth and stability of the modulation system. Initial "static" concentration studies of the CD signal were performed by introducing (-)-$Co(en)_3^{3+}$ solution with a peristaltic pump (Gilson Medical Electronics, Middleton, WI, Minipuls 2). Studies of both CD signal

linearity versus concentration and CD signal linearity versus laser power were performed. The results of these two studies are shown in Figures 24 and 25, respectively. The peristaltic pump replaced the chromatography system when it was used.

Results and Discussion

Optimization of the detection system signal-to-noise ratio (S/N) is required in order to produce the best analyte detectability. Since a laser is used because of its special qualities, the laser noise contribution must be well understood. A dye-laser exhibits large amplitude noise, or "flicker" noise, at lower frequencies (below 100 kHz) and drops off to the theoretical shot-noise limit a higher frequencies (near 10 MHz) (129). Similar behavior was anticipated for the argon ion laser in this work. The data plotted in Figure 26 support this idea. The peak-to-peak noise (PPN) was determined from the chart recording at various frequencies. PPN is abbreviated as N in Figure 26. The "signal", S, is measured using the absorbance configuration, while blocking one beam. S is equal to I_o in Equation 96. To obtain the solid line (Figure 26), the Pockels cell modulation system is turned off, while the light is still monitored by the lock-in amplifier at the appropriate input frequency. This, then, provides the flicker noise effective in a lock-in detection system. At 10 MHz, in Figure 26, the theoretical shot-noise limit is approached for the laser power used. Turning on the modulation system will physically modulate the laser beam. The result of this, using the CD configuration and conventional chromatography shown in Figure 23, is

Figure 24. Lock-in detected CD signal ΔI (μV), as a function of (+)-$Co(en)_3^{3+}$ concentration (mM), at constant laser power (ca 25 mW)

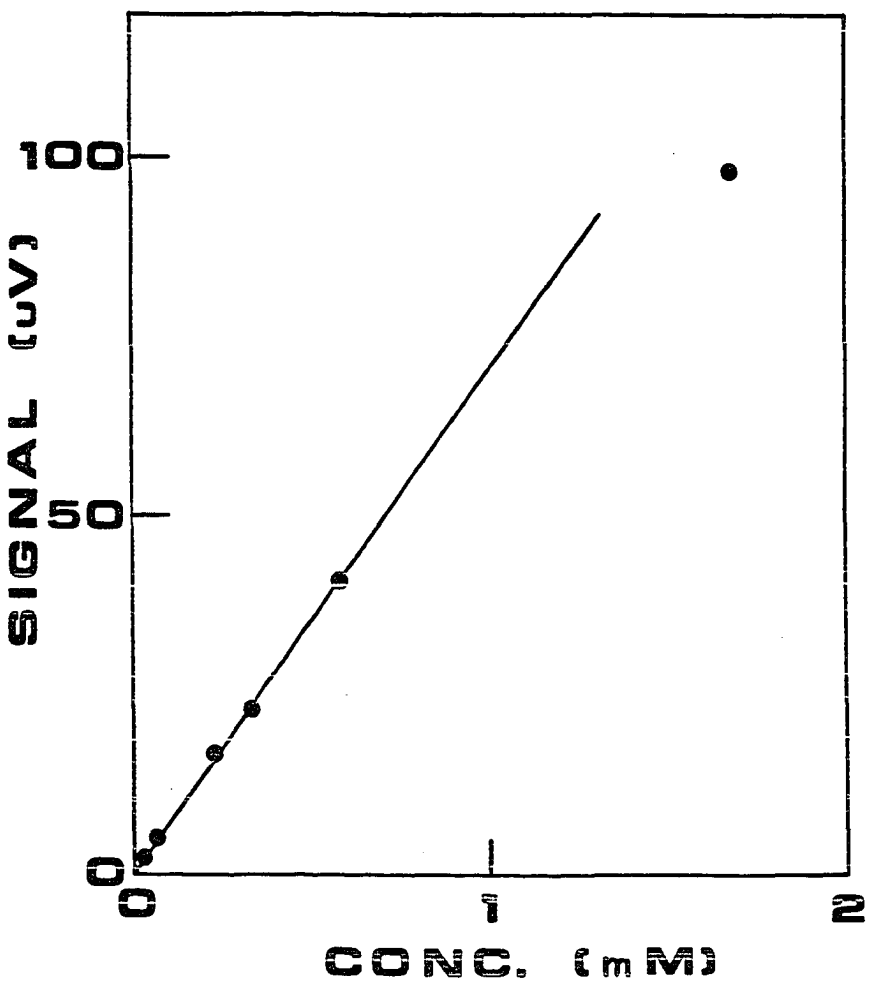
SIGNAL (uV)
100
50
0
0
1
2
CONC. (mM)

Figure 25. Lock-in detected CD signal, $\Delta I(\mu V)$, as a function of laser power (which is proportional to $I_o(mV)$), at a constant (+)-$Co(en)_3^{3+}$ concentration of 5.85×10^{-4} M

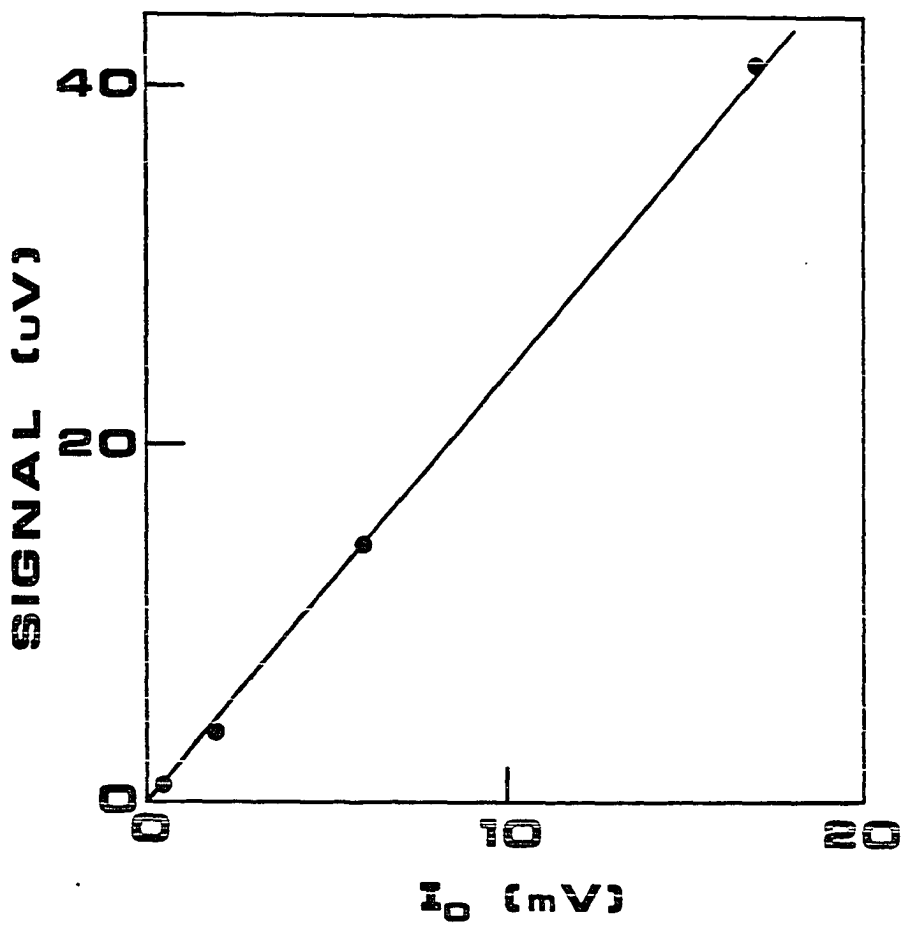
SIGNAL (uV)
40
20
0
0
10
20
I_o (mV)

Figure 26. Log (N/S) versus Log (Frequency)
20 mW laser power. Solid line: laser "flicker" noise.
Dashed line: experimentally measured noise in CD
configuration of Figure 23.

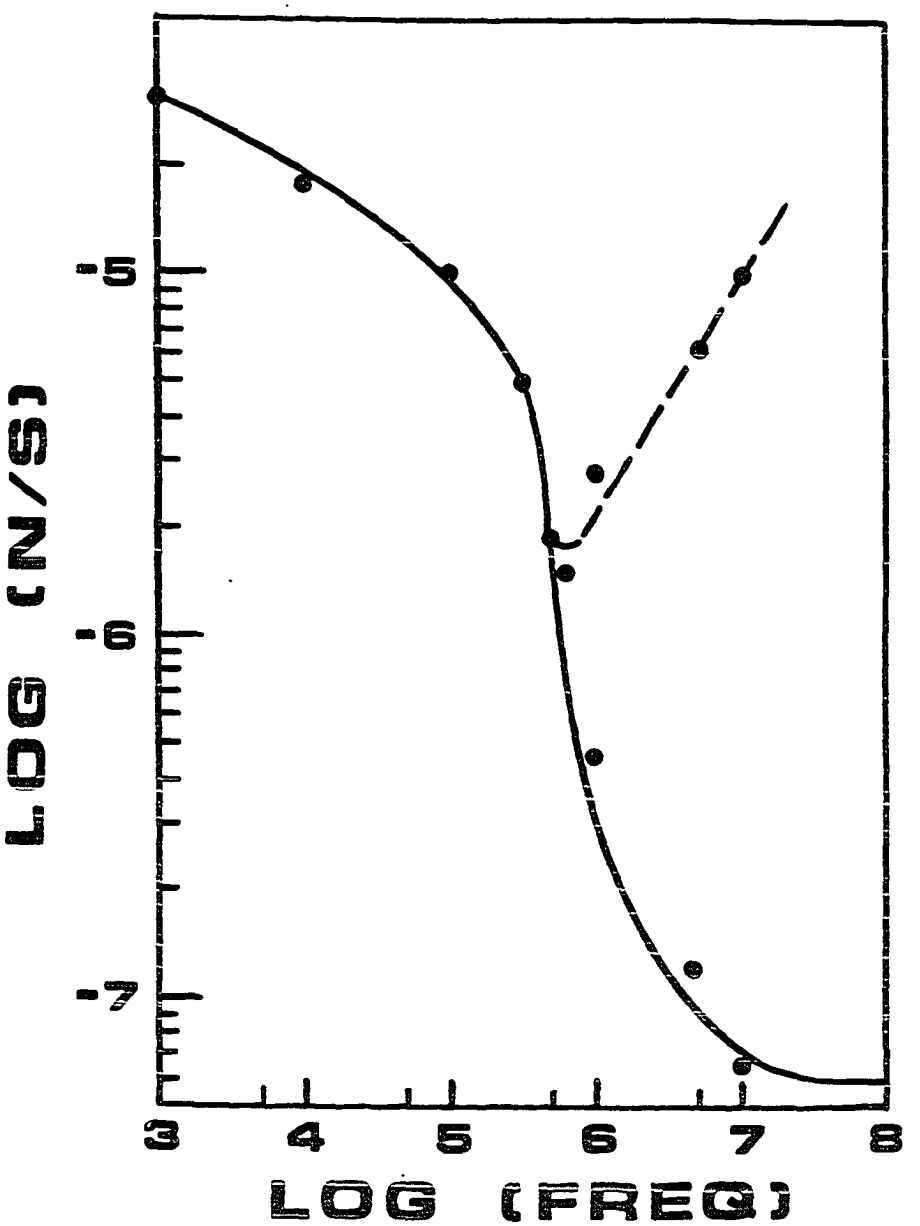
LOG (N/S)
-5
-6
-7
3
4
5
6
7
8
LOG (FREQ)

shown by the dashed line in Figure 26. Note that the conventional chromatography system did not limit the PPN/S data in any way. At frequencies below 500 kHz, the PPN/S is coincident with the solid line (i.e., flicker noise limited). Above 500 kHz the PPN/S is no longer laser flicker noise limited, but rather, affected by the electronic and mechanical instability of the modulation system. Thus, the shot-noise limit could not be reached with the present CD experimental configuration. An optimum PPN/S of 1.75×10^{-6} (500 kHz, 1 second time constant) was obtained with the CD system. If the LOD is taken as 1 x PPN (4) from Equation 96, the differential absorbance LOD is $\Delta A_{LOD} = 7.6 \times 10^{-7}$ AU for a 1-second time constant. This constitutes nearly a factor of 60 improvement relative to previous work (126, 127) for absolute CD absorbance detectability. Note that this noise level is equivalent to the shot-noise in a 1-μW light beam at 500 nm, which is characteristic of conventional light sources in CD spectrometers. So, it is the effort to stabilize the intensity by high-frequency modulation and not the high photon-flux that made the laser-based design superior.

The CD signal linearity was studied using a peristaltic pump for sample introduction, instead of chromatography (Figures 24 and 25). From experimental data, both figures yield a $\Delta\varepsilon$ value of 1.78. This is consistent with the literature value and sample purity. The upper limit on CD detection linearity for (+)-$Co(en)_3^{3+}$ is 1×10^{-3} M (Figure 24). The lower limit is effectively the ΔA_{LOD}. Above 1×10^{-3} M, the CD signal for (+)-$Co(en)_3^{3+}$ is attenuated by

background absorbance according to Equation 94. The ratio of $\varepsilon/\Delta\varepsilon$ was measured to be about 50. Thus, the background absorbance at the upper limit of linearity is roughly A = 0.10. The CD signal is attenuated from background absorbance by about 23% at this point. The useful range of absorbance spans over five orders of magnitudes (1.3×10^5). The linearity of the CD signal with laser power was studied using up to 25 mW of incident radiation and attenuating the laser beam by placing neutral density filters before the modulation system (Figure 25). The CD signal was found to be linear as a function of power for a 5.85×10^{-4} M (+)-$Co(en)_3^{3+}$ solution. Two orders of magnitude attenuation from 25 mW were spanned. The system PPN/S was the best at 25 mW and got worse (i.e., increased) as the laser beam was attenuated. Also, introduction of a highly absorbing yet non-CD active species gave no appreciable signal. Thus, Equation 94 and Equation 96 were substantiated. Furthermore, CD signals (i.e., ΔI) obtained experimentally could be calculated a priori with Equation 96 using available experimental and physical data (i.e., I_0,b,$\Delta\varepsilon$,C). The "I_0 offset effect" described by Equation 95 posed no problem for (+)-$Co(en)_3^{3+}$ since experimentally a $\Delta I_0/I_0$ better than 1×10^{-4} was maintained. Using a $\varepsilon/\Delta\varepsilon$ of 50, a value for R of 5×10^{-3} can be calculated with Equation 95 (i.e., 0.5% error). Note that for organic species in which $\varepsilon/\Delta\varepsilon$ can approach 1×10^5, the "I_0 offset effect" for the same $\Delta I_0/I_0$ as above would be problematic. Clearly, $\Delta I_0/I$ would need to be decreased to a much smaller level to make such determinations feasible.

The demonstration of the HPLC-CD detection system for a mixture of three metal complexes is shown in Figure 27. The CD chromatogram is shown in contrast to an absorbance chromatogram. Chromatographic data pertaining to Figure 27 are listed in Table 18. Note that there are solvent disturbances in both chromatograms of Figure 27 that occur at retention times earlier than the elution of $Co(NH_3)_5Cl^{2+}$. A LOD of 19 ng for (+)-$Co(en)_3^{3+}$ is calculated from Figure 27 (240 g/mole, 10 μL injected, 1 second time constant). The "spikes" observed in the CD chromatogram at the retention times of the other two complexes cannot be attributed to CD activity. Since they are quite narrow in width, the "spikes" do not produce very much area as compared to the (+)-$Co(en)_3^{3+}$ peak, thus, they can be tolerated. Most likely, these are artifacts due to thermal lensing at the absorption maximum, in turn deflecting the laser beam relative to the photodiode. Utilization of a 10 second time constant compared to a 1 second time constant is shown for the same mixture in Figure 28. Some rounding of the analyte peak occurs, yet a LOD of 10 ng was calculated, while the ΔA_{LOD} is better than 2.5×10^{-7} AU! A larger solvent peak is also observed. Shown in Figure 29, a (-)-$Co(en)_3^{3+}$ sample produced a peak that deflects in the opposite direction, as it should.

Microbore chromatography was demonstrated with the system described earlier. Figure 30 displays a chromatogram containing (+)-$Co(en)_3^{3+}$ as the CD-active analyte. A LOD of 2.8 ng is calculated from the analyte peak that occurs at nearly 5 minutes. Note that the $\Delta A_{LOD} = 2.5 \times 10^{-6}$ is about a factor of 3 worse than that in

Figure 27. HPLC detection of $Co(NH_3)_5Cl^{2+}$, $Cr(NH_3)_6^{3+}$, and $(+)\text{-}Co(en)_3^{3+}$

CD: circular dichroism. A: absorbance. 10 μL injected, 0.67 mL/min, 5×10^{-4}M $(+)\text{-}Co(en)_3^{3+}$, 500 kHz modulation frequency, 1 second time constant, and a 2 cm pathlength cell. Pertinent data are listed in Table 18.

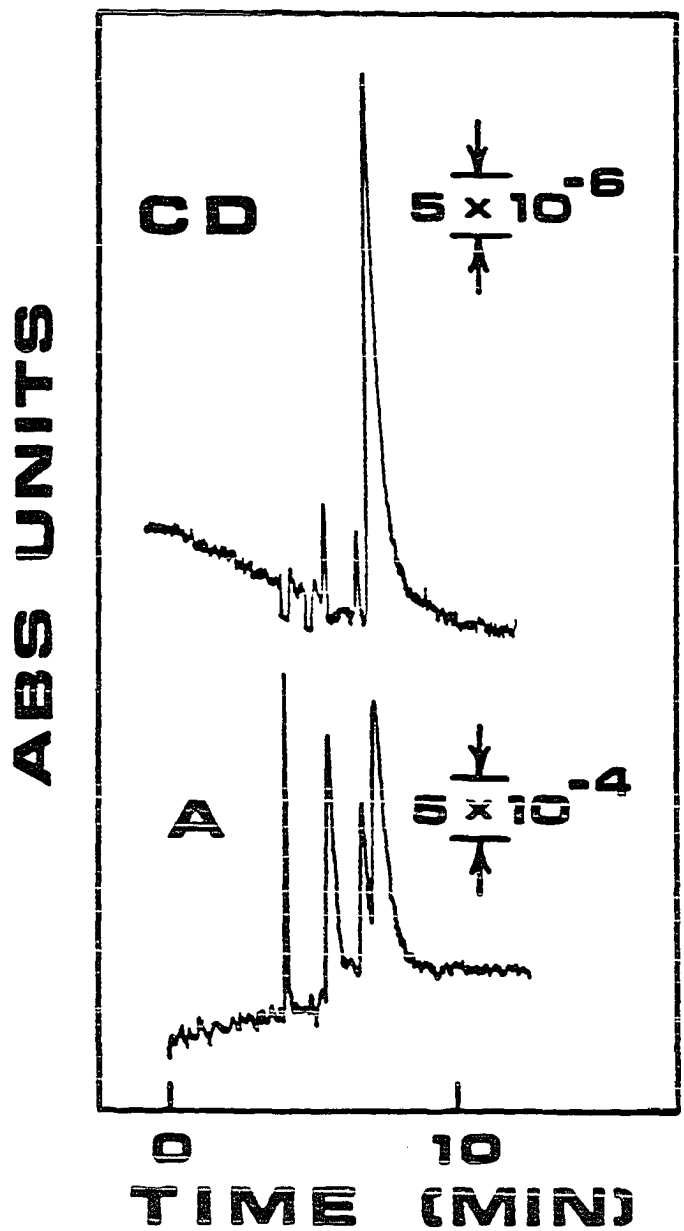
CD
5 x 10⁻⁶
A
5 x 10⁻⁴
ABS UNITS
0
10
TIME (MIN)

Table 18. Chromatographic data for peaks in Figure 27

Species[a]	Absorbance[b]	Retention Time (min)
$Co(NH_3)_5Cl^{2+}$	0.00231	5.7
$Cr(NH_3)_6^{3+}$	0.00165	6.8
$(+)\text{-}Co(en)_3^{3+}$	0.00251	7.3

[a]Concentrations: $(+)\text{-}Co(e)_3^{3+}$ is 5.0×10^{-4}M. $Co(NH_3)_4Cl^{2+}$ and $Cr(NH)_6^{3+}$ are at unknown concentrations. It is only required that they absorb similar to $(+)\text{-}Co(en)_3^{3+}$.

[b]Absorbance measured at the peak using $A=\log I_o/I$, from the absorbance chromatogram.

Figure 28. HPLC-CD detection of the same mixture as Figure 27 using two different time constants: 1 second time constant (upper), 10 second time constant (lower)

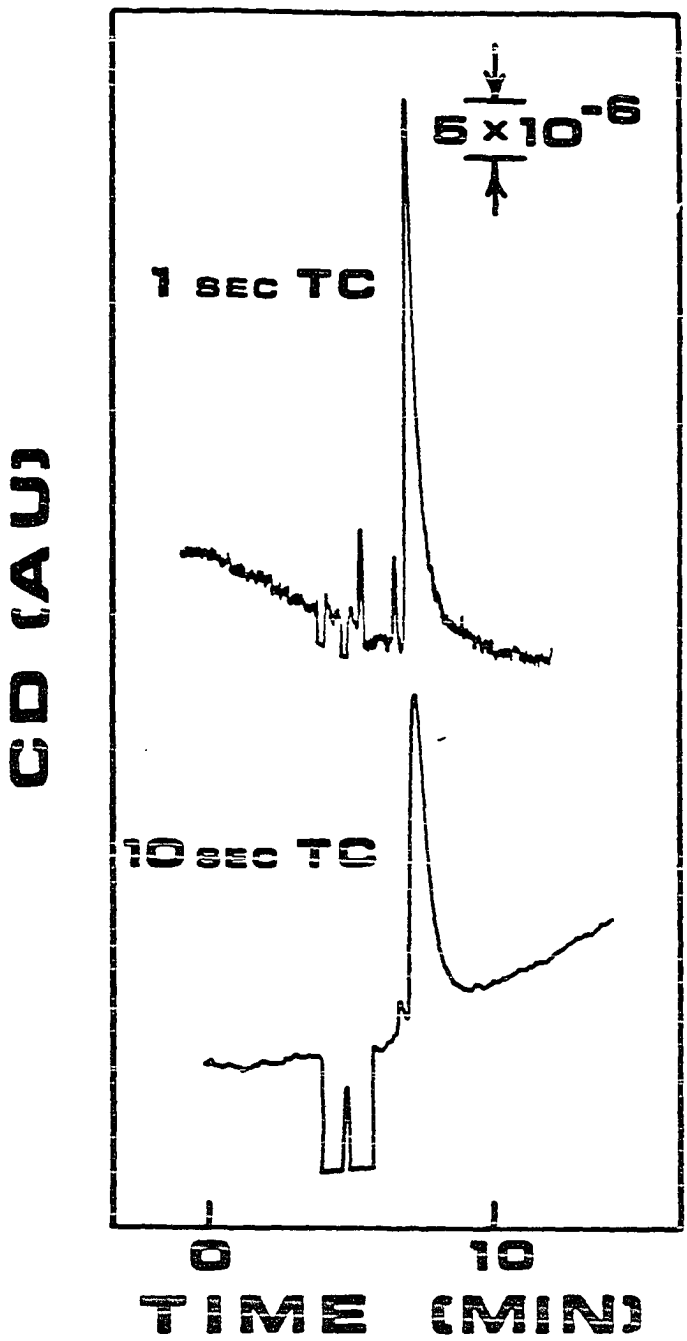
5 x 10⁻⁶
1 SEC TC
10 SEC TC
CD (A U)
0
10
TIME (MIN)

Figure 29. HPLC-CD detection of enantiomers

(A) HPLC-CD detection of (+)-$Co(en)_3^{3+}$.

(B) HPLC-CD detection of (-)-$Co(en)_3^{3+}$.

Recorder zero was adjusted between injections.

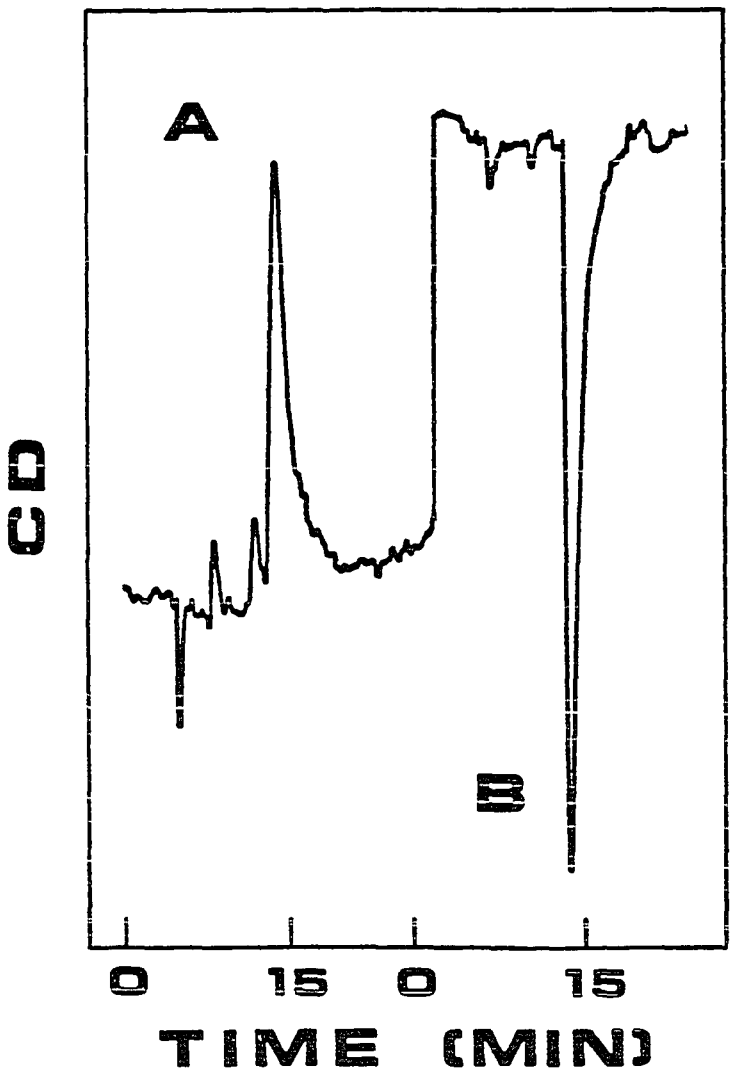
A
B
CD
0
15
0
15
TIME (MIN)

Figure 30. Microbore HPLC-CD detection of the same mixture as Figure 27

$(+)\text{-}Co(en)_3^{3+}$ is at 2.5×10^{-3}M. 0.5 µL injected, 40 µL/min, 1 second time constant, 500 kHz modulation frequency, and a 1-cm pathlength cell. Retention time at peak is 4.8 min. Solvent disturbance is before 4.0 min. LOD is 2.8 ng.

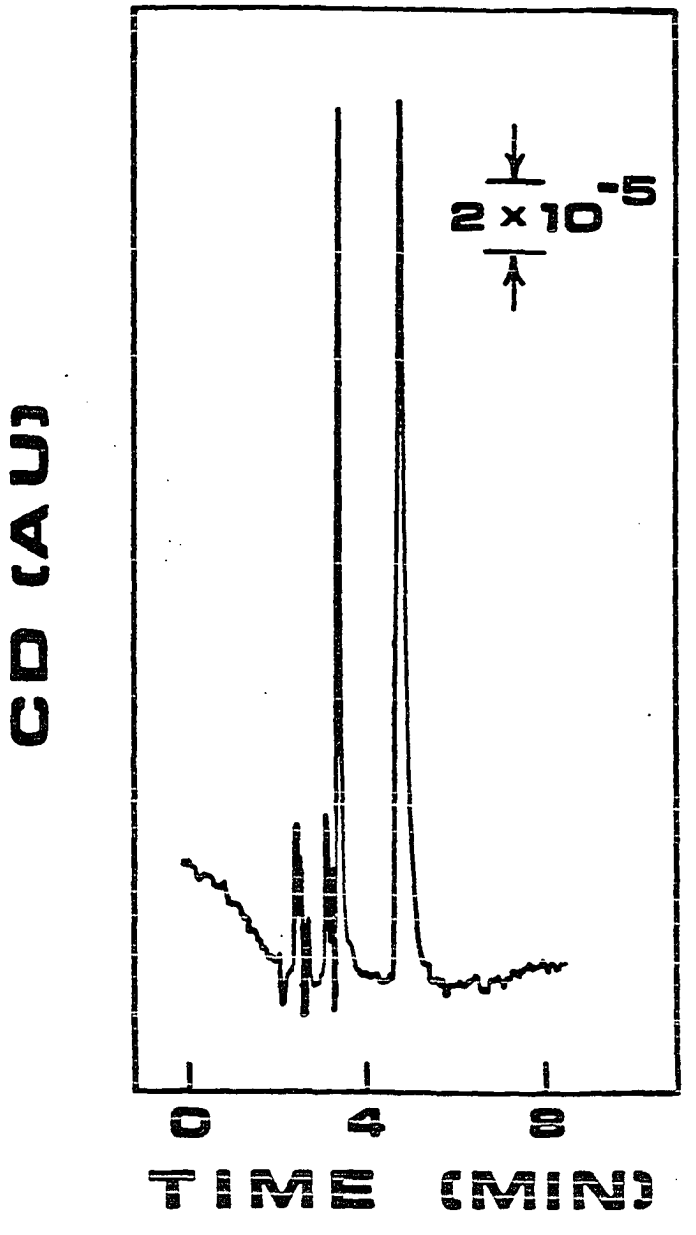
CD (A U)
2 x 10-5
0
4
8
TIME (MIN)

conventional chromatography with the same time constant (Figure 27). This is due to difficulties in stabilizing the optical configuration. Yet, microbore chromatography produced a LOD that is 6.8 times lower than in conventional chromatography (despite the shorter pathlength) for an analyte eluting at essentially the same capacity factor because of the smaller peak volume. The present cell has a volume that is marginal for microbore LC, but the laser beam waist here should readily clear a 1-μL flow cell (7). It is possible to remove the solvent disturbance by preparing the sample in the same solvent as the eluent, as shown for the microbore separation of (+)-$Co(en)_3^{3+}$ with CD detection (Figure 31).

Conclusion

A summary of the LODs for the various chromatographic conditions are listed in Table 19. It is interesting to compare the detectabilities obtained in this work to previously reported work. Assuming the same chromatographic dilution and broadening effects, and objectively compensating for inherent differences in analyte sensitivity, the microbore chromatography LOD of 2.8 ng shows an improvement in mass detectability of nearly a factor of 220 over previous work (127). Absolute detector sensitivity in AU for conventional chromatography with a 1 second time constant has improved by nearly a factor of 60. Clearly, the potential for HPLC-CD as a sensitive and specific analytical instrument can be appreciated. The present report is based on an Ar ion laser operating in the visible

Figure 31. Same as Figure 30

The sample is prepared in a solvent that is also the eluent. LOD is slightly worse, at 3.5 ng.

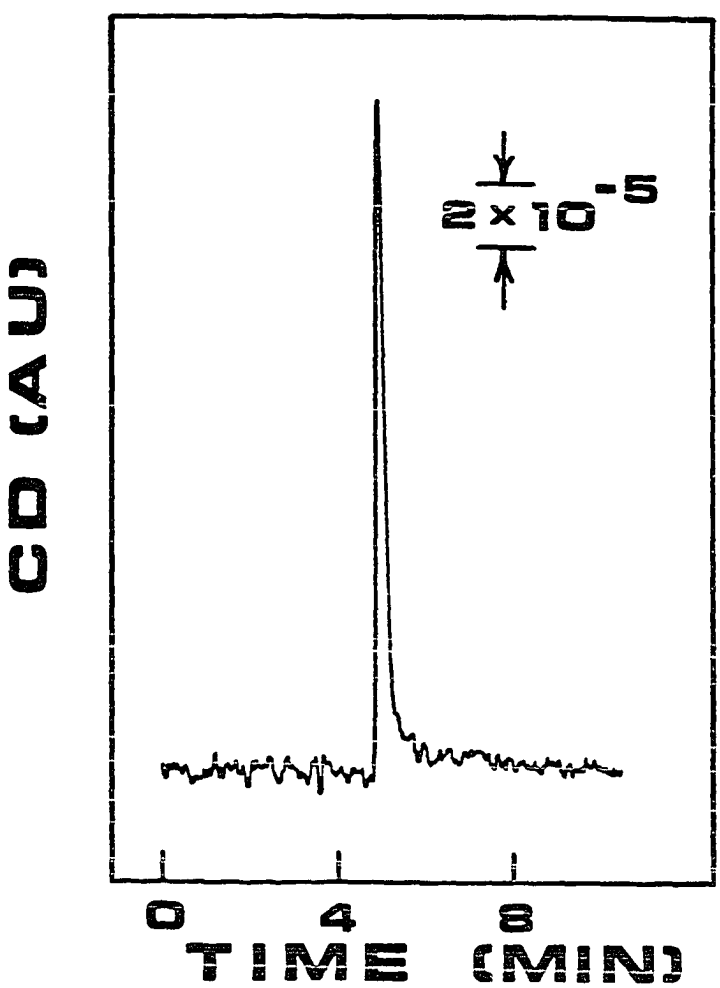
CD (A U)
2 x 10-5
0
4
8
TIME (MIN)

Table 19. LOD values for HPLC-CD detection using 500 kHz amplitude modulation

Chromatography System	Time Constant (s)	Pathlength, b(cm)	Injection Volume (μL)	ΔA LOD[a]	Mass LOD[b]
Conventional	1	2	10	7.5×10^{-7}	19 ng
Conventional	10	2	10	2.4×10^{-7}	10 ng
Microbore	1	1	0.5	2.5×10^{-6}	2.8 ng

[a]Using $\Delta I = 1 \times PPN$ for the LOD, Equation 96, and the PPN/I_0 from the chart recording.

[b]Calculated for (+)-$Co(en)_3^{3+}$ at 488 nm and k' ~ 1 in each case, from the detected signal and knowing the injected concentration and volume.

region. However, one can expect to obtain similar detectabilities using the frequency-doubled Ar ion laser output at 257 nm or the HeCd laser output at 325 nm to match other chromophores. Applications in a variety of select areas could benefit from an HPLC-CD system. Determination of optical purity of drugs, chiral-marker mapping of biological matrices, and studying stereoselective reactions in a variety of contexts (117) are just a few of the many situations that an HPLC-CD system may be invaluable.

CHAPTER 9.

FLUORESCENCE DETECTED CIRCULAR DICHROISM AS A DETECTION PRINCIPLE IN HIGH PERFORMANCE LIQUID CHROMATOGRAPHY

Introduction

High performance liquid chromatography (HPLC) is extensively applied in the analysis of complex, often biologically related, samples. If the separation process is not adequate in providing the extent of selectivity required in an analysis, a detector with appropriate selectivity must be chosen (3). Optical activity detection (OAD) is a method that can provide excellent selectivity in HPLC analyses. OAD-HPLC procedures using polarimetry as the detection principle have been reported for the analysis of carbohydrates in urine (54) and cholesterol in human serum (55). Optically active species in the samples are detected, exclusively, while optically inactive species pass through the detector unnoticed. Even greater selectivity in HPLC detection may be useful as complexity increases for the samples.

Riboflavin (Vitamin B_2) is an important chemical species that exhibits both strong fluorescence and optical activity. Various analytical procedures for its analysis have been reported (137, 138, 139). Using a commercially available fluorescence detector, with a conventional light source, and conventional HPLC, these procedures typically produced detectabilities of low nanogram levels of injected riboflavin. The need for a more sensitive procedure for riboflavin

was suggested (137). A laser fluorometric study of riboflavin provided data that imply picogram detectabilities are possible for conventional HPLC (140). Also, it is common for riboflavin to exist in a sample matrix that is quite complex, and traditional fluorescence detection, while selective to some extent, may not be adequate for the analysis. Circular dichroism (CD) spectroscopy of riboflavin and its analogs suggests that CD may provide an added dimension of selectivity when coupled with fluorescence (141).

The use of fluorescence detected circular dichroism (FDCD) in the analysis of biologically significant systems in static solutions (116) provided invaluable structural information. This application suggests the development of an HPLC detection principle based upon FDCD. Similarly, the report of a transmission detected (TD) CD detector for HPLC, in Chapter 8, supports the claims of improved selectivity and ample sensitivity that an FDCD detector for HPLC should provide.

A laser-based FDCD-HPLC system has been developed, and tested with a reversed phase chromatographic separation of a mixture containing riboflavin. Some of the problems associated with CD detection in dynamic (flowing) systems, as compared to static systems, are discussed in this Chapter. Also, experimental and technical considerations concerning FDCD-HPLC and TDCD-HPLC will be presented. FDCD-HPLC is found to provide ample sensitivity (170 pg limit of detection for riboflavin), while also providing the detection selectivity of optically active fluorophores in the presence of optically inactive fluorophores.

Theory

CD is defined as the difference in absorbance of left circularly polarized light (LCPL) and right circularly polarized light (RCPL). Since CD is dependent upon absorbance, the CD parameter, $\Delta\varepsilon$, is related to the molar absorptivities for LCPL and RCPL by

$$\Delta\varepsilon = \varepsilon_L - \varepsilon_R \tag{97}$$

where L indicates LCPL and R indicates RCPL. In order to use Equation 97 for FDCD, an expression relating the fluorescence, I_F, detected at 90° from an incident light source I_o, for small absorbances, is useful.

$$I_F = 2.303\ f(\theta)g(\lambda)\phi_F\varepsilon bcI_o \tag{98}$$

where $f(\theta)$ is a geometric collection efficiency factor, $g(\lambda)$ is a signal conversion factor depending upon wavelength, ϕ_F is a factor accounting for quantum efficiency of fluorescence, ε is the average molar absorptivity, b is the observed pathlength, and C is the concentration of a fluorophore.

Ideally, the light source incident upon a FDCD detection cell is modulated at a given frequency, so that one half-cycle is entirely RCPL and the second half-cycle is entirely LCPL. In practice, this is not the case, but rather

$$\Delta I_o = I_{o,L} - I_{o,R} \tag{99}$$

with

$$I_o = (I_{o,L} + I_{o,R})/2 \tag{100}$$

It is also useful to note that

$$\varepsilon = (\varepsilon_L + \varepsilon_R)/2 \tag{101}$$

for optically active species. Thus, for a lock-in detection system, the signal detected in the FDCD measurement, ΔI_F, will be related to the fluorescence intensity detected on each half-cycle of modulation

$$\Delta I_F = I_{F,R} - I_{F,L} \tag{102}$$

where $I_{F,R}$ is the fluorescence intensity due to RCPL, and $I_{F,L}$ is the fluorescence intensity due to LCPL. Taking Equations 97 and 98 and assuming ΔI_o is equal to zero, the FDCD signal is expressed by

$$\Delta I_F = -2.303\ f(\theta)g(\lambda)\phi_F\Delta\varepsilon bCI_o \tag{103}$$

The negative sign indicates that the FDCD signal is opposite in magnitude as compared to the TDCD signal, according to the definition of $\Delta\varepsilon$ in Equation 97. Equation 103 is consistent with what has previously been reported (142) for the FDCD measurement in static systems. Equation 103 is an ideal expression, since ΔI_o cannot be neglected in practice due to imperfections in the electro-optic modulation process and due to difficulties in balancing birefringent and reflection phenomena in the detection cell (143). The ΔI_o effect on ΔI_F can be included on an additive basis, since very small

absorbances are measured in a chromatography context. For an optically active fluorophore, $\Delta I_{F,OA}$ is given by

$$\Delta I_{F,OA} = 2.303\ f(\theta)g(\lambda)\phi_F bC[-\Delta\epsilon I_o \pm \epsilon\Delta I_o] \qquad (104)$$

where the first term in the brackets is for the CD effect, and the ± sign on the second term indicates that ΔI_o can arbitrarily be positive or negative relative to the first term. For an optically inactive fluorophore, an experimentally measured signal, $\Delta I_{F,OI}$, due entirely to ΔI_o may be observed

$$\Delta I_{F,OI} = 2.303\ f(\theta)g(\lambda)\phi_F bC[\pm \epsilon\Delta I_o] \qquad (105)$$

Note for a given measurement, the ± sign in Equations 104 and 105 will be the same.

It is possible to measure both the fluorescence and the FDCD signal (144) for the same chromatographic system. For an optically active fluorophore, using Equations 98 and 104, the ratio of $\Delta I_{F,OA}$ and I_F is given by

$$\frac{\Delta I_{F,OA}}{I_F} = -\frac{\Delta\epsilon}{\epsilon} \pm \frac{\Delta I_o}{I_o} \qquad (106)$$

where ϵ is defined as in Equation 101 and I_o is defined by Equation 100. For an optically inactive fluorophore, using Equations 98 and 105, the ratio of $\Delta I_{F,OI}$ and I_F yields

$$\frac{\Delta I_{F,OI}}{I_F} = \pm \frac{\Delta I_o}{I_o} \qquad (107)$$

Again, the ± sign in Equations 106 and 107 will be the same. Thus, if the effect due to ΔI_0 cannot be neglected, then the use of an optically inactive fluorophore, via Equation 107, provides a means to subtract off this unwanted contribution in Equation 106 for optically active fluorophores. This procedure will be confirmed in this work, by utilizing it in HPLC coupled with FDCD detection.

Experimental

Detection system

The detection system was laser-based, modulated by using polarization techniques, and can be seen in Figure 32. The 325-nm light from the HeCd laser (Liconix, Sunnyvale, CA, Model 4240NB) at about 8 mW power was sent through a 50-cm focal length quartz lens, and on through an electro-optic modulator (Lasermetric, Inc., Teaneck, NJ, Model 3030). After exiting the modulator, the light entered the chromatographic detection cell. The detection cell was approximately at the focal point of the quartz lens. Any fluorescence originating in the detection cell was collected 90° from the incident laser beam direction. This fluorescence passed through two filters (Corning Glass, Corning, NY, 4-65 and 0-52) before detection with a photomultiplier tube (RCA, Harrison, NJ, Type 1P28), which was biased at 1000 V. The detected signal was sent through an ac amplifier with a gain of 100, and on to a lock-in amplifier (Princeton Applied Research, Princeton, NJ, Model 5202), for phase-sensitive detection synchronized to the modulation frequency applied to the electro-optic

Figure 32. FDCD-HPLC system

(HC) - HeCd laser, 8 mW; (FL) - 50 cm focal length quartz lens; (PC) - electrooptic modulator (Pockels cell); (M) - modulation driver; (W) - waveform generator; (LCS) - liquid chromatography system; (WL) - waste liquid; (C) - detection cell (detailed in Figure 33); (S) - eam stop; (F1) - 4-65 Corning filter; (F2) - 0-52 Corning filter; (P) - photomultiplier tube; (H) - high voltage power supply; (A) - AC amplifier; (L) - lock-in amplifier; (R) - chart recorder.

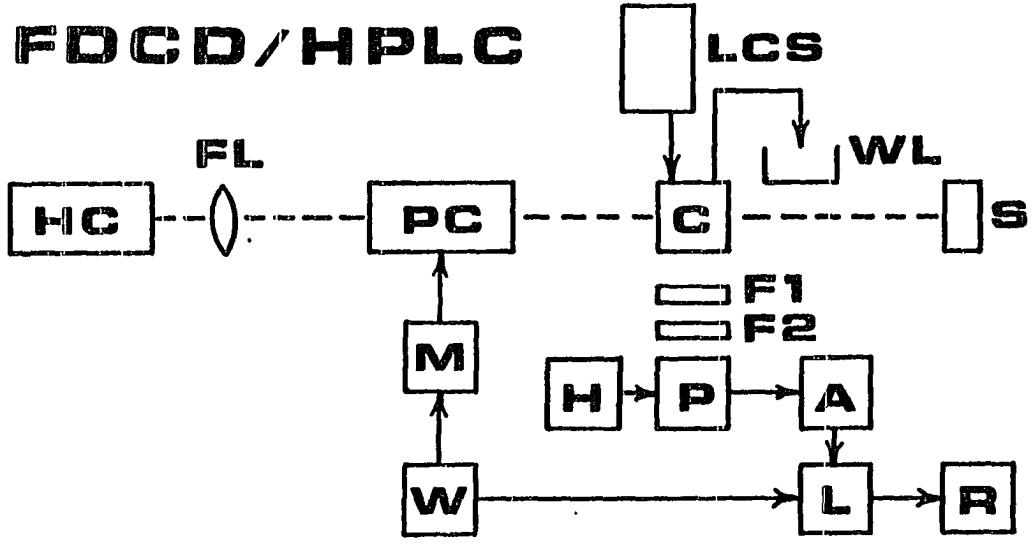
FDCD/HPLC
LCS
FL
WL
HC
PC
C
S
F1
F2
M
H
P
A
W
L
R

modulation device. The output from the lock-in amplifier was sent to a strip chart recorder operating at 1 V full scale.

The polarization of the laser beam initially was vertical to the plane of the optical table. The electro-optic modulator (i.e., Pockels cell) acts upon the polarized laser light, in conjunction with a modulation driver (Conoptics, Inc., Danbury, C.T., Model 25), which in turn was synchronized with the lock-in amplifier via a wave generator (Wavetek, San Diego, CA, Model 162). The system was operated at 150 kHz with a square wave from the wave generator. It was possible to obtain CPL directly from the Pockels cell without using a Fresnel rhomb prism. This was in contrast to the procedure used in TDCD detection (Chapter 8). By proper adjustment of the modulation driver bias voltage and input waveform peak-to-peak voltage, both right and then left CPL were produced (135). Yet, the production of CPL from the Pockels cell must be tested with a Fresnel rhomb, a polarizing prism, and a photodiode detector. Once CPL was obtained with the Pockels cell, the detection system for FDCD was simpler and just as effective as that reported for TDCD.

Chromatography system

The eluent consisted of 20% acetonitrile (Burdick and Jackson, Muskegon, MI, HPLC grade) and 80%, by volume, water, initially deionized and purified with a commercial system (Millipore, Bedford, MA, Milli-Q System). The liquid chromatography system consisted of a syringe pump (ISCO, Lincoln, NB, Model 314), an injection valve (Rheodyne, Berkeley, CA, Model 7410) with a 1-μL injection loop, and a

15 cm x 2.1 mm i.d. 5-μm C_{18} chromatography column (Alltech Associates, Inc., Deerfield, IL), which was connected to a detection cell (made in-house, shown in Figure 33), having an observed pathlength of 1.2 cm and a cell volume of 14 μL. A flow rate of 200 μL per min was used. The detection cell is positioned, with care, using a combination of translational and rotational stages (Aerotech, Inc., Pittsburgh, PA, Models ATS-301 and ATS-301R).

Samples studied

Both the optically active fluorophore (-)-riboflavin and the optically inactive fluorophore 4-methylumbelliferone were commercially available, reagent grade chemicals. They were found to be sufficiently pure for this work. Riboflavin and 4-methylumbelliferone both exhibit large absorptivities at 325 nm. Log ε values are 3.3 and 4.1, respectively, for these compounds. Also, they both exhibit intense fluorescence. The maximum fluorescence for riboflavin is near 535 nm, while that of 4-methylumbelliferone is below 500 nm. The filters were chosen to pass the fluorescence of riboflavin, but a significant amount of 4-methylumbelliferone fluorescence was also allowed to pass. From the literature (141), the optically active (-)-riboflavin has $\Delta\varepsilon$ values ranging from +1.5 to +2.5 L $cm^{-1}mol^{-1}$ in solvent systems such as that used in this study. Concentrations injected into the HPLC system were 1.05×10^{-5}M riboflavin and 4.25×10^{-6}M 4-methylumbelliferone. Riboflavin has a molecular weight of 376 g/mole.

Figure 33. Chromatographic detection cell
(B) - 1.8 cm total pathlength; (B') - 1.2 cm observed pathlength; (D) - 1.0 mm i.d. quartz tubing; (T) - chromatography tubing, inlet and outlet.

CELL DESIGN

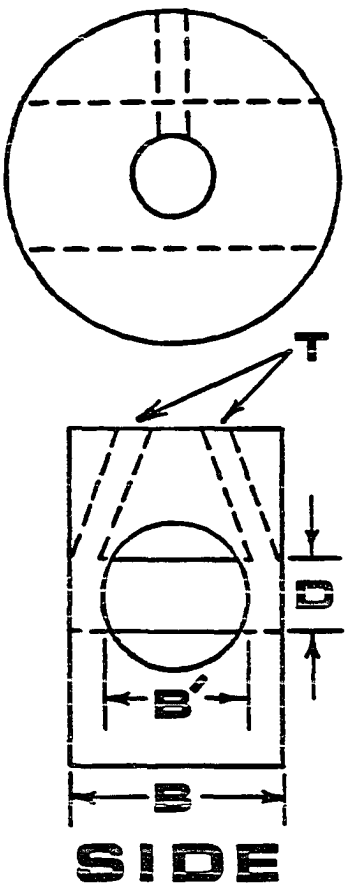

Fluorescence and FDCD measurements

A fluorescence chromatogram was obtained by inserting a Glan-Thompson polarizing prism (Karl Lambrecht Corp., Chicago, IL, Model MGLA-SN-8), after the Pockels cell but before the detection cell. The modulation system was adjusted to form a polarization modulated laser beam that is "on" for one half-cycle, and "off" for the other half-cycle. Lock-in detection provides a fluorescence signal proportional to that described by Equation 98. A series of at least three fluorescence chromatograms were obtained until good precision was substantiated by the reproducibility.

A FDCD chromatogram was obtained by removing the polarization prism and adjusting the modulation system to produce, alternately, RCPL and LCPL as a function of the modulation frequency. Lock-in detection provides a FDCD signal proportional to that described by Equations 104 and 105. This is done only after the ratio $\Delta I_o/I_o$ has been experimentally minimized to reduce this extraneous contribution to the signal (see Equations 106 and 107). FDCD chromatograms were collected until good reproducibility was confirmed, which was at least three trials.

Results and Discussion

Fluorescence and FDCD chromatograms

A mixture containing riboflavin and 4-methylumbelliferone was injected onto the chromatography system and the fluorescence was detected. The fluorescence chromatogram for one of these equivalent

trials is shown in Figure 34. Notice that the peak heights for both species are nearly identical. The FDCD detection system was then employed. The same sample mixture was injected onto the chromatography system with optimized FDCD detection. The FDCD chromatogram, for one of three trials, is shown in Figure 35.

It is apparent that the optically inactive 4-methylumbelliferone still provides a signal in FDCD detection. This is due to the magnitude of its molar absorptivity, ε, and the magnitude of the ratio $\Delta I_o/I_o$, in relation to the magnitude of $\Delta\varepsilon$ for typical optically active species. Recall that the "error", R, due to ΔI_o in a chromatography context for TDCD is given by

$$R = \frac{\Delta I_o \varepsilon}{I_o \Delta\varepsilon} \tag{108}$$

where R indicates the proportion of the offset signal as compared to the CD signal for optically active species.

Using the peak heights from the data in Figures 34 and 35, and knowing the relative difference for the vertical scales used in these figures, Equations 106 and 107 were applied. For the optically inactive 4-methylumbelliferone, using Equation 107, $\Delta I_o/I_o$ was found to be 5.5×10^{-4}. Using $\Delta I_o/I_o = 5.5 \times 10^{-4}$ in Equation 106, for optically active (-)-riboflavin, a $\Delta\varepsilon/\varepsilon$ of 4.9×10^{-4} was calculated. Substituting these values into Equation 108 yields an R value of 1.12. Thus, the fraction of the CD signal relative to the total signal measured in the FDCD experiment was calculated from the

Figure 34. Fluorescence chromatogram

(R) - (-)-riboflavin at 1.05 x 10^{-5}M; (M) - 4-methylumbelliferone at 4.25 x 10^{-6}M. 1 µL injected at these concentrations, at a flow rate of 200 µL/min. Column, 5-µm ODS 150 x 2.1 mm; eluent, 20:80 acetonitrile:water.

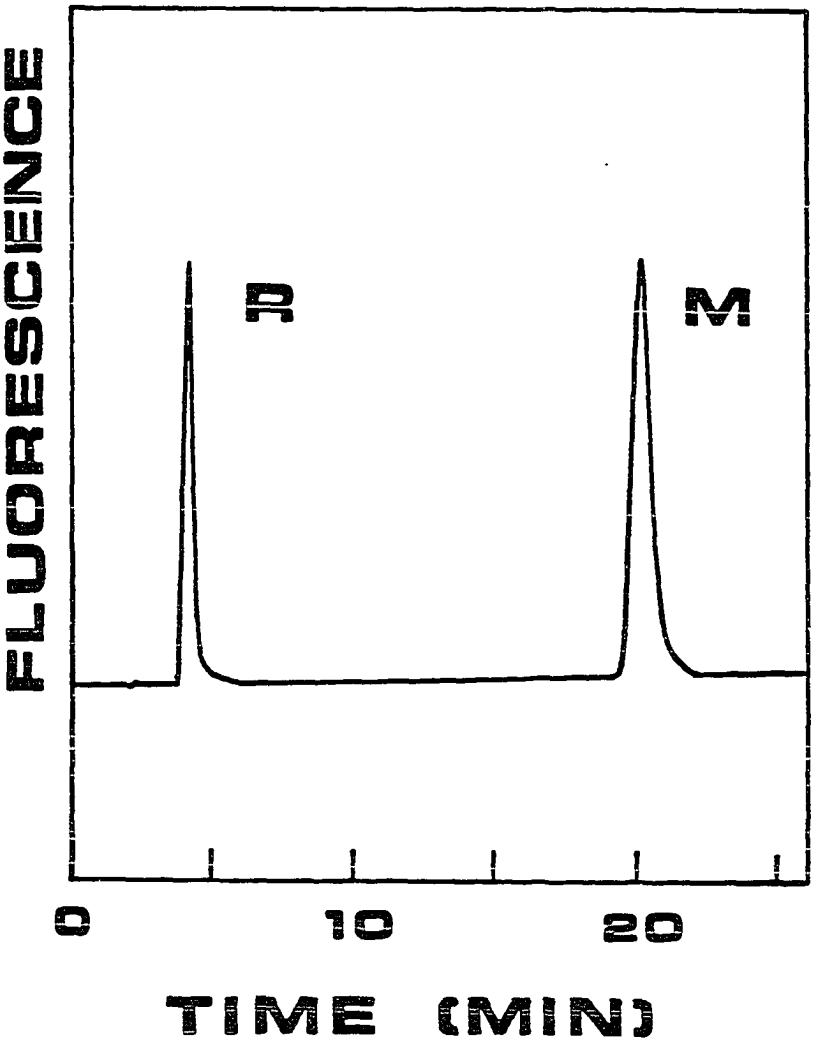
FLUORESCENCE
R
M
0
10
20
TIME (MIN)

Figure 35. FDCD chromatogram

(R) - (-)-riboflavin; (M) - 4-methylumbelliferone. Same chromatographic conditions and samples as Figure 34. A portion of the base line noise is amplified by a factor of 4 for comparison.

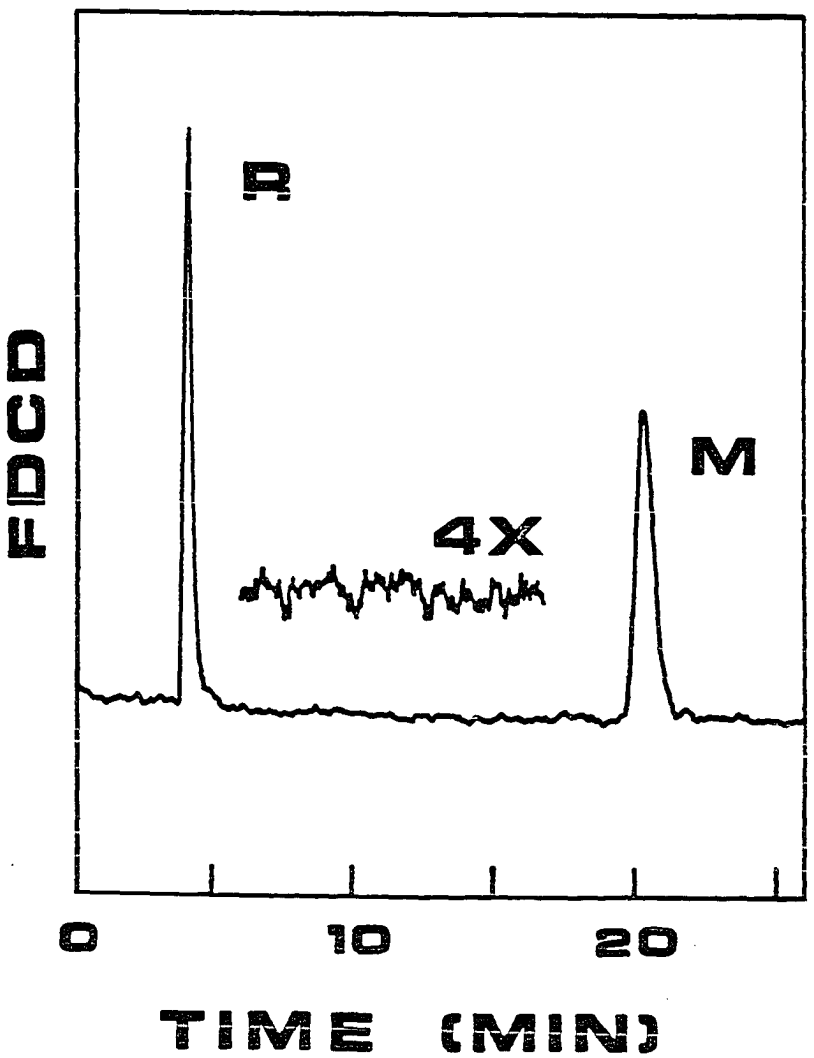
R
M
4X
FDCD
0
10
20
TIME (MIN)

definition of R, and was found to be 47%. The $\Delta\varepsilon/\varepsilon$ value for (-)-riboflavin at 325 nm is generally near 5.0×10^{-4} (141), for solvent systems similar to the chromatographic eluent used in this work. This value for $\Delta\varepsilon/\varepsilon$ compares favorably to the experimentally measured value of 4.9×10^{-4} found here. Note that the $\Delta I_o/I_o$ contribution in Equation 106 is added to the CD contribution, $\Delta\varepsilon/\varepsilon$. On different days, due to differences in alignment, the $\Delta I_o/I_o$ contribution was observed to either add or subtract from the CD contribution. The direction of the CD contribution to the total FDCD signal for (-)-riboflavin is however consistent with Equation 106, the literature $\Delta\varepsilon$ value, and the production of RCPL and LCPL via the modulation system.

Comparison of laser/modulation system combinations

It is interesting to compare the $\Delta I_o/I_o$ value obtained with FDCD-HPLC using a HeCd laser, with that obtained using an argon ion laser. Apparently, due to polarization instabilities in the HeCd laser and Pockels cell modulation system, a $\Delta I_o/I_o$ of 5×10^{-4} and a peak-to-peak noise to signal ratio (PPN/I_o) of 7×10^{-5} was the best obtainable. This was obtained at 150 kHz modulation frequency. Increasing or decreasing the modulation frequency had an adverse effect on these values. This is for either TDCD or FDCD measurements. In contrast, recent measurements with TDCD and FDCD systems using an argon ion laser yielded a $\Delta I_o/I$ of 6×10^{-5} and 1×10^{-4}, respectively. Also, the PPN/I_o was near 1×10^{-6} for the TDCD system with a 500 kHz modulation frequency, as discussed in

Chapter 8. Obviously, there are marked differences in the characteristics of these two laser/modulation system combinations. It was observed that transmission of the Pockels cell used is 90% at 488 nm and 75% at 325 nm. The absorption-induced heating at the latter wavelength probably caused the poorer performance. While the argon ion laser appears superior in considering $\Delta I_o/I_o$ and PPN/I_o, the HeCd laser was chosen since $\Delta\varepsilon/\varepsilon$ for riboflavin and other important biologically related fluorophores is more favorable at 325 nm (HeCd laser) than at 488 nm (argon ion laser).

Comparison of transmission and fluorescence detected circular dichroism

Comparing the nature of transmission and fluorescence detected CD measurements in the context of chromatography is quite useful. In the TDCD-HPLC system, the offset ratio, $\Delta I_o/I_o$, is readily observed on the lock-in amplifier as a steady DC signal shifted one way or the other from true zero. This is the chromatographic baseline. The elution of a highly absorbing species, assuming a large $\Delta I_o/I_o$, will cause the lock-in signal to swing back towards true zero, while a CD active species adds a contribution (hopefully significant) to this signal. In comparison, in the FDCD-HPLC system, the offset ratio, $\Delta I_o/I_o$, is not readily monitored since the correct choice of filters will produce nearly a zero light background at the photomultiplier tube at the chromatographic baseline. It is necessary in FDCD-HPLC to consider the use of a steady-state flow of some highly fluorescing, yet optically inactive, species from another pumping system separate from

the chromatography system. Thus, before a set of analyses are done on the FDCD-HPLC system, the offset ratio $\Delta I_o/I_o$ can be minimized with easy visualization on the lock-in amplifier. Once accomplished, the chromatography column can be connected to the detection cell to complete the FDCD-HPLC system. It should be emphasized that such careful adjustments to reduce $\Delta I_o/I_o$ is necessary to avoid artifacts in the chromatograms.

Quantitation calculations for the FDCD-HPLC system

It is of value to calculate the LOD for (-)-riboflavin in the FDCD-HPLC chromatogram (Figure 35). Using the 1X PPN as the LOD, and the CD fraction (47%) of the peak height, the mass detectability is 168 picograms injected (-)-riboflavin. The minimum concentration detectable is 4.5×10^{-7}M injected, using the 1-μL injection loop, 1.2 cm observed pathlength cell, and a 10-s time constant. A 10-s time constant was used because the FDCD measurement is, actually, the difference of two very large numbers, with respect to the chromatographic background, for an eluting fluorophore. The peak widths here are not substantially degraded at a 10-s time constant. A 1-s time constant was tested, and for this FDCD-HPLC system, provided slightly sharper chromatographic peaks but a poorer LOD by a factor of about 4, as compared to the 10-s time constant data. The precision for multiple trials with the FDCD-HPLC system yielded a relative standard deviation of about 11% for the peak heights shown in Figure 35. This indicates the presence of underlying polarization fluctuations within the measurement, that are hidden by the apparently

stable chromatographic baseline. As a regular fluorescence detector (Figure 34), the detection limit for riboflavin was about 300 femtograms, with a 10-s time constant.

Conclusion

A FDCD detection system, suitable for HPLC has been presented. The performance in terms of concentration detectability is better than that obtained for stopped-flow (static) or rapid-scanning CD detection systems (145, 146). The ability to do CD measurements in dynamic systems (HPLC) complements these published studies. The FDCD-HPLC system discussed here provides optical activity identification of eluting species that would not have been available in the wavelength region used, unless microgram quantities of optically active materials were injected (127). Thus, the system provides over a 10^3-fold improvement in mass detectability for fluorophores. The detectability is about 10 times better than the laser-based TDCD-HPLC system discussed in Chapter 8. With further refinements in laser sources and modulation systems (147), the selectivity of the measurement may be improved in the future. the present system provides the lowest detection limit available for indicating the optical activity of chromatographically separated species. Extension of this principle for microbore HPLC may improve this result, assuming a long enough pathlength can be maintained in detection without inducing too much

band broadening. The principle of FDCD-HPLC may prove invaluable in the analysis of biologically significant samples, where the optical activity of the sample components must be known.

REFERENCES

1. Poppe, H. Anal. Chim. Acta 1983, 145, 17.

2. Yeung, E. S. In "Microcolumn Separations: Columns, Instrumentation, and Ancillary Techniques", Novotny, M. V.; Ishi, D., Ed.; Elsevier Science Publishers: New York, 1985; p. 135.

3. DiCesare, J. L.; Ettre, L. S. J. Chromatogr. 1982, 251, 1.

4. Long, G. L.; Winefordner, J. D. Anal. Chem. 1983, 55, 712A.

5. Kucera, P.; Guiochon, G. J. Chromatogr. 1984, 283, 1.

6. Bobbitt, D. R.; Yeung, E. S. Anal. Chem. 1984, 56, 1577.

7. Bobbitt, D. R.; Yeung, E. S. Anal. Chem. 1985, 57, 271.

8. Synovec, R. E.; Yeung, E. S. Anal. Chem. 1985, 57, 2162.

9. Synovec, R. E.; Yeung, E. S. Anal. Chem. submitted.

10. Synovec, R. E.; Yeung, E. S. Anal. Chem. 1984, 56, 1452.

11. Wilson, S. A.; Yeung, E. S. Anal. Chim. Acta 1984, 157, 53.

12. Wilson, S. A.; Yeung, E. S.; Bobbitt, D. R. Anal. Chem. 1984, 56, 1457.

13. Mho, S.; Yeung, E. S. Anal. Chem. 1985, 57, 2253.

14. Skogerboe, K. J.; Yeung, E. S. Anal. Chem. 1984, 56, 2684.

15. Synovec, R. E.; Yeung, E. S. Anal. Chem. 1983, 54, 1599.

16. Synovec, R. E.; Yeung, E. S. J. Chromatogr. 1984, 283, 183.

17. Synovec, R. E.; Yeung, E. S. J. Chromatogr. Sci. 1985, 23, 214.

18. Synovec, R. E.; Yeung, E. S. In "Characterization of Heavy Crude Oils and Petroleum Residues", B. Tissot, Ed.; Editions Technip: Paris, France, 1984, p. 268.

19. Synovec, R. E.; Yeung, E. S. Anal. Chem. 1985, 57, 2606.

20. Synovec, R. E.; Yeung, E. S. J. Chromatogr. submitted.

21. Miller, J. C.; George, S. A.; Willis, B. G. Science 1982, 218, 241.

22. Hoshimo, T.; Sanda, M.; Hondo, T.; Saito, M.; Tohei, S. J. Chromatogr. 1984, 316, 473.

23. Krstulovic, A. M.; Colin, H. TRAC 1984, 3, 43.

24. Van Der Wal, S. J.; Snyder, L. R. J. Chromatogr. 1983, 255, 463.

25. Harris, J. M.; Leach, R. A. J. Chromatogr. 1981, 218, 15.

26. Buffett, C. E.; Morris, M. D. Anal. Chem. 1983, 55, 376.

27. Skogerboe, K. J.; Yeung, E. S. Anal. Chem. 1986, 58, 1014.

28. Nolon, T. G.; Hart, B. K.; Dovichi, N. J. Anal. Chem. 1985, 57, 2703.

29. Collette, T. W.; Parekh, N. J.; Griffin, J. H.; Carreira, L. A.; Rogers, L. B. Applied Spectroscopy 1986, 40, 164.

30. Sepeniak, M. J.; Yeung, E. S. J. Chromatogr. 1980, 190, 377.

31. Gluckman, J. C.; Shelly, D. C.; Novotny, M. V. J. Chromatogr. 1984, 317, 443.

32. Gluckman, J. C.; Shelly, D. C.; Novotny, M. V. Anal. Chem. 1985, 57, 1546.

33. Slais, K.; Krejci, M. J. Chromatogr. 1982, 235, 21.

34. Caudill, W. L.; Ewing, A. G.; Jones, S.; Wightman, R. M. Anal. Chem. 1983, 55, 1877.

35. Lunte, C. E.; Kissinger, P. T.; Shoup, R. E. Anal. Chem. 1985, 57, 1541.

36. Cassidy, R. M.; Elchuk, S. J. Chromatogr. Sci. 1983, 21, 454.

37. Woodruff, S. D.; Yeung, E. S. Anal. Chem. 1982, 54, 1174.

38. Wilson, S. A.; Yeung, E. S. Anal. Chem. 1985, 57, 2611.

39. Stolyhwo, A.; Colin, H.; Guiochon, G. J. Chromatogr. 1983, 265, 1.

40. Zarrin, F.; Dovichi, N. J. Anal. Chem. 1985, 57, 1826.

41. Niessen, W. M. A.; Poppe, H. J. Chromatogr. 1985, 323, 37.

42. Conroy, C. M.; Griffiths, P. R.; Jinno, K. Anal. Chem. 1985, 57, 822.

43. Johnson, C. C.; Taylor, L. T. Anal. Chem. 1984, 56, 2642.

44. Hayes, M. J.; Schwartz, H. E.; Vouros, P.; Karger, B. L.; Thurston, A. D., Jr.; McGuire, J. Anal. Chem. 1984, 56, 1229.

45. Blakley, C. R.; Vestal, M. L. Anal. Chem. 1983, 55, 750.

46. Alborn, H.; Stenhagen, G. J. Chromatogr. 1985, 323, 47.

47. Dorn, H. C. Anal. Chem. 1984, 56, 747A.

48. Bayer, E.; Albert, K. J. Chromatogr. 1984, 312, 91.

49. Loude, D. A., Jr.; Lee, R. W. K.; Wilkins, C. L. Anal. Chem. 1985, 57, 1464.

50. McGuffin, V. L.; Novotny, M. V. J. Chromatogr. 1981, 218, 179.

51. Gluckman, J. C.; Novotny, M. V. J. Chromatogr. 1984, 314, 103.

52. LaCourse, W. R.; Kruss, I. S.; Bratin, K. Anal. Chem. 1985, 57, 1810.

53. Locke, D. C.; Dhingra, B. S.; Baker, A. D. Anal. Chem. 1982, 54, 447.

54. Kuo, J. C.; Yeung, E. S. J. Chromatogr. 1981, 223, 321.

55. Kuo, J. C.; Yeung, E. S. J. Chromatogr. 1982, 229, 293.

56. Lovelock, J. E.; Maggs, R. J.; Adlard, E. R. Anal. Chem. 1971, 43, 1962.

57. Lovelock, J. E. J. Chromatogr. 1974, 99, 3.

58. Hirschfelder, J. O.; Curtiss, C. F.; Bird, R. B. "Molecular Theory of Gases and Liquids", Wiley: New York, 1964, p. 852.

59. Yeung, E. S. In "Advances in Chromatography", Giddings, J. C.; Grushka, E.; Brown, P. R.; Eds.; Marcel Dekker, Inc.: New York, 1983.

60. Woodruff, S. D.; Yeung, E. S. Anal. Chem. 1982, 54, 2124.

61. Skoog, D. A.; West, D. M. "Principles of Instrumental Analysis", 2nd Ed.; Saunders: Philadelphia, 1980; p. 374.

62. "CRC Handbook of Chemistry and Physics", Weast, R. C.; Astle, M. J.; Eds.; CRC Press: Boca Raton, 1978.

63. Snyder, L. R. J. Chromatogr. Sci. 1978, 16, 223.

64. Yeung, E. S.; Steenhoek, L. E.; Woodruff, S. D.; Kuo, J. C. Anal. Chem. 1980, 52, 1399.

65. Hamming, M. C.; Foster, N. G. "Interpretation of Mass Spectra of Organic Compounds", Academic: New York, 1972.

66. "High Performance Mass Spectrometry: Chemical Applications", Gross, M. L., Ed., ACS Symposium Series 70, American Chemical Society: Washington, D.C., 1978.

67. "Laboratory Methods in Infrared Spectroscopy", Miller, R. G. J.; Stace, B. C., Eds., 2nd ed., Heyden: London, 1972.

68. Jinno, K.; Fujimoto, C.; Ishii, D. J. Chromatogr. 1982, 239, 625.

69. Bevington, P. R. "Data Reduction and Error Analysis for the Physical Sciences", McGraw-Hill: New York, 1969, Chapter 6.

70. Younger, M. S. "Handbook for Linear Regression", 1st ed., Duxbury Press: North Scituate, MA, 1979, p. 234.

71. Brown, R. S.; Hausler, D. W.; Taylor, L. T. Anal. Chem. 1980, 52, 1511.

72. Zinbo, M.; Parsons, J. L. J. Chromatogr. 1971, 55, 55.

73. Craig, L. C.; Hausmann, W.; Ahrens, E. H., Jr.; Harfenist, E. J. Anal. Chem. 1951, 23, 1326.

74. Modern Plastics Encyclopedia 1982, 59, 623.

75. Sepaniak, M. J.; Yeung, E. S. J. Chromatogr. 1981, 211, 95.

76. Brown, R. S.; Hausler, D. W.; Taylor, L. T.; Carter, R. C. Anal. Chem. 1981, 53, 197.

77. Brown, R. S.; Taylor, L. T. Anal. Chem. 1983, 55, 273.

78. Johnson, C. C.; Taylor, L. T. Anal. Chem. 1983, 55, 436.

79. Alexander, G.; Hazai, I. J. Chromatogr. 1981, 217, 19.

80. Beckman, H., Ed. Geology of Petroleum, Vol. 5: "Composition and Properties of Petroleum", Halsted Press: New York, NY, 1981, Chapters 1 and 2.

81. Bobbitt, D. R.; Reitsma, B. H.; Rougvie, A.; Yeung, E. S.; Aida, T.; Chen, Y. Y.; Smith, B. F.; Squires, T. G.; Venier, C. G. Fuel 1985, 64, 114.

82. Matsunaga, A. Anal. Chem. 1983, 55, 1375.

83. Garrigues, P.; Ewald, M. Anal. Chem. 1983, 55, 2155.

84. Alexander, R.; Kagi, R. I.; Sheppard, P. N. J. Chromatogr. 1983, 267, 367.

85. Cookson, D. J.; Rix, C. J.; Shaw, I. M.; Smith, B. E.; J. Chromatogr. 1984, 312, 237.

86. Karger, B. L.; Snyder, L. R.; Eon, C. J. Chromatogr. 1976, 125, 71.

87. Billiet, H. A. H.; Van Dalen, J. P. J.; Schoenmakers, P. J.; DeGalan, L. Anal. Chem. 1983, 55, 847.

88. Dolan, J. W.; Gant, J. R.; Snyder, L. R. J. Chromatogr. 1979, 165, 31.

89. Snyder, L. R.; Glajch, J. L. J. Chromatogr. 1982, 248, 165.

90. Fritz, J. S.; Scott, D. M. J. Chromatogr. 1983, 271, 193.

91. Haley, G. A. Anal. Chem. 1971, 43, 371.

92. Ostvold, G. J. Chromatogr. 1983, 282, 413.

93. Dark, W. A. J. Liq. Chromatogr. 1982, 5, 1645.

94. Miller, R. L.; Ettre, L. S.; Johansen, N. G. J. Chromatogr. 1983, 259, 393.

95. O'Brien, A. P.; Ray, J. E. Analyst 1985, 110, 593.

96. Liphard, K. G. Chromatographia 1980, 13, 603.

97. Ogan, K.; Katz, E. Anal. Chem. 1982, 54, 169.

98. Haw, J. F.; Glass, T. E.; Dorn, H. C. Anal. Chem. 1981, 53, 2332.

99. Taraszewski, W. J.; Haworth, D. T.; Pollard, B. D. Anal. Chim. Acta 1984, 157, 73.

100. Foley, J. P.; Dorsey, J. G. Chromatographia 1984, 18, 503.

101. "Nomenclature, Symbols, Units and Their Usage in Spectrochemical Analysis-II", Spectrochim. Acta B 1978, 33B, 242.

102. Foley, J. P.; Dorsey, J. G. J. Chromatogr. Sci. 1984, 22, 40.

103. Smit, H. C.; Walg, H. L. Chromatographia 1975, 8, 311.

104. Wichmann, B. A.; Hill, I. D. Applied Statistics 1982, 31, 188.

105. Muller, M. E. "Generation of Normal Deviates", Technical Report No. 13, Statistical Techniques Research Group, Department of Mathematics, Princeton University.

106. Lephardt, J. O. In "Transform Techniques of Chemistry" Griffiths, Peter R.; ed.; Plenum Press: New York, 1978, 294-301.

107. Barnett, W. B.; Bohler, W.; Carnrick, G. R.; Slavin, W. Spectrochim. Acta 1985, 40B, 1689.

108. Woodruff, S. D.; Yeung, E. S. J. Chromatogr. 1983, 260, 363.

109. Laeven, J. M.; Smit, H. C. Anal. Chim. Acta 1985, 176, 77.

110. Saadat, S.; Terry, S. C. Amer. Lab. 1984, 16(5), 90.

111. Wright, N. A.; Villalanti, D. C.; Burke, M. F. Anal. Chem. 1982, 54, 1735.

112. Lam, R. B.; Sparks, D. T.; Isenhour, T. L. Anal. Chem. 1982, 54, 1927.

113. Maestre, M. F.; Katz, J. E. Biopolymers 1982, 21, 1899.

114. Warner, I. M.; Patonay, G.; Thomas, M. P. Anal. Chem. 1985, 57, 463A.

115. Tinoco, I., Jr.; Williams, A. L. Ann. Rev. Phys. Chem. 1984, 35, 329.

116. Turner, D. H.; Tinoco, I., Jr.; Maestre, M. F. Biochemistry 1975, 14, 3794.

117. Allenmark, S. G. TRAC 1985, 4, 106.

118. Schippers, P. H.; Dekkers, H. P. J. M. Anal. Chem. 1981, 53, 778.

119. Collingwood, J. C.; Day, P.; Denning, R. G.; Quested, P. N.; Snellgrove, T. R. J. Physics E: Sci. Inst. 1974, 7, 991.

120. Goodwin, T. J.; Williams, P. A. Inorg. Chim. Acta 1984, 86, L73.

121. deWeerd, R. J. E. M.; van Hal, H. M. P. M.; Buck, H. M. J. Org. Chem. 1984, 49, 3413.

122. Han, S. M.; Atkinson, W. M.; Purdie, N. Anal. Chem. 1984, 56, 2827.

123. Atkinson, W. M.; Han, S. M.; Purdie, N. Anal. Chem. 1984, 56, 1947.

124. Crone, T. A.; Purdie, N. Anal. Chem. 1981, 53, 17.

125. Gaffney, J. S.; Premuzic, E. T.; Orland, T.; Ellis, S.; Snyder, P. J. Chromatogr. 1983, 262, 321.

126. Drake, A. F.; Gould, J. M.; Mason, S. F. J. Chromatogr. 1980, 202, 239.

127. Westwood, S. A.; Games, D. E.; Sheen, L. J. Chromatogr. 1981, 204, 103.

128. Yeung, E. S. In "Analytical Applications of Lasers", Laser Spectroscopy for Detection in Chromatography, Piepmeir, E. H., Ed.; Wiley-Interscience: New York, 1985, in press.

129. Ducloy, M.; Snyder, J. J. Proc. SPIE 1983, 426, 87.

130. McCaffery, A. J.; Mason, S. F.; Ballard, R. E. J. Chem. Soc. 1965, 519, 2883.

131. Nimura, N.; Toyama, A.; Kinoshita, T. J. Chromatogr. 1984, 316, 547.

132. Buckingham, D. A. J. Chromatogr. 1984, 313, 93.

133. Yoneda, H. J. Chromatogr. 1984, 313, 59.

134. Buckingham, D. A.; Clark, C. R.; Oeva, M. M.; Tasker, R. F. J. Chromatogr. 1983, 262, 219.

135. Young, M. In "Optics and Lasers", MacAdam, D. L., Ed.; Springer Series in Optical Sciences: Germany, 1977, Vol. 5, pp. 188-190.

136. Angelici, R. J. In "Synthesis and Technique in Inorganic Chemistry", 2nd Ed., W. B. Saunders Co.: Philadelphia, PA, 1977, pp. 13-25, 39-45, 71-80.

137. Watada, A. E.; Tran, T. T. J. Liq. Chromatogr. 1985, 8, 1651.

138. Vandemark, F. L.; Schmidt, G. J. J. Liq. Chromatogr. 1981, 4, 1157.

139. Ang, C. Y. W.; Moseley, F. A. J. Agric. Food Chem. 1980, 28, 483.

140. Ishibashi, N.; Ogawa, T.; Imasaka, T.; Kunitake, M. Anal. Chem. 1979, 51, 2096.

141. Tollin, G. Biochemistry. 1968, 7, 1720.

142. Tinonco, I. Jr.; Turner, D. H. J. Am. Chem. Soc. 1976, 98, 6453.

143. Jensen, H. P.; Schellman, J. A.; Troxell, T. Applied Spectrosc. 1978, 32, 192.

144. Lobenstine, E. W.; Turner, D. H. J. Am. Chem. Soc. 1980, 102, 7787.

145. Anson, M.; Bayley, P. M. J. Physics E: Scientific Instruments 1974, 7, 481.

146. Hatano, M.; Nazawa, T.; Murakami, T.; Yamamoto, T.; Shigehisa, M.; Kimura, S.; Takakuwa, T.; Sakayanagi, N.; Yano, T.; Natanabe, A. Rev. Sci. Instrum. 1981, 52, 1311.

147. Hipps, K. W.; Crosby, G. A. J. Physical Chem. 1979, 83, 555.

APPENDIX.

STATISTICAL DERIVATIONS FOR USE IN CHAPTER 3

The following contains the derivations of several key equations in the main text of Chapter 3. It is shown how a consideration of the propagation of errors can lead to an estimate of the confidence level associated with the best-fit elution order.

To determine the effect of propogation of errors in Equation 24 in Chapter 3 the partial derivatives of $S_3^{x'} \equiv S$ with respect to each term.

$$dS = \left(\frac{\partial S}{\partial S_1^x}\right) dS_1^x + \left(\frac{\partial S}{\partial S_2^x}\right) dS_2^x + \sum_{i=j}^{3} \sum_{j=A}^{B} \left(\frac{\partial S}{\partial S_i^j}\right) dS_i^j \qquad \text{(A-1)}$$

It is easy to see that

$$\frac{\partial S}{\partial S_1^x} = \frac{a}{c} \qquad \text{(A-2)}$$

and

$$\frac{\partial S}{\partial S_2^x} = \frac{b}{c} \qquad \text{(A-3)}$$

Considering the numerator in Equation 24 as f and the denominator there as g, one has

$$\frac{\partial f}{\partial S_1^A} = -S_3^B S_2^x \qquad \text{(A-4)}$$

and

$$\frac{\partial q}{\partial S_1^A} = -S_2^B \qquad \text{(A-5)}$$

Combining Equations A-4 and A-5,

$$\frac{\partial S}{\partial S_1^A} = \frac{-cS_3^B S_2^x + S_2^B(aS_1^x + bS_2^x)}{c^2} \qquad \text{(A-6)}$$

Each of the other terms in Equation A-1 can thus be similarly calculated. Now, one can square both sides of A-1, neglecting cross items, and obtain variances. The result is

$$\begin{aligned} \text{var } S_3^{x'} = [&a^2 \text{ var } S_1^x + b^2 \text{ var } S_2^x + (S_3^{x'} S_2^B - S_2^x S_3^B)^2 \text{ var } S_1^A + \\ &(S_1^x S_3^B - S_3^{x'} S_1^B)^2 \text{ var } S_2^A + (S_2^x S_3^A - S_3^{x'} S_2^A)^2 \text{ var } S_1^B + \\ &(S_3^{x'} S_1^A - S_1^x S_3^A)^2 \text{ var } S_2^B + (S_2^x S_1^B - S_1^x S_2^B)^2 \text{ var } S_3^A + \\ &(S_1^x S_2^A - S_2^x S_1^A)^2 \text{ var } S_3^B]/c^2 \end{aligned} \qquad \text{(A-7)}$$

To derive Equation 28 in Chapter 3 one first replaces the weighting factors in either Equation 25 or 26 by w. To a first approximation, one can consider the weights w and the total area, $\Sigma|S^x|$, to be constants, i.e., the propagation of errors from these terms are only second-order in nature. So

$$\sigma^2 = \frac{\Sigma w(S^{x'} - S^x)^2}{\text{const}} \qquad \text{(A-8)}$$

One can define each residual squared as μ, so

$$\sigma^2 = \frac{\Sigma w\mu}{\text{const}} \tag{A-9}$$

and

$$\text{var } \sigma^2 = (\Sigma w^2 \text{var}\mu)/\text{const}^2 \tag{A-10}$$

For each of the terms μ,

$$d\mu = \frac{\partial \mu}{\partial S^{X'}} dS^{X'} + \frac{\partial \mu}{\partial S^{X}} dS^{X} \tag{A-11}$$

$$d\mu = 2(S^{X'} - S^{X})dS^{X'} - 2(S^{X'} - S^{X})dS^{X} \tag{A-12}$$

Squaring and neglecting cross-terms,

$$\text{var } \mu = 4(S^{X'} - S^{X})^2[\text{var } S^{X'} + \text{var } S^{X}] \tag{A-13}$$

It can also be shown that

$$\text{var } \sigma = \frac{1}{2\sigma} \text{var } \sigma^2 \tag{A-14}$$

Combining Equations A-10, A-13, and A-14, one obtains Equation 28 in Chapter 3.

To obtain the confidence level for a separation of Δ for the two lowest values of σ_1 and σ_2 as calculated from Equation 25 or 26 with $\sigma(\sigma)$ of s_1 and s_2, respectively, one can refer to the two Gaussian-shaped distribution curves that give the probability of σ_1 having a

particular value x and the probability of σ_2 having a particular value y. These are

$$P\sigma_1(x) = \frac{1}{s_1\sqrt{2\pi}} \exp\ (-x^2/2s_1^2) \tag{A-15}$$

and

$$P\sigma_2(y) = \frac{1}{s_2\sqrt{2\pi}} \exp\ [-(y-\Delta)^2/2s_2^2] \tag{A-16}$$

Now, for σ_1 taking on a value of x, the probability of σ_2 taking on values <u>smaller</u> than x is given by

$$P\sigma_2(y < x) = \int_{-\infty}^{x} \frac{1}{s_2\sqrt{2\pi}} \exp\ [-(y-\Delta)^2/2s_2^2]dy \tag{A-17}$$

So, the total probability of having σ_2 <u>larger</u> than σ_1 in future experiments is a confidence level

$$C.L = 1 - \int_{-\infty}^{\infty} \frac{1}{s_1\sqrt{2\pi}} \exp(-x^2/2s_1^2) \int_{-\infty}^{x} \frac{1}{s_2\sqrt{2\pi}} \exp[-(y-\Delta)^2/2s_2^2]dydx \tag{A-18}$$

By numerical integration, it was found that if $s_1 - s_2 = s$, the C.L. is the worst for a given $\Delta = \sigma_2 - \sigma_1$. For example, Δ = 0, s, 2s, and 3s gives C.L. = 50%, 76%, 92%, and 98%, respectively. If $s_1 \neq 0$ and $s_2 = 0$, then for $\Delta = s_1$ and $2s_1$, one gets C.L. = 84% and 97.8%, respectively.

ACKNOWLEDGMENTS

It is difficult to thank, in an appropriate manner, all those having an important role in my personal and professional development. Yet, I would like to start from Iowa State University and work my way back in time.

Dr. Edward S. Yeung, my research advisor at ISU, has been a constant influence, guiding my graduate work and professional development, with much interest and effort. Dr. Yeung and my committee are gratefully acknowledged for the opportunities made available, and pursued, through their supervision. The Chemistry Department at ISU continuously has an excellent group of graduate students and staff. Friendships with many of these people have helped to make graduate school an enjoyable experience.

One cannot go to graduate school without first graduating from undergraduate studies. My experience of going to Bethel College in St. Paul, Minnesota, has helped me to put many things in life into perspective. Dr. Dale Stephen's interest in my future, and a career choice is very appreciated. The Chemistry, Mathematics, and Physics departments at Bethel College have many "good folks", each having a large impact on my academic interests.

I am indebted to the teachers at Canby High School, in Canby, Minnesota, a small town of roughly 2,000 people. It is important to never forget one's roots, but Canby is as far back as I'll go!

Finally, I would like to thank my immediate family. My sisters, Dianne and Debra, and brother, Ryan, are fun to grow up with, and are appreciated and loved. My father, Eugene Synovec, and mother, Joan Synovec, are probably the best parents in the world, or at least in Minnesota! But seriously, they are very understanding, supportive, loving, and just plain fun. For my wife, Kristy, I acknowledge her interest in both of our careers, our love for each other, and the hope for a good life together.